## INFORMATION TO USERS

This dissertation was produced from a microfilm copy of the original document. While the most advanced technological means to photograph and reproduce this document have been used, the quality is heavily dependent upon the quality of the original submitted.

The following explanation of techniques is provided to help you understand markings or patterns which may appear on this reproduction.

1. The sign or "target" for pages apparently lacking from the document photographed is "Missing Page(s)". If it was possible to obtain the missing page(s) or section, they are spliced into the film along with adjacent pages. This may have necessitated cutting thru an image and duplicating adjacent pages to insure you complete continuity.

2. When an image on the film is obliterated with a large round black mark, it is an indication that the photographer suspected that the copy may have moved during exposure and thus cause a blurred image. You will find a good image of the page in the adjacent frame.

3. When a map, drawing or chart, etc., was part of the material being photographed the photographer followed a definite method in "sectioning" the material. It is customary to begin photoing at the upper left hand corner of a large sheet and to continue photoing from left to right in equal sections with a small overlap. If necessary, sectioning is continued again – beginning below the first row and continuing on until complete.

4. The majority of users indicate that the textual content is of greatest value, however, a somewhat higher quality reproduction could be made from "photographs" if essential to the understanding of the dissertation. Silver prints of "photographs" may be ordered at additional charge by writing the Order Department, giving the catalog number, title, author and specific pages you wish reproduced.

**University Microfilms**

300 North Zeeb Road
Ann Arbor, Michigan 48106

A Xerox Education Company

THE UNIVERSITY OF OKLAHOMA

GRADUATE COLLEGE

# DISSIPATION OF ENERGY IN A SELF-INTERACTING, MULTIPLY-CONNECTED SUPERCONDUCTING LOOP

A DISSERTATION

SUBMITTED TO THE GRADUATE FACULTY

in partial fulfillment of the requirements for the

degree of

DOCTOR OF PHILOSOPHY

BY

LESTER K. SISEMORE

Norman, Oklahoma

1972

DISSIPATION OF ENERGY IN A SELF-INTERACTING,

MULTIPLY-CONNECTED SUPERCONDUCTING LOOP

APPROVED BY

Keith J. Engvold

Stephen C. Whitmore

R. R. Bowrasser

R. Kantowski

Gene B. Hocker

DISSERTATION COMMITTEE

ACKNOWLEDGMENT

First and foremost, I would like to express my sincere appreciation for the time and effort spent by Dr. Keith J. Carroll in directing this work. I acknowledge Dr. Paul T. Sikora for reading the dissertation and offering helpful suggestions which greatly improved my understanding of this work.

Special thanks are due Dr. Ronald Bourassa, Dr. Ronald Kantowski, Dr. Gene Walker, and Dr. Stephen Whitmore who, along with Dr. Carroll and Dr. Sikora, spent time in reading this dissertation.

Appreciation goes to my friend Dr. James E. Nicholson for his help in writing the computer program and for his help, along with Mr. Wallace Pryor, in the laboratory. Recognition goes to Mr. Gene Scott for the construction of the cryostat used in this experimental investigation.

I would like to thank the Research Corporation for partial financial support of this project.

I would like to thank the National Defense and Education Association (NDEA) and the National Aeronautics and Space Administration (NASA) from whom I held fellowships during part of the time spent on this work.

My deepest gratitude goes to my wife, Frances, for her encouragement and understanding during the years in school. Her help in typing this dissertation was invaluable.

TABLE OF CONTENTS

LIST OF TABLES

LIST OF ILLUSTRATIONS

LIST OF ILLUSTRATIONS--Continued

# DISSIPATION OF ENERGY IN A SELF-INTERACTING, MULTIPLY-CONNECTED SUPERCONDUCTING LOOP

## CHAPTER I

## INTRODUCTION

A superconducting device which has evolved into several useful forms is the persistatron, first described in 1958 by Buckingham[1] as a low temperature memory element. Since then, the device has been modified to become a persistent-mode switch for superconducting magnets[2], and a "flux-pump"[3]. Furthermore, Sikora has suggested that a doubly-connected superfluid helium system should exhibit analogus behavior[4], and this conjecture has been verified.[5]

### Coupled Persistatron

Recently, the persistatron has been modified into a coupled superconducting circuit in which the two branches of the device are deliberately made interacting,[6] as shown in Fig. 1. This multiply-connected, self-interacting superconducting circuit is referred to as a "coupled persistatron". The current $i_s$ in the coil of inductance L produces a field $H_s$ at the central wire. Thus, the transport current $i_w$ carried by the wire is influenced by $i_s$. The behavior of the system, that is, the apportionment of the currents $i_s$ and $i_w$ between the two parts or branches, can be predicted by using only the principles that (a) a dissipation-producing

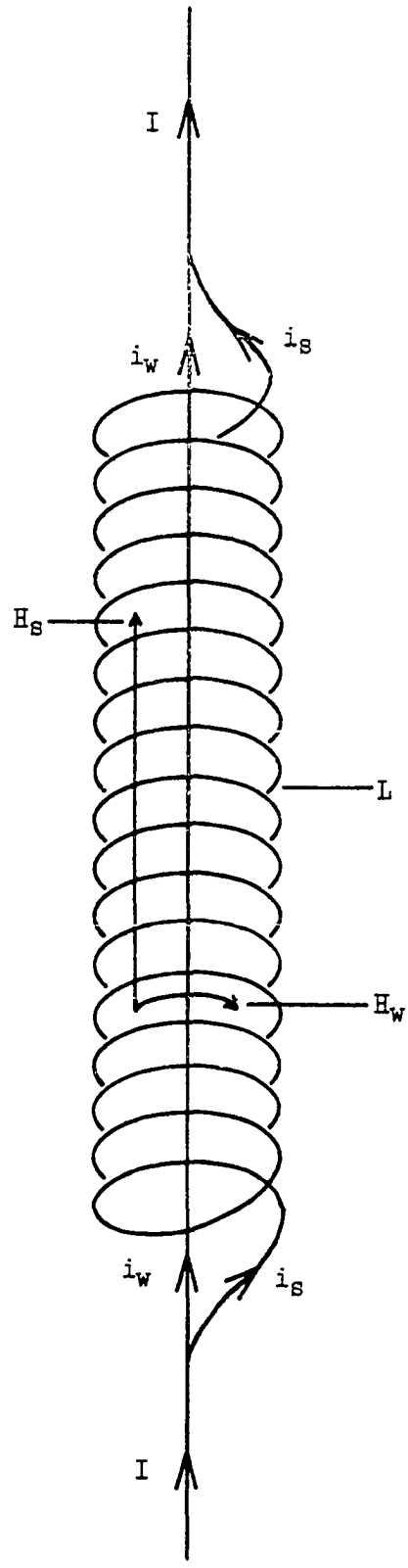


Fig. 1.--The coupled persistatron circuit.

flow apportionment is dynamically unstable against a loss-less apportionment whenever the latter is possible for a given total current, and (b) the quantization of system energy due to flux conservation when the multiply-connected system is in the superfluid state prevent any further current changes once a loss-less flow pattern has been attained. Experimental results in this laboratory for $i_s$ and $i_w$ as a function of input current I agree very well with the theoretical predictions.[6] (cf. Fig. 2)

The steady state of the coupled persistatron is a delicate balance of currents which exist only when there is no dissipation in the straight wire (assuming that the solenoid is in the superconducting state well below the critical current transition). This characteristic of the coupled persistatron can be used to study the dissipation of energy in a current-carrying superconducting wire. This investigation will be concerned with using the coupled persistatron to study the following: (i) the current at which dissipation begins in the wire, (ii) the behavior of the wire when the current is increased above this threshold value, and (iii) the properties of the equilibrium state to which the system tends once such an increase is made.

## Destruction of Superconductivity

If a metal is to remain superconducting, the net momentum of the superelectrons must not exceed a certain value.[7] For this reason there is a limit to the density of resistanceless current that can be carried by any region in the metal. This critical current density applies to both a current transported through the specimen from an external source and to screening currents which shield the specimen from an applied magnetic field. As a result of this critical current density, a sufficiently

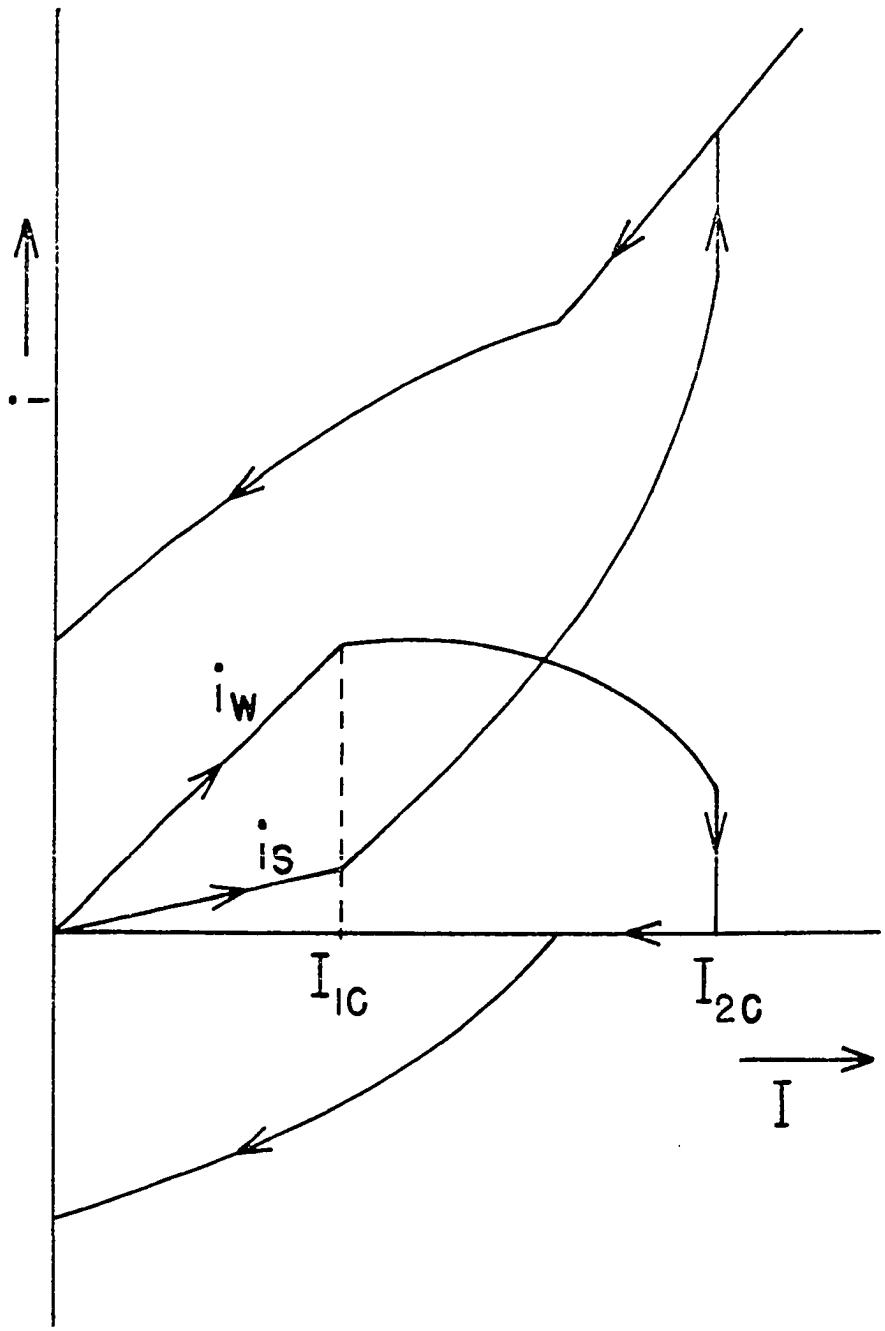


Fig. 2.--The complete cycle for the coupled persistatron.

strong magnetic field will destroy the superfluid state in a superconductor. This field $H_c$ is called the critical magnetic field and is a function of temperature.

The question may be raised as to which is the more fundamental variable, the magnetic field or the current, for a superconductor. Actually, these two modes of description are equivalent. However, when the collective behavior of the superelectrons is treated thermodynamically, the temperature and magnetic field strength are taken as the fundamental variables. On the other hand, when the superconductor is part of a circuit in which current flows, the most convenient mode of description for its behavior is in terms of current, transport and shielding.

Microscopically, from the BCS theory, one might say that the fundamental quantity for a superconductor is the minimum excitation energy required to split a Cooper pair. In other words, superconductivity is destroyed when the superelectrons receive a sufficient amount of energy to cross the energy gap $2\Delta$. This energy may be supplied in several different ways, the most common of which are the raising of the temperature, the application of a magnetic field, and the introduction of a transport current.

## Surface Currents

An applied magnetic field produces a flux density in the nonmagnetic material of a superconductor.[7] However, screening currents generate an internal flux density which everywhere is exactly equal and opposite to that produced by the applied field, and consequently the net magnetic field is zero inside the superconductor.

The fact that a superconductor does not allow a magnetic field to exist in its interior has an important effect on the current that flows

along it; currents cannot pass through the bulk of a type-I superconductor, but must flow only on the surface. This can be seen by considering the relation between the magnetic flux and current density,

$$\vec{\nabla} \times \vec{B} = \mu_0 \vec{J}.$$

If the specimen is superconducting $\vec{B}$ and $\vec{\nabla} \times \vec{B}$ are zero inside of it. It follows, therefore, that the current density $\vec{J}$ must also be zero within the superconductor. The current then flows not through the specimen but on the surface. This is true of currents passed along the superconductor from some external source (these are called "transport" currents because they transport charge into and out of the material), as well as diamagnetic screening currents. In the absence of an applied magnetic field, the transport current not only must flow on the surface but must also flow along the length of the wire without spiraling relative to it.

On the other hand, currents cannot be confined entirely to the surface because the current sheet would have no thickness and the current density would be infinite. In fact the currents flow within a very thin surface layer. Consequently, the flux density does not fall abruptly to zero at the boundary but dies away within the region where the currents are flowing. The depth within which the currents flow is called the "penetration depth $\lambda$", because it is the depth to which the flux of the applied magnetic field appears to penetrate.

## Critical Current

There is a relation between the supercurrent density at any point and the magnetic flux density at that point. This relation holds whether the supercurrent is a screening current, a transport current, or a combination of both. If the total current flowing on a superconductor is

sufficiently large, the current density at the surface will reach the critical value and the associated magnetic field at the surface will have a value $H_c$. This leads to the following general hypothesis: a superconductor loses its zero resistance when, at any point on the surface, the total magnetic field, due to transport current and applied magnetic field, exceeds the critical field $H_c$.[7] This implies that the critical current of a wire is the maximum amount of transport current which can be passed along a superconducting wire without resistance appearing. It should be emphasized that this defines the critical current of a specimen as the current at which it ceases to have zero resistance. One of the purposes of this investigation is just to determine the universality of this definition.

If there is no applied magnetic field the only magnetic field will be that generated by a transport current. In this case, the critical current will be that current which generates the critical magnetic field $H_c$ at the surface of the conductor. This special case of the general rule stated above is known as Silsbee's hypothesis[8]. Consider a cylindrical wire of diameter d. If, in the absence of any externally applied magnetic field, a current i is passed along the wire, a magnetic field will be generated at the surface,

$$H = (2/5d)\ i, \tag{1}$$

where d is in centimeters, i in amperes, and H in gauss. The critical current of a wire will then be

$$i_c = (5d/2)\ H_c, \tag{2}$$

according to Silsbee's hypothesis.

## Intermediate State

Although the description of a macroscopic superconductor in the presence of an external field $H_e$ presented is formally correct, it is sometimes more convenient to replace it by an equivalent one which treats such a superconductor as a magnetic body with an interior field $H_i$, magnetization $M_i$, and no surface current density.[9] According to this diamagnetic mode of description, the field strength inside the superconductor is given by

$$H_i = H_e - 4\pi D M_i, \tag{3}$$

where D is the demagnetization coefficient of the specimen. For an infinite cylinder with its axis parallel to $H_e$, $D = 0$; for an infinite cylinder transverse to the field, $D = 1/2$; and for a sphere, $D = 1/3$.

This says that when a magnetic field is applied to a superconducting specimen, the transition to the normal state may or may not be abrupt depending on its demagnetization coefficient. In the region

$$(1 - D) H_c \leq H \leq H_c, \tag{4}$$

the specimen is neither entirely normal nor entirely superconducting. This is referred to as the intermediate state. This intermediate state exists, in some field interval, for any geometry other than that of a quasi-infinite cylindrical sample parallel to the external field.

The domain structure in the intermediate state has been investigated experimentally by many workers. The first of these were Meshkovsky and Shalnikov.[10] Photographs of the intermediate state in aluminum plates were obtained by Faber,[11] using a powder technique. More recently Baird[12] has studied the penetration of magnetic flux into superconducting indium using the Faraday effect (the ability of a paramagnetic glass in a magnetic field to rotate the plane of polarization of polarized light).

The motion of flux and of superconducting-normal boundaries in the intermediate state implies dissipation of energy. Direct observations on the time behavior of magnetic flux penetration in flat indium plates subjected to a transverse magnetic field have been reported.[13-14]

Though an intermediate state does not appear in a straight wire in a longitudinal field, one may be induced by a current. The full normal resistance does not appear at a sharply defined value of current but over a considerable current range. In fact, at the critical current, the wire goes into an intermediate state of alternate superconducting and normal regions each of which occupies the full cross-section of the wire.[15] The current passing along the wire now has to flow through the normal regions, so at the critical current the resistance should jump from zero to a fraction of the resistance $R_o$ of the completely normal wire, as in Fig. 3. Extensive research has been done on this resistance transition.[16] Of particular interest is the work done by Scott[17] and by Meissner and Zdanis[18]. The detailed configuration of the normal and superconducting regions which must appear when a current exceeding the critical current is passed along a wire has not yet been determined experimentally, and it is a complicated problem to deduce the pattern from theoretical considerations.[19]

Whenever an externally applied magnetic field and a transport current are present at the same time in a superconductor, there is an interaction between the two.[20] The subsequent flux motion is known to produce power dissipation.[21]

## Metallurgical Annealing

The metallurgical behavior[22-26] of a single-component crystalline metal is of special interest in this investigation. When a crystalline

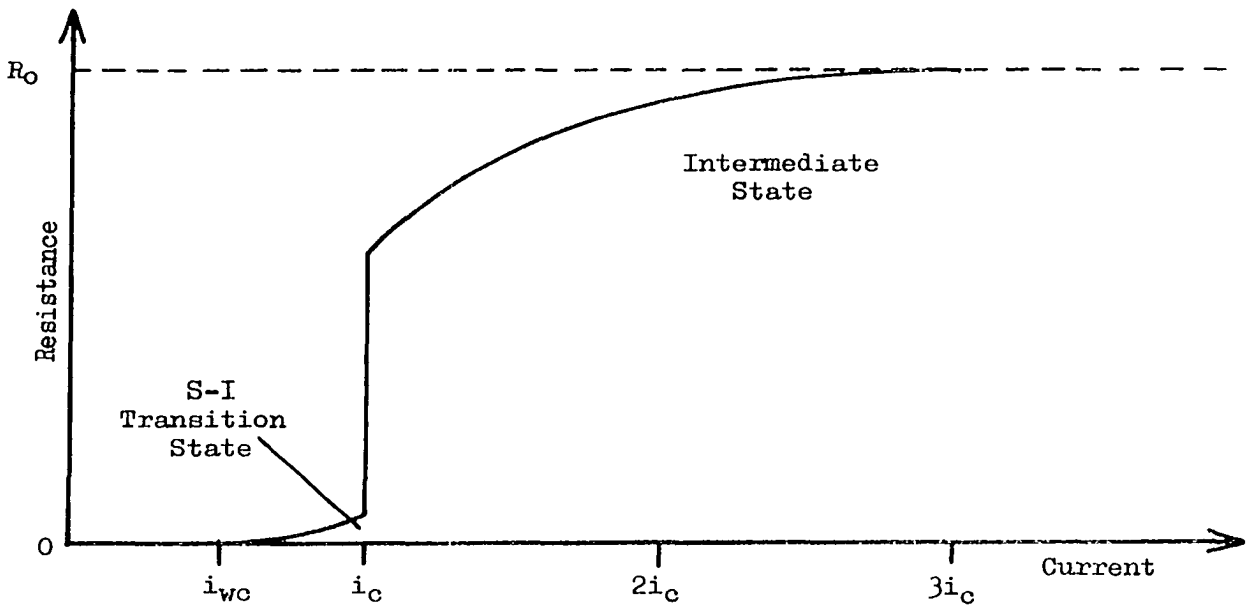


Fig. 3.--A resistance transition curve.

metal is severely deformed at a temperature less than its melting point, it loses its crystal structure. If the metal is subjected to a suitable heat treatment, new crystals or grains begin to form from the deformed metal. This process is referred to as recrystallization and, for indium, occurs at a temperature somewhere between liquid nitrogen temperature and room temperature[27].

After recrystallization the metal is polycrystalline, consisting of many different grains. The layer of atoms which constitute the zone of contact between adjacent grains having differently oriented space lattices is called a grain boundary. This investigation will try to observe the effect these grain structures and boundaries have on flux movement or dissipation in a superconductor.

Grain growth occurs during and after the recrystallization process whenever the metal is annealed. The process of heating a metal to a certain temperature, maintaining it there for a given time, and then cooling it is called annealing. Generally, this implies that the metal is slowly cooled after heating, but this is not always the case. Cast metals do not show grain growth--recrystallization is possible only in metals that have been cold-worked.[24]

Each grain in a single-component metal has the same composition and crystal structure, but they differ in size, shape, and orientation. The appearance of definite grain boundaries at the interfaces between adjacent crystals is the result of different orientations.

As the result of the interaction of two independent sets of bonding forces, the last atom to freeze in the region of the grain boundary will actually come to rest at some intermediate point representing a compromise between two possible equilibrium positions. Since the position

of any given atom is determined by the attractive forces of all the atoms that surround it, displacement of an atom at the interface results in correspondingly smaller displacements of the atoms in the layers on each side of the interface. This causes still smaller displacements of the atoms in the next deeper layer within each crystal, and so on to a depth of perhaps five to twenty interatomic distances from the interface.[25]

Grain boundaries are actually distorted layers of atoms between normal grains, within which there occurs a transition from the orientation of one crystal to that of the other. The width of the grain-boundary layer and the degree of distortion within it depend on the relative orientations of the crystals between which it exists.

Grain-boundary atoms have an energy above that of atoms within the grains. This is due to the fact that they do not exist in the positions of minimum-energy they would occupy in an undistorted crystal. Consequently, grain boundaries are regions of abnormally high free energy.

In accordance with the second law of thermodynamics, the solid tends to reduce its free energy by approaching a condition of minimum grain-boundary energy. The major means by which a polycrystalline metal does this is grain growth, in which one crystal grows at the expense of another. Because a small grain has more surface per unit volume, it has more surface energy than a large one. This instability tends to cause the larger grain to grow at the expense of the smaller one.

In a pure metal the mechanism of grain growth is described as grain-boundary migration. This involves a slow encroachment of one crystal into the region initially occupied by its smaller neighbor. The grain boundary between them shifts toward the center of the smaller crystal.

Finally, the smaller crystal is completely absorbed, the grain boundary disappears, and the increment of free energy represented by the boundary is dissipated as heat.

The ultimate tendency of grain growth is to eliminate grain boundaries. This reduces a polycrystalline metal to the minimum-energy condition of a single crystal. The following are variables that influence the rate of grain growth:

1) differences in original grain size,

2) temperature,

3) initial grain size,

4) extent of cold working,

5) duration of annealing,

and perhaps on other factors not yet recognized.

It should be emphasized that the connection between the metallurgical state and the superconducting properties to be studied in this investigation is only qualitatively known. The metallurgical effects studied in this work will also be treated only qualitatively.

# CHAPTER II

## THEORY

Even though a quantitative theory on the nature of the dissipation in a current-carrying superconducting wire cannot be presented here at the present time, the macroscopic or collective behavior as observed using the coupled persistatron can be treated. The current apportionment within the circuit can be predicted[6], and so can the steady state of the system characterized by a loss-less apportionment. The apportionment of the current in the circuit, the characteristics of the equilibrium state to which the system tends, and the nature of the time behavior of the system will give important information about the dissipation in a superconducting wire.

### Coupled Persistatron

#### System Behavior

As an external control current, $I = i_s + i_w$, is impressed upon the coupled persistatron, virtually all of the current appears in the straight wire branch so that flux may be conserved. That is

$$\phi = Li_s - L'i_w = 0 \qquad (5)$$

where $L'$ is the inductance of the branch containing the wire sample. Now $L \gg L'$ so that

$$i_s = \frac{L'}{L} i_w \ll i_w .$$

Typically

$$i_s = 0.025\, i_w \ .$$

This reversible situation continues until at some input $I = I_{1c}$ (first critical point), the current $i_w$ attains a threshold value $i_{wc}$. Beyond this value of $I_{1c}$, any further current increase must appear as an increase in $i_s$, which will reduce $i_w$ through its dependence on $H_s$.

Mathematically, in the region $I > I_{1c}$, an increment of input current can be written

$$dI = di_w + di_s \tag{6}$$

and since $i_{wc} = i_{wc}(H_s)$,

$$di_w = \left( \frac{\partial i_w}{\partial H_s} \right)_c dH_s \ .$$

Now

$$H_s = k_s i_s \tag{7}$$

so

$$di_w = k_s \left( \frac{\partial i_w}{\partial H_s} \right)_c di_s$$

and from Eq. (6)

$$dI = di_s + k_s \left( \frac{\partial i_w}{\partial H_s} \right)_c di_s$$

which yields

$$\frac{di_s}{dI} = \frac{1}{1 + k_s(\partial i_w/\partial H_s)_c} \ . \tag{8}$$

Also from Eq. (6)

$$dI = di_w + \frac{di_w}{k_s(\partial i_w/\partial H_s)_c}$$

which yields

$$\frac{di_w}{dI} = \frac{k_s(\partial i_w/\partial H_s)_c}{1 + k_s(\partial i_w/\partial H_s)_c} \ . \tag{9}$$

Since $(\partial i_w/\partial H_s)_c < 0$ for a type-I superconductor,

$$\frac{di_s}{dI} > 0 \quad \text{and} \quad \frac{di_w}{dI} < 0 \ .$$

Thus, in the region beyond $I_{1c}$, $i_s$ increases and $i_w$ decreases, until for some input current $I = I_{2c}$ (second critical point), $di_s/dI$ and $di_w/dI$ become discontinuous at

$$\frac{1}{k_s} = -\left( \frac{\partial i_w}{\partial H_s} \right)_c \ . \tag{10}$$

At this "singularity point", $i_w$ decreases abruptly to zero and $i_s$ becomes equal to I.

The system behaves reversibly for $I > I_{2c}$. If I is decreased to zero, a circulating current is left in the loop formed by the branches. A fuller account of these ideas may be found in Ref. 6.

An attempt is now made to express the condition for the singularity point in terms of observables. Consider the relation

$$H_{tot}^2 = H_s^2 + H_w^2 \ , \tag{11}$$

where $H_{tot}$ is the total field at the surface of the wire. Now

$$H_w = k_w i_w \tag{12}$$

so Eq. (11) may be rewritten as

$$\frac{H_s^2}{H_{tot}^2} + \frac{i_w^2}{(H_{tot}/k_w)^2} = 1 \ . \tag{13}$$

Taking the partial derivative of Eq. (11) with respect to $H_s$ and rearranging yields the relation

$$\left( \frac{\partial H_{tot}}{\partial H_s} \right)_c = \frac{H_s}{H_{tot}} + \frac{i_w}{(H_{tot}/k_w)} k_w \left( \frac{\partial i_w}{\partial H_s} \right)_c \ .$$

Making use of Eq. (10) the following is obtained:

$$\frac{i_w}{H_{tot}/k_w} = \frac{k_s}{k_w}\frac{H_s}{H_{tot}}\left[1 - \frac{H_{tot}}{H_s}\left(\frac{\partial H_{tot}}{\partial H_s}\right)_c\right]$$

Substitution of this into Eq. (13) and multiplication by $(H_{tot}/H_s)^2$ produces

$$1 + \left(\frac{k_s}{k_w}\right)^2\left[1 - \frac{H_{tot}}{H_s}\left(\frac{\partial H_{tot}}{\partial H_s}\right)_c\right]^2 = \left(\frac{H_{tot}}{H_s}\right)^2 . \qquad (14)$$

This equation describes the point at which the coupled persistatron ceases to function as such, that is, at $I_{2c}$.

## Equilibrium State

The total magnetic field at the surface of the wire is given by

$$H_{tot}^2 = H_s^2 + H_w^2 .$$

When the system reaches the steady state, then the field at the surface of the wire might be expected to be the bulk critical field $H_c$. According to Silsbee's rule, the critical current is that current for which the total field $H_{tot}$ equals $H_c$,

$$i_c = \left(\frac{H_c^2 - H_s^2}{k_w^2}\right)^{\frac{1}{2}} . \qquad (15)$$

From the observations of Scott[17] and of Meissner and Zdanis[18], it may be conjectured that dissipation begins at a current less than critical (refer to Fig. 3). In other words,

$$i_{wc} = S_i\, i_c(H_s) \qquad (16)$$

where $i_{wc}$ is referred to as the threshold current, $S_i$ is a factor less than unity called the threshold current ratio, and $H_s$ is a longitudinally applied magnetic field.

Because of Eq. (16),

$$H_c^2 = H_s^2 + (k_w i_c)^2$$

will not accurately describe the equilibrium state of the system. Instead,

a more accurate description of the steady state of the system is

$$H_c'^2 = H_s^2 + (k_w S_i i_c)^2, \tag{17}$$

where $H_c'$ is the steady-state value of the total field at the surface of the wire and will be called the threshold field. Using Eq. (15) this becomes

$$H_c' = \left[(1 - S_i^2) H_s^2 + S_i^2 H_c^2\right]^{\frac{1}{2}} . \tag{18}$$

This says that the threshold field for a current-carrying superconducting wire is a function of the longitudinally applied field. If $S_i = 1$, that is, there is no Silsbee violation, then $H_c' = H_c$. If the field is due entirely to a transport current, $H_s = 0$, then $H_c' = S_i H_c$ which will be discussed later in Chapter IV.

Perhaps a more convenient way to express Eq. (18) is to use Eq. (7) and, recalling that $i_s = I - i_w$, make the substitution

$$H_s = k_s I (1 - i_w/I)$$

to obtain

$$H_c' = \left[(1 - S_i^2) k_s^2 I^2 (1 - i_w/I)^2 + S_i^2 H_c^2\right]^{\frac{1}{2}} . \tag{19}$$

An experimental fit to this curve $H_c'$ vs. $i_w/I$ will be a verification of Eq. (16).

## Critical Region

Behavior of the coupled persistatron which is not predicted by the preceding treatment is the following: in the range $I_{1c} < I < I_{2c}$ (I increasing), changes in the external control current I do not immediately appear as new steady-state currents $i_w$ and $i_s$. Rather, once a change in I (typically 1.0 amp) is effected, these currents take several minutes to proceed to their final steady-state values. In other words, after an increase in I, the variables have a time dependence until the steady state

is reached. This range of I will be referred to as the "critical region", and the dynamics in this region should yield some important information on the dissipation in a wire.

## Flux Penetration

As the external control current I is increased through the reversible region ($0 < I < I_{1c}$), the wire is experiencing a magnetic field which is composed of two parts. The first part is the longitudinal component $H_s$ produced by the current in the solenoid, while the second part is the azimuthal component $H_w$ produced by the current in the wire itself. However, in this reversible region the circuit is a complete superconducting loop and is thus capable of conserving flux. When the current in the wire $i_w$ reaches some threshold value $i_{wc}$, dissipation is observed to occur. This dissipation manifests itself as a current reapportionment within the device at constant I and indicates a breakdown in the conservation of flux. Once the circuit loses its ability to conserve flux, the magnetic field begins to "penetrate" the closed loop by means of the straight wire.

Note that there is some question as to the physical meaning of the term "enter" or "penetrate" when applied to a multiply-connected loop. In the case of a simple loop, such as a circle, it is easy to think of a magnetic field penetrating the circuit. Nonetheless, flux penetration will be used in reference to the coupled persistatron even though its appearance may be difficult to visualize physically. (This is not to suggest that flux penetration is not the appropriate mechanism. It can be seen that the connectivity of the coupled persistatron is no different from that of a circular loop by noting that the coupled persistatron can be gotten from the simple loop simply by bending the longer segment appropriately.) Flux penetration will refer to flux motion or dissipation in the straight wire.

The picture of a magnetic field penetrating the superconducting loop is a method of describing the fact that a breakdown in flux conservation results in a persistent current being trapped in the loop when the external control current is reduced to zero.

The current in the wire reaches its threshold value $i_{wc}$ at the first critical point $I_{1c}$. As I is increased above this value of $I_{1c}$, the circuit enters into the critical region ($I_{1c} < I < I_{2c}$). It is in this region that the time behavior of the current reapportionment is observed and a net flux enters the closed loop. The total magnetic field is a resultant of the previously mentioned components, and consequently spirals along the surface of the wire at a pitch angle defined by the components, as in Fig. 4.

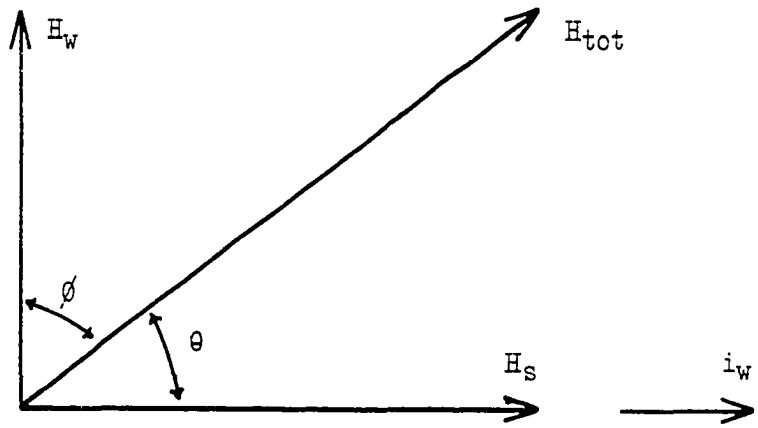


Fig. 4.--The pitch angle $\phi$ of the magnetic field.

The different portions of the critical region are defined by the ratio of the field due to the wire $H_w$ to the field due to the solenoid $H_s$. This ratio dictates the value of the field pitch angle

$$\phi = -\theta + \pi/2$$

where

$$\theta = \tan^{-1}(H_w/H_s). \tag{20}$$

Initially the field $H_{tot}$ at the surface of the wire is composed chiefly of the azimuthal field $H_w$ produced by the transport current $i_w$ in the wire. When this is the case, the pitch angle $\phi$ is small and the field spirals very "tightly" around the wire. As I approaches $I_{2c}$, the longitudinal field $H_s$ becomes the dominating component. In this latter case, the pitch angle $\phi$ is approximately $\pi/2$ and the field spirals along the wire very "loosely". A convenient way to represent the critical region is by the function

$$f(H_s, H_w) = \cos \phi = \sin \theta.$$

The behavior of this function is shown in Fig. 5. Several points are labled on the curve; for example, the steady-state values for I = 18.0 amp and I = 28.0 amp are indicated.

The portion of the critical region where $\sin \theta \approx 0.95$ is referred to as the "plateau". For the circuit used here, this condition holds true for $I \leq 19.0$ amp. However, the values I = 15.0 through 18.0 amp are chosen to be the "plateau values", because for these particular currents in the plateau region, the changes in equilibrium values of $i_w$ from one value of I to another is very small (approximately 0.5 per cent).

After an increase in I is effected and current reapportionment takes place, the system reaches a steady state. Observations indicate

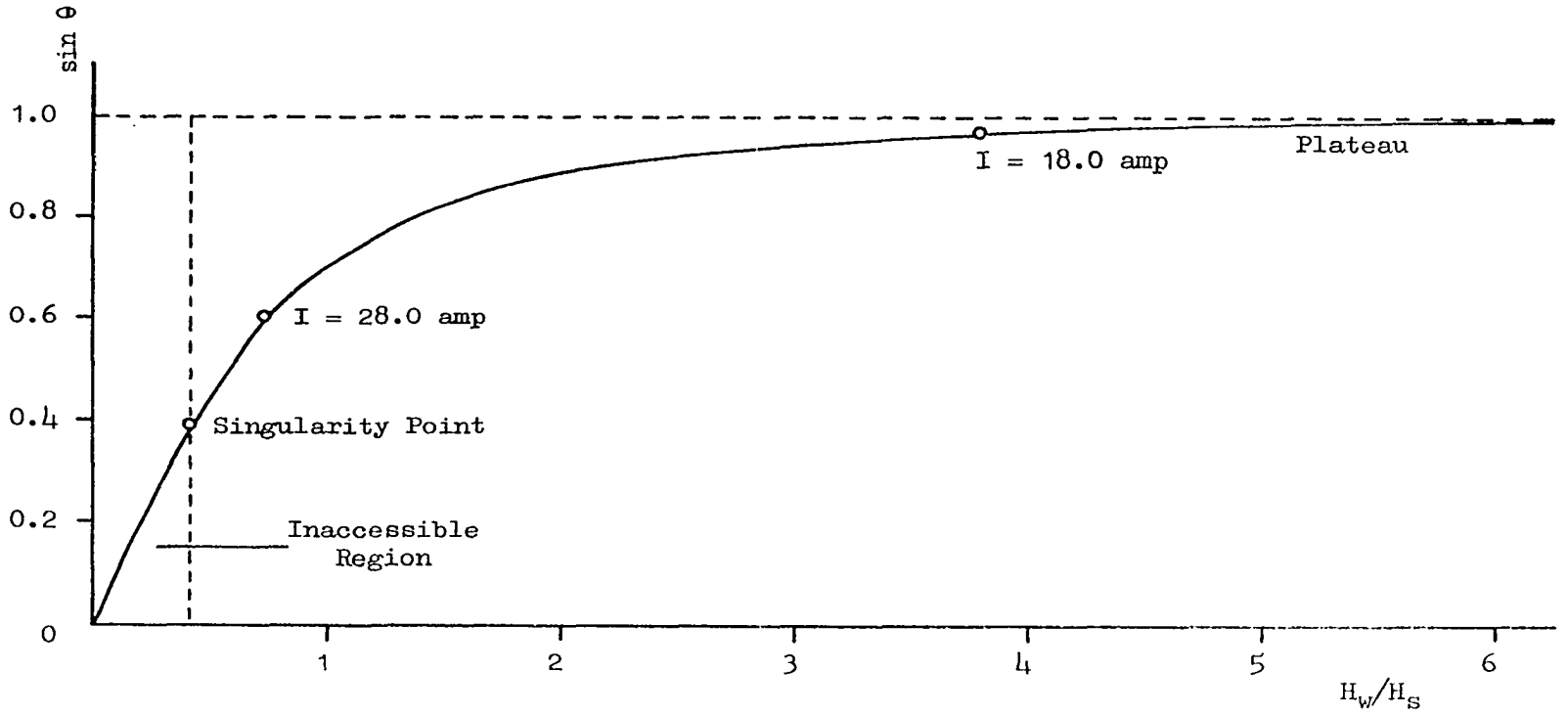


Fig. 5.--Behavior of the sin Θ function.

that this is a stable equilibrium. As the system approaches this equilibrium state, the total magnetic field at the surface of the wire is defined by

$$(H_w/H_{tot})^2 + (H_s/H_{tot})^2 = 1,$$

a simple result from magnetostatics. In a more useful form,

$$H_{tot} = I \left[k_w^2 (i_w/I)^2 + k_s^2 (1 - i_w/I)^2\right]^{\frac{1}{2}} \qquad (21)$$

where

$$H_w = k_w i_w \; ; \quad H_s = k_s i_s \; .$$

The hyperbolic curve defined by Eq. (21) allows one to look at how $H_{tot}$ varies with current apportionment. In the critical region, there is a whole family of such curves, one for each value of I. One of the curves is presented in Fig. 6. When I is increased, the system is moved to a new $H_{tot}$ curve.

Each of the $H_{tot}$ curves has a minimum defined by

$$dH_{tot}/di_w)_I = 0.$$

This leads to the condition that

$$i_w/I = k_s^2/(k_s^2 + k_w^2) \qquad (22)$$

at the minimum. This relation is identical to Eq. (14) for the case where $H_{tot} = H_c$. Note that the point at which the minimum occurs is dependent only on the physical constants of the circuit and thus occurs at the same value of $i_w/I$ for every curve. The total magnetic field at the minimum point is dependent on the value of the external control current and increases in direct proportion to I. For the circuit used in this experiment, from Eq. (22),

$$i_w/I)_{min} = 0.408,$$

and from Eq. (21),

$$H_{min} = 4.791 \; I. \qquad (23)$$

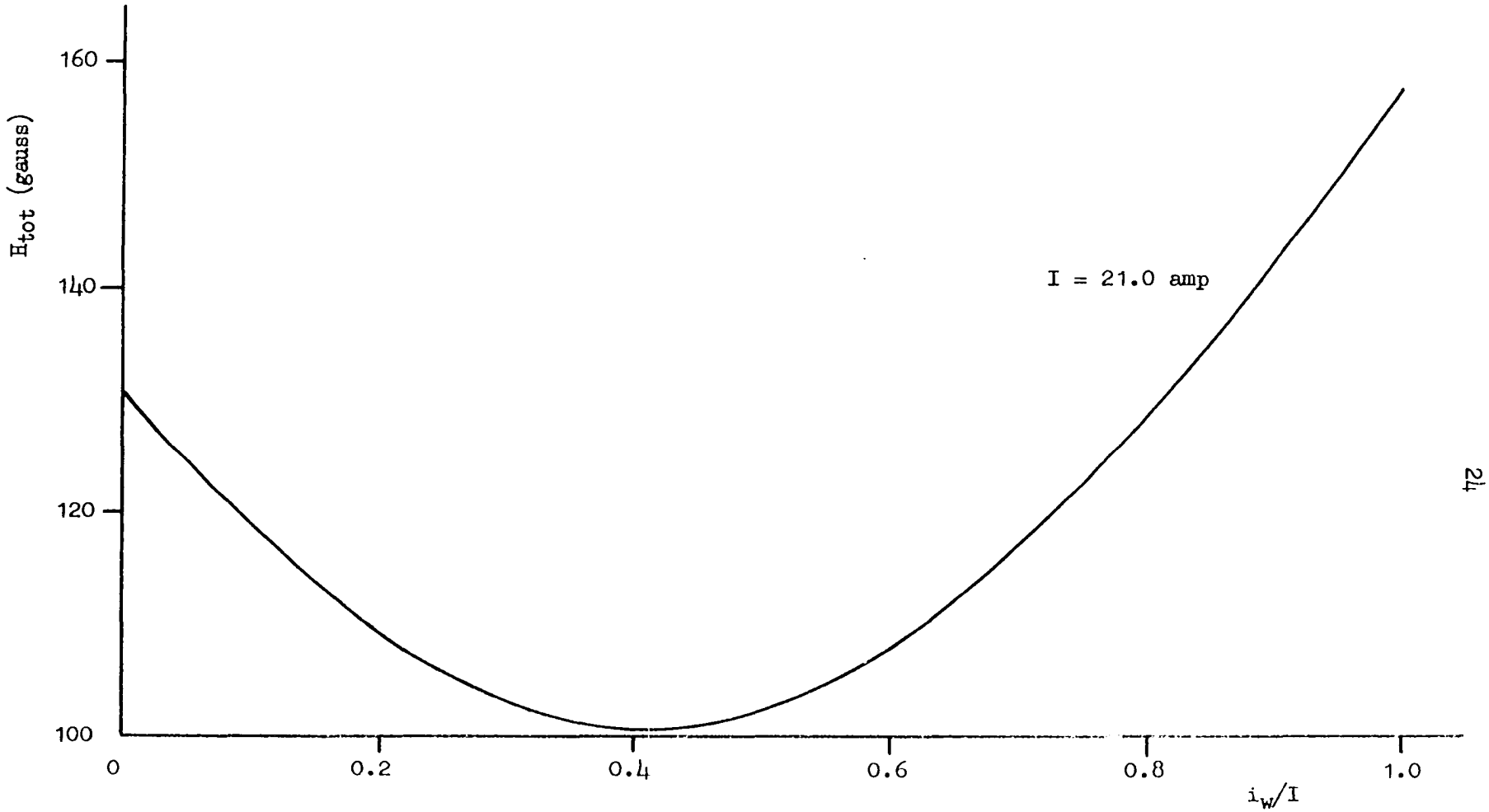


Fig. 6.--A typical total-field curve in the region over which it is mathematically defined by the circuit used in this investigation.

This minimum point turns out to be important in describing the behavior of the system. For example, one might expect that, since the magnetic field $H_{tot}$ increases with decreasing $i_w$ beyond the minimum point, the system would cease to function as a superconducting circuit beyond this point. Because of Eq. (18), the system will be able to come to equilibrium beyond this minimum point. The behavior in this region will be discussed later.

## Effective Voltage

If the input current is increased beyond the point $I = I_{1c}$, it will go into the straight wire. It always enters the straight wire initially because of lowest-energy considerations. However, when this happens, the wire is suddenly in an unstable situation. It is carrying a supercritical current $i_w > i_{wc}$ and cannot continue to do so without energy loss, that is, energy dissipation.

It is of interest how the system copes with this somewhat complex situation. When magnetic flux conservation breaks down, the straight wire gives up current in an attempt to reach a current-field apportionment for which dissipation ceases. When the wire loses current to the solenoid, the longitudinal field at the surface of the wire is increased, thus reducing the current-carrying capacity of the wire. As the wire gives up current, there is a current increase in the solenoid giving rise to a magnetic field which changes in time. This is the transient behavior of the system as equilibrium is approached at constant I.

Consider Maxwell's equation

$$\vec{\nabla} \times \vec{E} = - \partial\vec{B}/\partial t,$$

or, in integral form, Faraday's law for electromotance

$$\oint \vec{E}\cdot\vec{dl} = -\,\partial\Phi/\partial t$$

where

$$\Phi = \int \vec{B}\cdot\vec{dA}.$$

Now inductance is a quantity depending solely on the geometry of the circuit. When multiplied by the current in the circuit it gives the total flux linkage

$$\Phi = L\,i\ .$$

The electromotance equation then becomes

$$\oint \vec{E}\cdot\vec{dl} = -L(\partial i/\partial t).$$

The coupled persistatron exhibits this type of time behavior. Whenever current reapportionment occurs in the circuit, some of the current carried by the straight wire is directed into the solenoid. In other words, the percentage of total current carried by the wire is reduced. Since this reapportionment of current takes place at constant external control current I, the increase of current in the solenoid, along with the corresponding decrease in the straight wire, may be thought of as an independent current (reapportionment current i) "flowing" in the closed loop. As this current flows into the solenoid, an electromotance is produced by the changing magnetic field (or the current producing the field) in the same way an electromotance is produced in an electromagnet when the current is switched on or off,

$$E_S = L(di/dt),$$

where L is the self-inductance of the solenoid.

Kirchoff's second law says that the sum of the product of current and resistance for every conductor in a closed conducting loop is equal to the sum of the electromotance in the loop. If the product of current

and resistance is referred to as electromotance, then the sum of the electromotance in a closed conducting loop is equal to zero.

In order that the sum of electromotances around the coupled persistatron be zero, there must be a corresponding electromotance produced by the straight wire

$$E_w = i\,R\ ,$$

where R is a "resistance" giving rise to the corresponding electromotance and is associated with dissipation of energy. The equation which explains the behavior of a L-R circuit is

$$E - i\,R - L(di/dt) = 0.$$

Since there is no internal source of electromotance in the coupled persistatron,

$$i\,R + L(di/dt) = 0. \tag{24}$$

Integration of this equation

$$\int_{i_o}^{i} di/i = -(R/L)\int_{0}^{t} dt$$

yields

$$i = i_o \exp(-Rt/L).$$

Although the inductance L is referred to as being the self-inductance of the solenoid, rigorously it also contains a mutual-inductance term and should be written as

$$L = L_s - M_{ws}\ .$$

The reapportionment current i is not directly observable. It must be defined in terms of observable quantities,

$$i = i_w(t) - i_{wf}\ . \tag{25}$$

where $i_{wf}$ is the final value of the wire current that is observed. Here

i is defined in terms of the wire current, a quantity which can readily be deduced from the observables. A more straight-forward definition might be in terms of the solenoid current $i_s$. However, the magnitude of the time rate of change of these two currents are equal for constant I, and it is the wire that is of particular interest in this investigation. Though this definition may be somewhat arbitrary, it is certainly useful. The resulting exponential relation is

$$i_w(t) - i_{wf} = (i_{wo} - i_{wf}) \exp(-Rt/L) \tag{26}$$

where

$$\begin{aligned} i_{wo} &= i_w(0) \ ; \\ i_{wf} &= i_w(\infty) \end{aligned} \tag{27}$$

The logarithm of Eq. (26) yields

$$\ln \frac{i_w(t) - i_{wf}}{i_{wo} - i_{wf}} = -\frac{R}{L} t \ . \tag{28}$$

Consider two different times during the reapportionment at constant I,

$$\ln \frac{i_w(t_1) - i_{wf}}{i_{wo} - i_{wf}} = -\frac{R}{L} t_1$$

and

$$\ln \frac{i_w(t_2) - i_{wf}}{i_{wo} - i_{wf}} = -\frac{R}{L} t_2 \ .$$

Substraction of these two equations produces

$$\ln \frac{i_w(t_1) - i_{wf}}{i_w(t_2) - i_{wf}} = -\frac{R}{L}(t_1 - t_2) = \frac{R}{L}\Delta t \ .$$

From this equation, the time constant associated with the time behavior of the current reapportionment is taken to be, in general,

$$\frac{R}{L} = \sum_n \frac{1}{\Delta t} \ln \frac{i_w(t_n) - i_{wf}}{i_w(t_{n+1}) - i_{wf}} \tag{29}$$

where

$$\Delta t = t_{n+1} - t_n \ . \tag{30}$$

In principle the sum over n is from zero to infinity; however, in practice a cut-off value is chosen. Experimentally, Eq. (28) is plotted when I is changed to a new value and the linear portion of the resulting curve is used to determine the number of experimental points n to be used.

The precise physical meaning of the resistance R is not a closed question; however, the time constant R/L is taken to be a "resistance" exhibited by the straight wire to the "magnetic pressure". Therefore, R/L is a "normalized resistance"; that is, though R is dimensionally a resistance, R/L is not.

The "effective voltage" associated with the resistance R/L of the wire may be estimated by using the relation

$$V = L(\Delta i_s/\Delta t) \ . \tag{31}$$

For this investigation, the above voltage range is on the order of $2 \times 10^{-10}$ volts for the final part of a measurement to $4 \times 10^{-7}$ volts for the initial part of a measurement. This is the voltage that appears between the ends of the solenoid due to the changing current or magnetic field. In this connection, the observation might be made that the effective voltage which appears depends on the properties of the parallel inductances and not purely on the properties of the axial wire. Thus, if flux migrates into the axial wire at some given rate, the voltage is produced because of a Lenz's law reaction opposing the buildup of magnetic flux, trapped in the loop. The same rate of flux migration in a wire in a four-probe setup certainly need not produce this "back emf" and would not obviously be required to produce the same voltage.

## Perfect Diamagnetism

Consider a cylindrical superconducting wire in a longitudinal magmetic field $H_S$. In order to shield the interior of the superconductor from this field, shielding currents $i_{WS}$ are set up in such a way as to cause $B \approx 0$ inside the wire. For the longitudinal field, the currents are azimuthal.

Now suppose a transport current $i_W$ is introduced into the wire. This longitudinal current will combine with the shielding current to produce a resultant current[7] $i_{WT}$ that will follow a helical path along the wire with a pitch angle $\theta$.

The transport current gives rise to a magnetic field $H_W$ and this, combined with the longitudinally applied field, produces the resultant field $H_{tot}$[9] that is also helical. According to the Maxwell equation,

$$\vec{\nabla} \times \vec{B} = \mu_o \vec{J},$$

the resultant field is perpendicular to the resultant current as in Fig. 7.

This picture of the current is referred to as the "perfect diamagnetism" model. It assumes that the wire is in the superconducting state and remains so for all values of the magnetic field less than critical. When the wire is completely superconducting, the current is carried in a surface layer while the interior is current free. The current is free to choose the path it follows (in the surface layer) and, according to the Maxwell equation, will flow in a direction perpendicular to the field. The interior of the wire is also completely free from any magnetic field.

At the surface of the wire, there is an interaction between the magnetic field and the current,

$$\vec{dF} = i \vec{dl} \times \vec{B}.$$

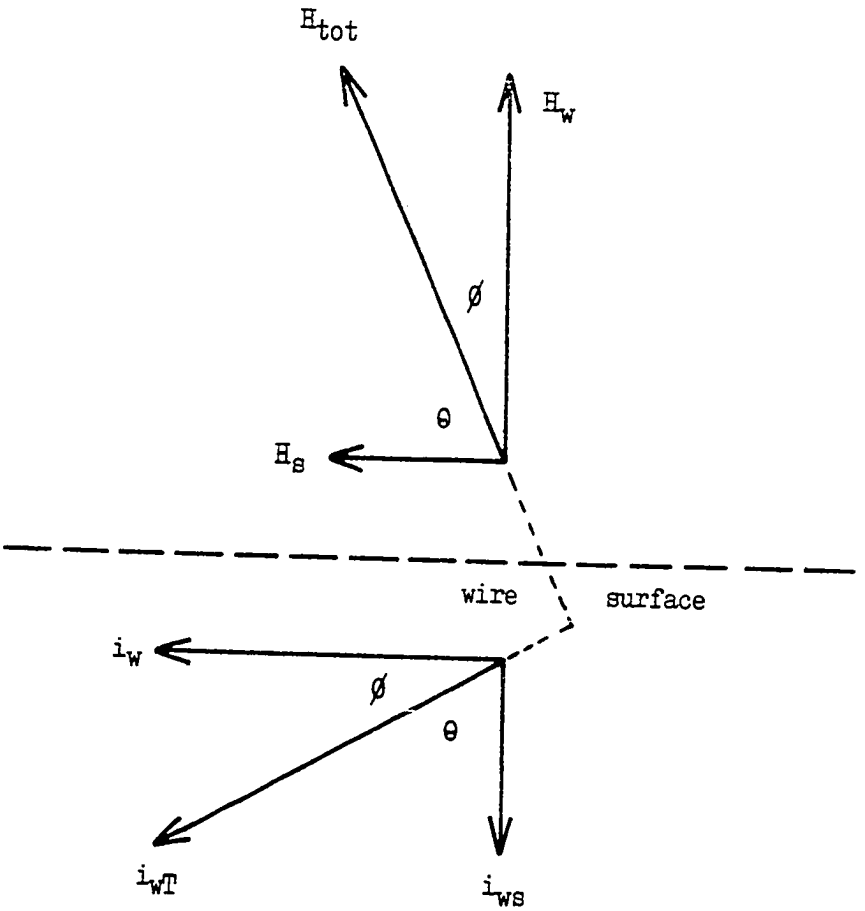


Fig. 7.--The resultant field and current.

This is referred to as the Lorentz force and can be expressed in the following way:

$$F = i\, l\, B \sin\alpha \tag{32}$$

where F is in newtons, B in webers/meter$^2$, l in meters, and i in amperes. To be consistent with the convention used in this paper, a unit change is made by using

$$\text{weber/meter}^2 = 10^{-4} \text{ gauss.}$$

Thus

$$F = i\, l\, B \sin\alpha \times 10^{-4}$$

or

$$F_L = i\, B \sin\alpha$$

is the normalized Lorentz force per unit length. The units associated with $F_L$ are $10^4$ newtons/meter where i is in amperes and B in gauss. For the particular case studied here

$$F_L = i_{wT}\, H_{tot} \sin(\pi/2) = i_{wT}\, H_{tot}.$$

However,

$$i_{wT} = i_w/\sin\theta \tag{33}$$

so that

$$F_L = i_w\, H_{tot}/\sin\theta \tag{34}$$

where

$$\theta = \tan^{-1}(H_w/H_s).$$

Note that the direction of this force is into the wire; thus it has a tendency to cause the field to penetrate the wire, producing dissipation.

The "Lorentz force" introduced here is better called the "magnetic pressure". The Lorentz force is usually calculated for some specific entity. For the case considered here, it is better to talk of force/area or magnetic pressure; however, both terms will be used.

# CHAPTER III

# EXPERIMENTAL TECHNIQUE

## Circuit Design

The first step in preparing this experiment is to design a practical circuit utilizing the principle of the coupled persistatron. The circuit should be designed as a single or self-contained unit so that it may be removed from the cryostat without disturbing the superconducting joints. The solenoid should be one of practical size and should yield an uniform field over a given length. The straight wire should be mounted securely in the solenoid so that the magnetic field it experiences is reproducible.

The superconducting wire used to make the solenoid is one that will remain in the superconducting state throughout the experiment. This means that it is able to carry thirty to fifty amperes without approaching its critical current. The wire that was initially used in this experiment was Ersin Multicore solder consisting of 60 per cent tin and approximately 40 per cent lead. Its diameter was 1.2 mm. Because of its inhomogeneity, this commercial solder wire was abandoned. It was replaced by solid Pb-Sn wire of the same composition and 1.02 mm diameter.

The Pb-Sn wire is made by melting solder and removing the resin flux. The molten solder is slowly poured into cold water, thus forming pellets. These pellets are then melted, heated to about 230°C, agitated

for approximately thirty minutes, and allowed to solidify in a one-half inch tube at room temperature. This slug is forced through a 1 mm steel die with high pressure at room temperature to form the wire. However, the pressure required (over 30 tons on a 3.5 inch ram) is at the limit of the available equipment. Consequently, pure lead (Pb) wire, being softer, came to be used in this experiment. This lead wire still has a high critical current and can be made using the procedure just described. It has a diameter approximately equal to 1.0 mm.

The width of the critical region of the coupled persistatron is determined by the coil constant and the radius of the center wire. If the radius of the wire is fixed, the coil constant (or turn density) is chosen to make the width of the critical region reasonably large. To do this, the following assumption is made: the total field at the surface of the wire when the system ceases to function as a coupled persistatron is the bulk critical field for the material used as the straight wire,

$$H_{tot} = H_c = \text{constant.}$$

Using this assumption, Eq. (14) becomes

$$\left( \frac{k_s}{k_w} \right)^2 + 1 = \left( \frac{H_c}{H_s} \right)^2 \quad . \tag{35}$$

The point described by Eq. (35) is near but not at the singularity point. However, Eq. (35) makes it possible to choose the approximate extent of the critical region,

$$I_{1c} \leq I \leq I_{2c} \ ,$$

by adjusting the parameters $k_s$ and $k_w$.

This point is arbitrarily chosen so that

$$H_s = 0.8 \ H_c \ .$$

This choice allows data to be taken over the major portion of the region

(or current-field range) covered by the I-H curve (as determined using Silsbee's rule). Consequently, the coil constant for a given radius of the wire is given by

$$k_S = \frac{3}{20\ r} . \tag{36}$$

As a first approximation, the turn density is assumed to be that for an infinite solenoid

$$n = \frac{5k_S}{2\pi} = \frac{3}{8\pi\ r} .$$

A wire of radius approximately 0.25 mm is chosen, which dictates that

$$n \approx 5 \text{ turns/cm.}$$

Since n is the physical parameter most easily adjusted, the infinite solenoid approximation has been used to get a value for the turn density. Using this approximate turn density, the coil constant is now obtained from the finite solenoid equation

$$k_S = \frac{n\pi\, l/5}{\left[(1/2)^2 + r^2\right]^{\frac{1}{2}}} , \tag{37}$$

where l is the length of the coil and r is the radius. The resulting coil constant is

$$k_S = 6.22 \text{ gauss/amp.}$$

The singularity point is the point beyond which the system cannot come to equilibrium; that is, it is the second critical point of the circuit. This point is estimated by Eq. (35). For the constants of the circuit used in this experiment,

$$k_W = 7.505 \text{ gauss/amp}$$

$$k_S = 6.226 \text{ gauss/amp,}$$

this equation yields

$$H_s = 0.77\ H_c$$

at the singularity point. If the critical magnetic field is taken to be

$$H_c(2^\circ K) = 180 \text{ gauss},$$

then

$$H_s = 138.6 \text{ gauss}$$

when the system becomes unstable and all of the current leaves the wire.

The uniformity of the magnetic field produced by the solenoid can be found making use of the equation

$$H = (n\pi i/5)(\cos\theta_1 + \cos\theta_2) \qquad (38)$$

$$= K(\cos\theta_1 + \cos\theta_2).$$

The angles $\theta_1$ and $\theta_2$ are defined in Fig. 8. For the center of the solenoid $\theta_1 = \theta_2$ and

$$H = 1.980\ K.$$

For a point on the axis 1.5 cm from the center

$$H = 1.973\ K.$$

This value is 99.6 per cent of the value at the center. Therefore, over a length of 3 cm in the center of the solenoid, there is a field variation of approximately 0.4 per cent.

After the solenoid is constructed, the indium wire must be mounted inside of it to form a complete superconducting loop. The wire is first mounted securely on a phenolic form or sample holder. This holder is made by cutting a solid phenolic rod (11.5 cm in length) along its diameter. The resulting surface is then polished smooth. For the first holder used, two grooves about 4 cm long, 0.08 cm deep, and 0.16 cm wide were cut in each end. Superconducting leads of the same wire used to make the solenoid were placed in these grooves. This left a flat area 3 cm long in the center of the holder on which the indium wire was mounted. The wire position

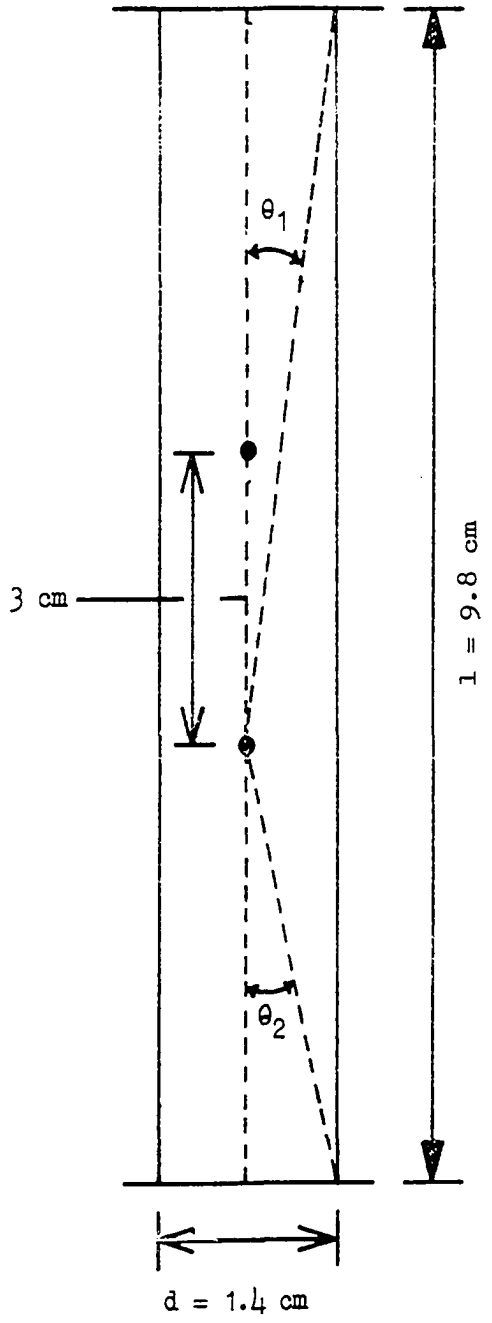


Fig. 8.--Variables used to calculate the field inside the solenoid.

on a flat, smooth surface allows the liquid helium to better surround the wire and thus cool it effectively.

It was discovered in the course of experimentation that the indium wire would not remain straight while resting on the flat surface. The cooling and warming process caused the wire to bend so that it was no longer longitudinal with the magnetic field of the solenoid. This was corrected by cutting a groove for the wire in the phenolic holder 0.30 mm deep and 0.50 mm wide and putting epoxy near the junctions and at each end. The epoxy mechanically isolates the wire and prevents it from being bent during construction of the circuit. However, a mistake in design occurred at this point in that this groove was on the axis with the larger grooves. This made it necessary to bend the wire to make the junction between the leads and the indium, creating two places on the sample that were not longitudinal. This problem was solved by cutting grooves for the lead-in wires off of the axis as shown in Fig. 9.

This phenolic holder with the sample mounted on it is inserted into the phenolic tube (1.3 cm o.d., 1.1 cm i.d.) on which the solenoid is wound. The two branches are soldered together on a copper mount at either end of the coil form, thus making a closed superconducting circuit similar to the one used in the earlier coupled persistatron.[28] The physical circuit for the coupled persistatron is presented in Fig. 10.

## Sample Preparation

After the construction of the first circuit, a process of trial and error took place to determine a method for producing an indium sample in the form of a wire most suitable for the studies involved in this experiment. The bending of the indium wire on the flat surface nullified

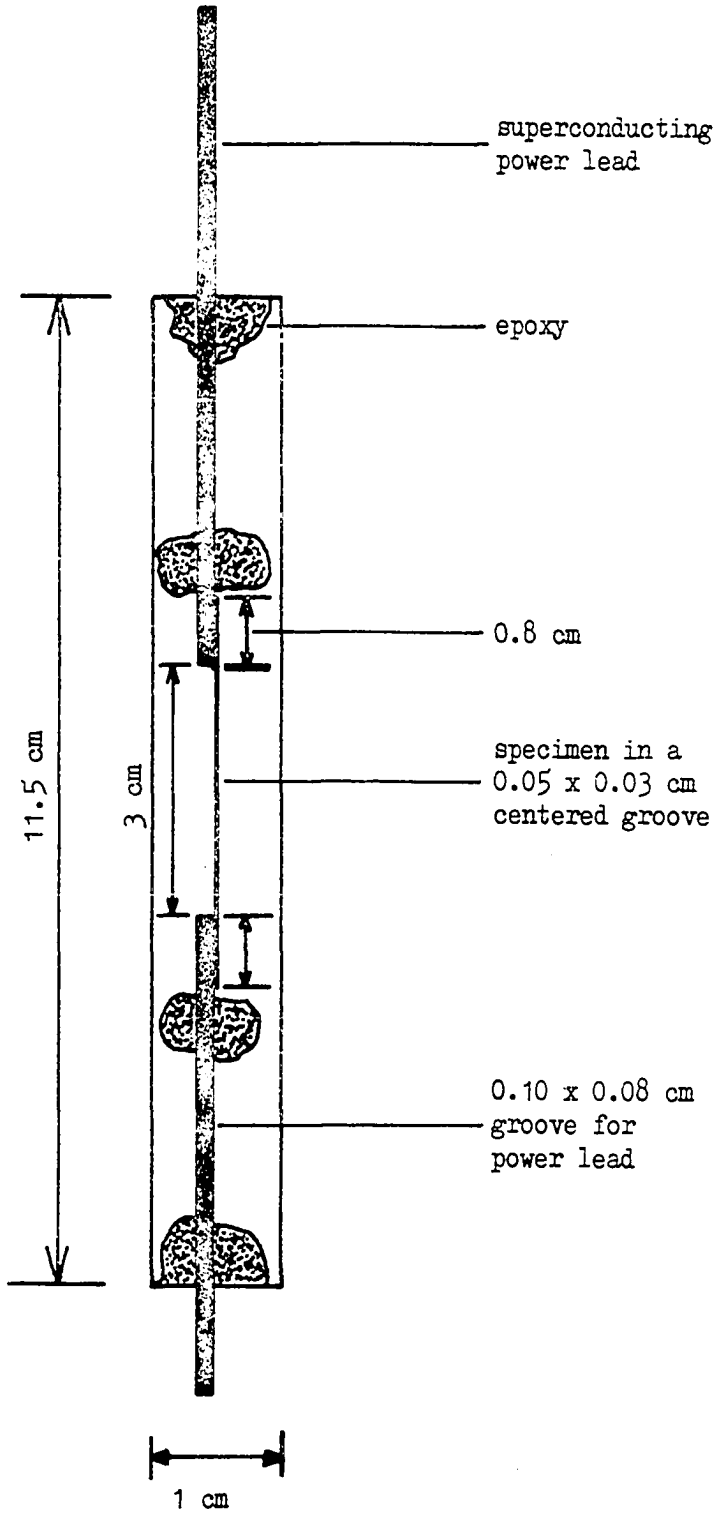


Fig. 9.--The phenolic holder for the low inductance branch of the coupled persistatron.

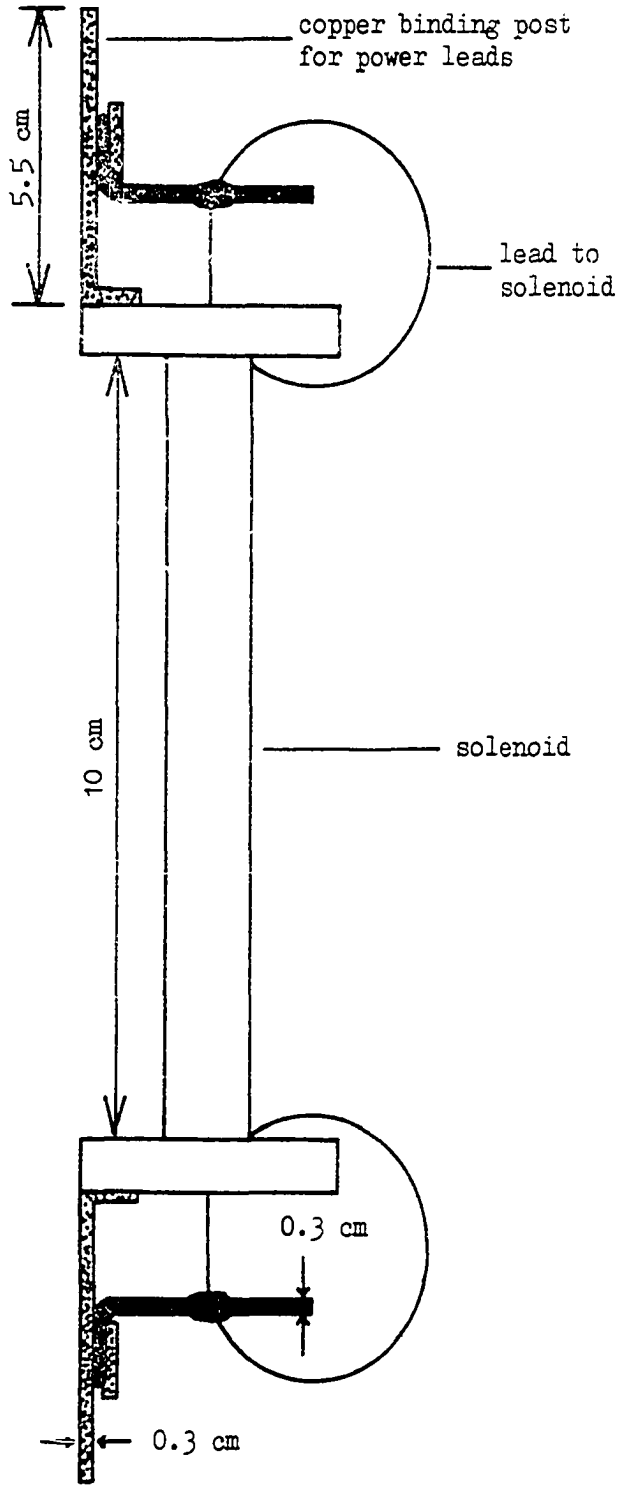


Fig. 10.--The physical circuit used in the experiment.

the first few experiments. The grooved holder was then used. The experiments that followed this were not reproducible. There were many variations in the time curves. The wire would appear to "superheat" taking all of the increase in the external control current at times. Abrupt changes in the slope of a curve were also observed. This "trouble" was blamed on the wire used in the coil, so pure lead (Pb) was used as well as a Pb-Sn alloy. Changes made in the coil had no effect on the behavior, so the wire sample itself was examined.

The 3 cm sample was replaced by a long sample running the entire length of the coil similar to the one used in the experiments on tin.[28] The same coil design was used with this 12 cm sample as with the 3 cm sample. However, with the 12 cm sample a groove 0.8 mm deep and 0.8 mm wide was cut in the phenolic form from one end to the other. This ensured that the long wire remained longitudinal to the magnetic field for the entire length of the solenoid. Use of this long wire eliminated the joints inside the solenoid.

Several experiments with this design revealed that the curve characteristics are functions of the amount of annealing the indium wire has undergone. The wires were cold rolled; that is, to help straighten them for experimentation, they were rolled between two flat surfaces at room temperature. Their time curves, which were then measured several times, indicated a marked difference in their behavior.

The best way to check the effect of annealing consists of starting with a wire that has not been annealed at all and taking measurements as it anneals. Here annealing refers to allowing the wire to remain undisturbed (usually at a temperature approximately two-thirds of the melting

point) for long periods of time. The specific metallurgical processes taking place during such a procedure have been previously discussed. The indium wire that was first used was a commercial wire (ESPI, 0.5 mm, 5-9 purity), the age of which was unknown. Therefore, it was necessary to make new wire using the extrusion process.

Indium shot (Cominco American Inc., 6-9 purity) is melted and cast into a slug 0.7 cm in diameter. This is then placed in a steel cylinder, and by means of a piston, extruded at room temperature through a 0.5 mm steel die under high pressure. Care must be taken to apply the pressure at a constant rate to ensure uniformity in the diameter of the wire.

The exact diameter of the wire is determined by using a microscope with a flier eyepiece. The eyepiece has a calibration of 0.0827 mm/rev. The diameter is measured several times at one spot on the wire. This is done for nine different spots along the length of the wire. The readings at one spot are averaged to minimize the reading error (to approximately $\pm$0.003 mm). The values thus obtained from each set are then averaged to give the mean diameter of the wire.

The extruded wires have longitudinal grooves or scratches on their surfaces because of the irregularity of the steel die. These grooves can be removed by etching with a 70 per cent solution of nitric acid. However, etching had no noticeable effect on the behavior of the wires. Consequently, the effect that the grooves may have is ignored and, generally, the samples are not etched after extrusion.

## Experimental Design

The experimental design used in these experiments with indium is basically the same as the one used in the experiments on tin.[28] However,

a few alterations were necessary because of the longer time required to run the indium experiments--four to six hours. This requires much more liquid helium (approximately 10 liters). In order to get this much helium in the dewar, it is necessary to provide additional ventilation. This is done by drilling a one-half inch hole in the top of the cryostat that can be closed during the experiment, by shortening the effective length of the transfer tube, and by placing baffles at intervals all the way to the top of the vacuum jacket on the helium dewar. Without these modifications, the pressure built up during the transfer of liquid heilum is too great to collect ten liters, and the boil-off is to great to sustain a run for a long enough time. If the transfer tube is too long, the superfluid helium will flow up the tube until it reaches a place hot enough to vaporize it. The resulting vapors are forced back down the tube into the liquid helium bath.

The completed circuit is mounted at the bottom of the cryostat by means of brass clamps and the power leads connected, as in Fig. 11. These power leads must be small enough to minimize the helium boil-off due to heat flowing into the bath through the wires (conduction heat leak), but large enough to minimize boil-off due to Joule heating of the wires. Sharp bends in the power leads should also be avoided.

Knowing the average current load of the circuit the optimum cross-sectional area of the electrical leads can be calculated.[29] Consider a conductor of cross-sectional area A and length l, running directly from the room temperature part of the cryostat down into liquid helium. The amount of heat conducted per second into the dewar by the wire may be written

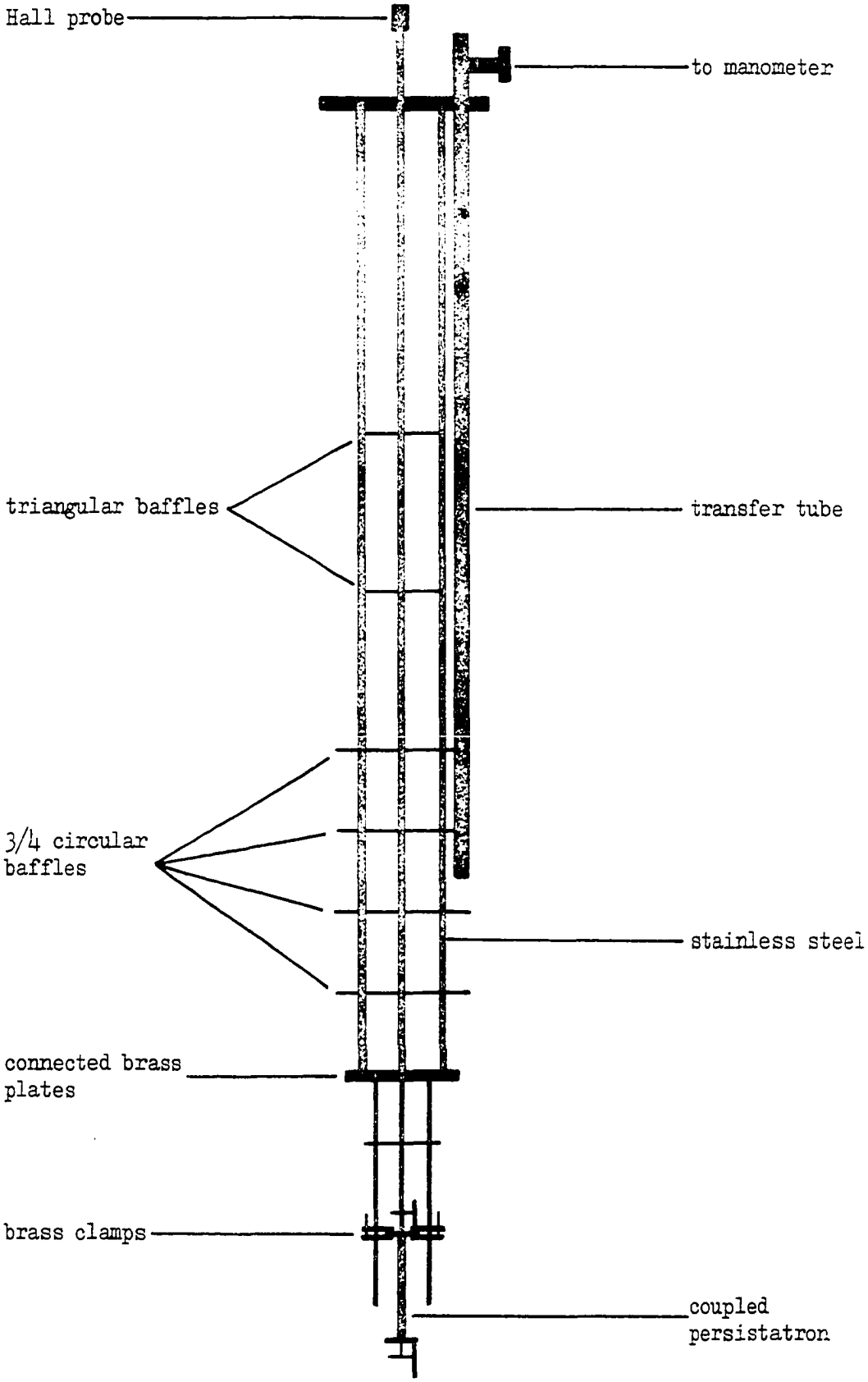


Fig. 11.--Cryostat used in this investigation.

$$Q_c = K A ,$$

where K is a constant which includes the average thermal conductivity of the metal. It can be shown that the optimum cross-section is given by

$$A_{opt} = I^2 R/K ,$$

where R is the total electrical resistance of the conductor and I is the current to be carried. It has been found by experiment that, for a copper conductor 70 cm long, the heat conducted per square centimeter of cross-sectional area is enough to evaporate 5.2 liters of liquid helium per hour.[30] The electrical conductance of copper is found to be about $2.4 \times 10^4$ mho $cm^{-2}$. Substitution of these values into the above equation yields

$$r_{opt}^2 = (4I/\pi) \times 10^{-4} \text{ cm}^2 . \qquad (39)$$

It turns out that the average current load for this investigation can be as high as 30 amperes. Since the time curves measured are longer for large currents (28 to 30 amp), the electrical leads are selected to produce the least heat leak at these currents. Also, the heat leak due to conduction at the lower currents is much less than that due to Joule heating at the higher currents (by observation). Therefore, for a current load of 30 amp the optimum radius is

$$r_{opt} = 0.62 \text{ mm.}$$

When the sample holder is mounted in the coil form, half of the tube is left vacant. It is into this vacancy that a Hall probe (see item #6 of the equipment list in Appendix B) is placed. This probe monitors the magnetic field $H_s$ of the solenoid as a function of time and external control current I. The geometry of the probe is such that it is insensitive to the azimuthal field $H_w$ produced by the straight wire; therefore, the field it measures is stricktly the longitudinal component,

produced by the coil, of the total magnetic field. Control of the Hall probe is done by a current of 35 milliamp supplied by a D. C. regulated power supply (item #11). The resulting Hall voltage $V_H$ is directed through a nulling circuit[28] which is controlled by another D. C. power supply (item #10).

A signal from this Hall probe nulling circuit is monitored by a voltmeter (item #3). The chart recorder is operated through the voltmeter on a 1 volt, 1 milliamp signal, that is, 1 volt from a special output of the voltmeter corresponds to a full scale deflection. There is a potential divider between the voltmeter and the chart recorder. This is used to calibrate the chart recorder, insuring that a full scale deflection on the voltmeter corresponds to a full scale deflection on the recorder. Six inch wide chart paper is used in the recorder and is divided into 10 major divisions and 50 minor divisions. Divisions on the chart paper along the time axis are spaced 0.25 inch apart.

The nulling circuit allows the voltmeter and recorder to be set at any given reference; that is, a back emf can be supplied to cancel a signal entering the circuit. This allows differences in the Hall probe reading to be measured rather than absolute values. Consequently, all of the data can be taken on the same scale, greatly increasing the sensitivity of the readings.

External control current to the coupled persistatron is supplied through a 10 gauge solid strand cable by a regulated D. C. power supply (item #8) capable of supplying 45 amperes at 20 volts (maximum current of 50 amp). The power supply is operated in the constant current mode, and this current is monitored by an ammeter (item #2) whose scale is divided

into one-half ampere intervals. A scale with divisions of 0.1 ampere can be used, if needed for smaller control currents. Since the scale cannot be changed during the course of an experiment, a scale must be selected that will allow all possible values of the external control current to be read.

The above mentioned equipment is mounted on an instrument cart that is mobile. Included on the cart is also the nulling circuit, a digital voltmeter, an extra power supply, a null detector, a 0 to 15 amp D. C. ammeter, 0 to 50 ma D. C. milliammeter, and several electronic components.

The experimental design is shown schematically in Fig. 12.

## Experimental Procedure

After the cryostat, with the circuit mounted in it, is placed in the dewar and liquid helium transferred in, the system is pumped down to the desired temperature (usually 2°K for this experiment) using a large mechanical pump (item #15 in Appendix B). The extra large mechanical pump is needed here since the four-inch helium dewar itself is used as the evaporation refrigerator. A better method would be to use a small metal inner dewar in which the experiment is conducted. The glass helium dewar would be used as a heat shield and a liquid helium reservior. With this system a much smaller mechanical pump could be used to maintain the low temperatures desired. The only disadvantage being the requirement of a diffusion pump system to evacuate the vacuum jacket on the inner refrigerator.

A steady rate slow enough to take advantage of the cooling capacity of the helium vapors is used to reduce the pressure. At first, the pumping line is not opened completely; however, once the lambda point is reached the two-inch line is opened completely until the desired temperature is approached. The large pumping line is then closed. A parallel

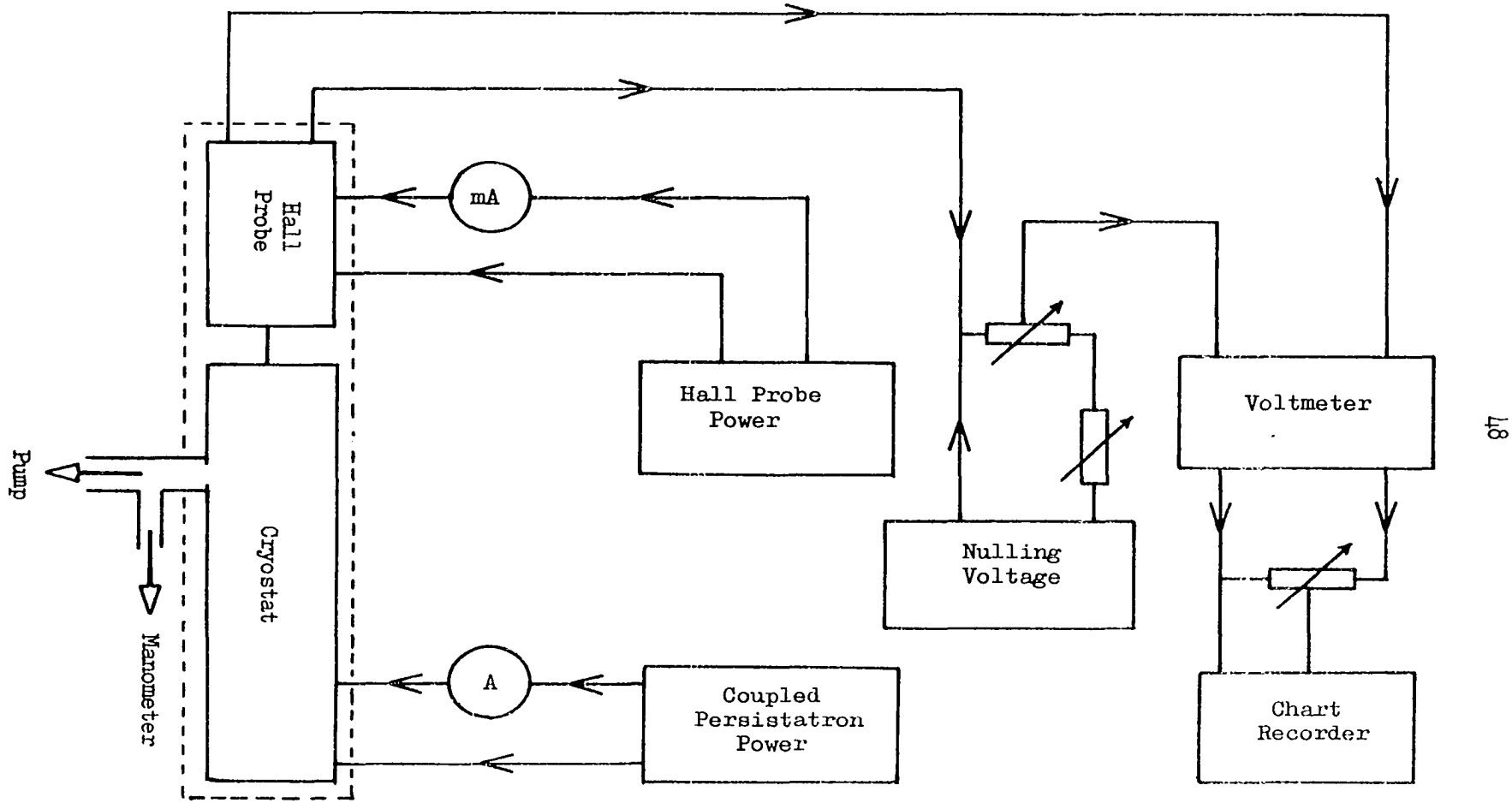


Fig. 12.--Schematic of the experimental arrangement.

valve system consisting of a one-half inch valve and a one-eighth inch valve controls the pressure, and thus the temperature. Pressure fluctuations due to current input, etc., are compensated for with the one-eighth inch valve, while the one-half inch valve is set for the desired pumping rate.

The pressure is monitored by a mercury manometer with which the temperature can be held within 1.5 millidegrees. As the helium level drops the pumping rate must be reduced because there are more baffles above the bath, there is less of the power line in the bath, and the volume of the bath is smaller so the amount of helium that has to be evaporated to maintain the temperature is less.

Once the temperature has been reached and stabilized, current is fed into the coupled persistatron. This external current I is increased in two-ampere intervals until the first critical point $I_{1c}$ of the circuit is approached. Then the current is carefully increased until the indium wire begins to lose current to the solenoid. The circuit is then allowed to come to equilibrium. This initial increase in Hall voltage $V_H$ is recorded and nulled out.

A chart speed is selected which will give a sufficient number of data points to present a clear picture of the time curves. (The speeds available are 0.75, 1.5, 3, 6, and 12 inches/minute or inches/hour.) The external control current I is suddenly increased by one ampere, for the first time curve. An increase in the magnetic field $H_S$ of the solenoid is observed as the current reapportionment within the circuit begins to take place. With I held constant, the change in $H_S$ is recorded as a function of time. The circuit is allowed to reach a new equilibrium. This

increase in Hall voltage $V_H$ is again nulled, and another increase in I is effected. This process is repeated until the helium supply is exhausted or the critical region is traversed and the second critical point $I_{2c}$ reached.

If the second critical point $I_{2c}$ is reached before 50 per cent of the helium supply is exhausted, the entire process is carefully repeated. When the external control current I is reduced to zero, a certain amount of persistent current remains in the circuit. This persistent current is removed by reversing the polarity of the power input and supplying a sufficient amount of current to cancel the current left in the circuit. During this process, the nulling circuit is switched out and the system is returned to the original residual Hall voltage, indicating an absense of magnetic field.

The data points are read from the chart at the given time intervals with a steel rule marked off in divisions corresponding to 0.01 inch. Across the chart the divisions are 3/32 inches wide and on the 1 mv scale this corresponds to 0.02 mv. An approximate reading A is taken by reading the division on the chart which the curve has just crossed. The distance from this mark to the curve is measured in inches and converted to mv by use of the relation

$$x = 0.2133\ f\ , \tag{40}$$

where f is the distance from the nearest mark (not exceeding) to the curve in inches and x is the correction to the approximate chart reading in mv. The actual chart reading used in computations is given by

$$x + A = CR\ . \tag{41}$$

This chart reading represents the amount of increase in the Hall voltage over the reference value. The initial values of the Hall voltage for each

value of external current I must be determined. This is done by keeping a running sum of the changes in the Hall voltage for each current change.

When the chart speed is slow (greater than or equal to ten seconds per interval) the increase in external current can be made on one of the chart time intervals. However, at faster speeds this cannot be done precisely and a correction must be made so that the data points can be taken at the time intervals as marked on the chart. Along the length of the chart, each division is 1/4 inch wide and corresponds to a given time interval; for example, five seconds when the chart speed is three inches per minute. The conversion is

$$t_i = 20\ s\ , \tag{42}$$

where s is the distance in inches from the first mark after the increase in external current I to where the curve starts and $t_i$ is the correction to the time in seconds. In other words, the first data point is taken $t_i$ seconds after the curve starts and every $\Delta t$ (say five) seconds thereafter.

# CHAPTER IV

## RESULTS AND DISCUSSION

Here again the objectives of this investigation are stated. The dissipation of energy in a current-carrying superconducting wire is to be studied here experimentally. In studying dissipation, the first thing one might want to do is to determine the point at which dissipation can first be observed. This point is usually taken to be the critical current. This should be checked. Once dissipation begins in the wire, the next item of interest is the behavior of the wire when the point of initial dissipation is exceeded, assuming the wire is able to change its current load as is the case for the coupled persistatron. Knowing that equilibrium states exist for the coupled persistatron for which there is no dissipation observed, the properties of such a steady state should be of interest.

### Preliminary Tests

The purpose of the preliminary tests is to determine whether or not the onset of dissipation in fact occurs at the critical current as defined by Silsbee's hypothesis from the bulk critical field $H_c$. Two techniques are used. The first is the traditional four-probe technique, and the second is the coupled persistatron technique.

## Current-Characteristic Curves

The first of these tests involves the determination of the threshold field curve (I-H curve). In this case, the critical current of the wire is measured as a function of an externally applied longitudinal magnetic field. This also gives a value for the critical magnetic field in the longitudinal direction as the current in the wire approaches zero.

It is assumed that the polycrystalline nature of the indium wire and the individual "defects" introduced during extrusion (including impurities) do not alter, to any great extent, the superconducting properties of the different specimens used in the experiment. This is to say that such properties as the critical field, critical current, and critical temperature are not altered by the particular procedure used in sample preparation. Therefore, one sample may be chosen to be representative of all the samples as far as the I-H characteristics are concerned. Based on this assumption, one wire was constructed and the results for this one are taken to be valid for all wire made from the same indium shots, using the same extrusion method, and run at the same temperature (for example, $T = 2^{o}K$).

The method used to determine the critical current is the conventional four-probe technique[31]. This method consists of attaching four conducting leads to the sample. Two of the leads are used to introduce a transport current into the specimen, and the other two leads are used to detect the potential which may be produced by the transport current. The experimental arrangement is identical to that of the coupled persistatron except that the solenoid and straight wire branches are not connected but are operated separately, each with its own power supply.

The sample holder is the same as the one previously described; however, on this holder provisions are made for potential leads (B&S 36 gauge copper wire) to be connected to the specimen. Nicholson[36] found that reproducible results could best be obtained when pressure contacts were used to connect the potential leads to the specimen. This is done by means of copper bars pressed across the sample and the copper leads simultaneously. Pressure contacts are used to avoid soldering or welding techniques which are not judged to be reproducible and are possibly damaging to the wire. The copper bars are placed between the junctions connecting the indium wire and the lead (Pb) current leads. The copper leads are connected to a low thermal coaxial cable which leads to the instrument cart.

The procedure used is to apply a specific external magnetic field parallel to the indium wire using the solenoid, then to increase the current it is carrying until an arbitrarily selected potential drop is observed along the length of the wire. This potential drop or voltage is recorded by a sensitive voltmeter (item #14 in the equipment list of Appendix A).

Ideally the critical current at a given applied magnetic field is that current which first produces a voltage along the length of the wire. Therefore, the reference voltage chosen should be vanishingly small. The particular value used depends on the limitations of the equipment or experimental arrangement. Various values have been chosen by different researchers doing this type of measurement. Levy and Meincke[31] defined the critical current as the current at which the voltage decreased to the noise level of 0.003 $\mu$V. Winter, et al.[32], took it to be the current at

which a voltage of 0.01 $\mu$V first appears. Still others (Swartz and Hart[33]) defined the critical transport current as that current producing a voltage drop of 1.4 $\mu$V/cm.

The critical current for this test is taken to be that which produces a voltage drop of 0.1 $\mu$V along the wire. This value is selected because it is the first value which can be clearly distinguished above the noise. The field is increased in regular increments and the critical current measured at each point, then the field is decreased in the same increments and the critical current remeasured. Fig. 13 shows the results of such measurements. (Data for this graph are given in Table 1 of Appendix B.) These data were taken at 2°K using a wire of diameter 0.555 mm after it had been annealed at 100°C for ten days. The same measurements were made on the wire before it was annealed, but since no noticeable differences were observed between the two sets of data only the results for the annealed wire are presented. (A more complete set of data was taken for the annealed wire.)

Notice that the critical field was measured to be

$$H_c = 163.43 \text{ gauss.}$$

This is less than may be expected. The value interpolated for indium at 2°K from tables published by Shaw, et al.[35] is

$$H_c = 180.03 \text{ gauss.}$$

The four-probe experiment done here then yields a critical field value of about 90 per cent of this expected value. The four-probe technique was only used on one wire; the copper bars pressed into the wire, possibly damaging it; and the junctions might have been weak. For these reasons, the value for $H_c$ as obtained with this method, being 90 per cent of the

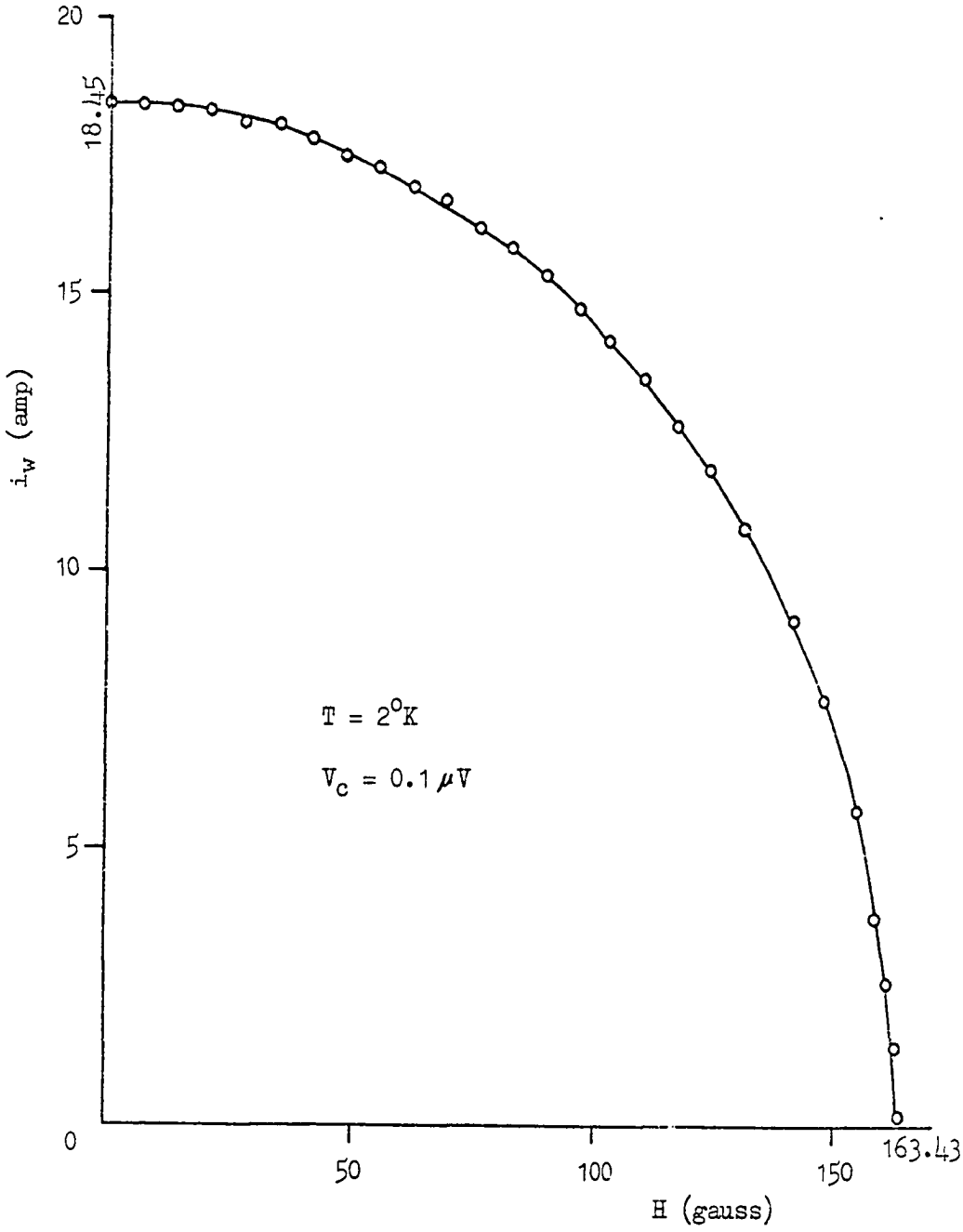


Fig. 13.--Threshold field curve obtained using the four-probe technique.

value found by Shaw, et al.[35], is considered very good. It is not the purpose of this part of the investigation to obtain an accurate value for the critical field. The purpose of this section is determine whether or not a voltage can be detected for a current below the value predicted by Silsbee's hypothesis. Consequently, the value of 180 gauss will be used in the calculations done in this work. (Further justification for this will be given later.)

The purpose of this section, to consider the critical current, is accomplished in part by noting that the critical current is not that obtained by Silsbee's rule

$$i_c = (5d/2)\, H_c = 22.7 \text{ amp},$$

but is instead

$$i_c = 18.45 \text{ amp}.$$

To illustrate the "dependence" of the critical current on the reference voltage chosen, the above measurements were repeated using 1 $\mu$V as the reference voltage. For this case the critical magnetic field remains relatively unchanged but the critical current is

$$i_c = 21.2 \text{ amp},$$

which is closer to the value predicted by Silsbee's rule, suggesting more uncertainty in determining $i_c$ than the longitudinal $H_c$.

The dependence of the critical current on the reference voltage indicates that the resistance transition from the superconducting to the normal state is wider when it is induced by current than it is when induced by a longitudinal magnetic field. This is an expected result. A transport current restores only part (60 to 75 per cent) of the normal state resistance to the wire at the critical current; thus, the wire passes

into an intermediate state (cf. Fig.3). Consequently, the resistance observed in zero field due entirely to a transport current could be an intermediate state resistance, which is sensitive to the reference voltage chosen. Because of the vanishingly small demagnetization coefficient of the straight wire, a longitudinal magnetic field will not produce an intermediate state between the normal and superconducting states. As a result, the resistance restored due to a longitudinal field rises rapidly to the normal resistance when a current is applied. This rapid rise makes the critical field less sensitive to the reference voltage.

Besides measuring the critical current as a function of magnetic field, the traditional four-probe technique is also used for resistance transition experiments[18]. These experiments study the sudden reappearance of electrical resistance as the current is increased in a superconductor by measuring the voltage produced along the length of the wire for a given current. The results are usually displayed by plotting the resistance ratio, $R/R_n$ ($R_n$ being the value of the resistance measured just above the normal transition temperature, or measured in an externally applied magnetic field of greater than critical intensity) as a function of current or current ratio, $i/i_c$.

Similar measurements are made in connection with this experiment. They consist of recording the current required to produce a given range of voltage drops for a particular applied magnetic field. This is only different from the I-H measurements in that, in practice, the current is treated as the independent variable and the voltages produced by a given current range are measured.

Typical results for this test are shown in Fig. 14. (The set of data for this graph is presented in Table 2 of Appendix B.) Several

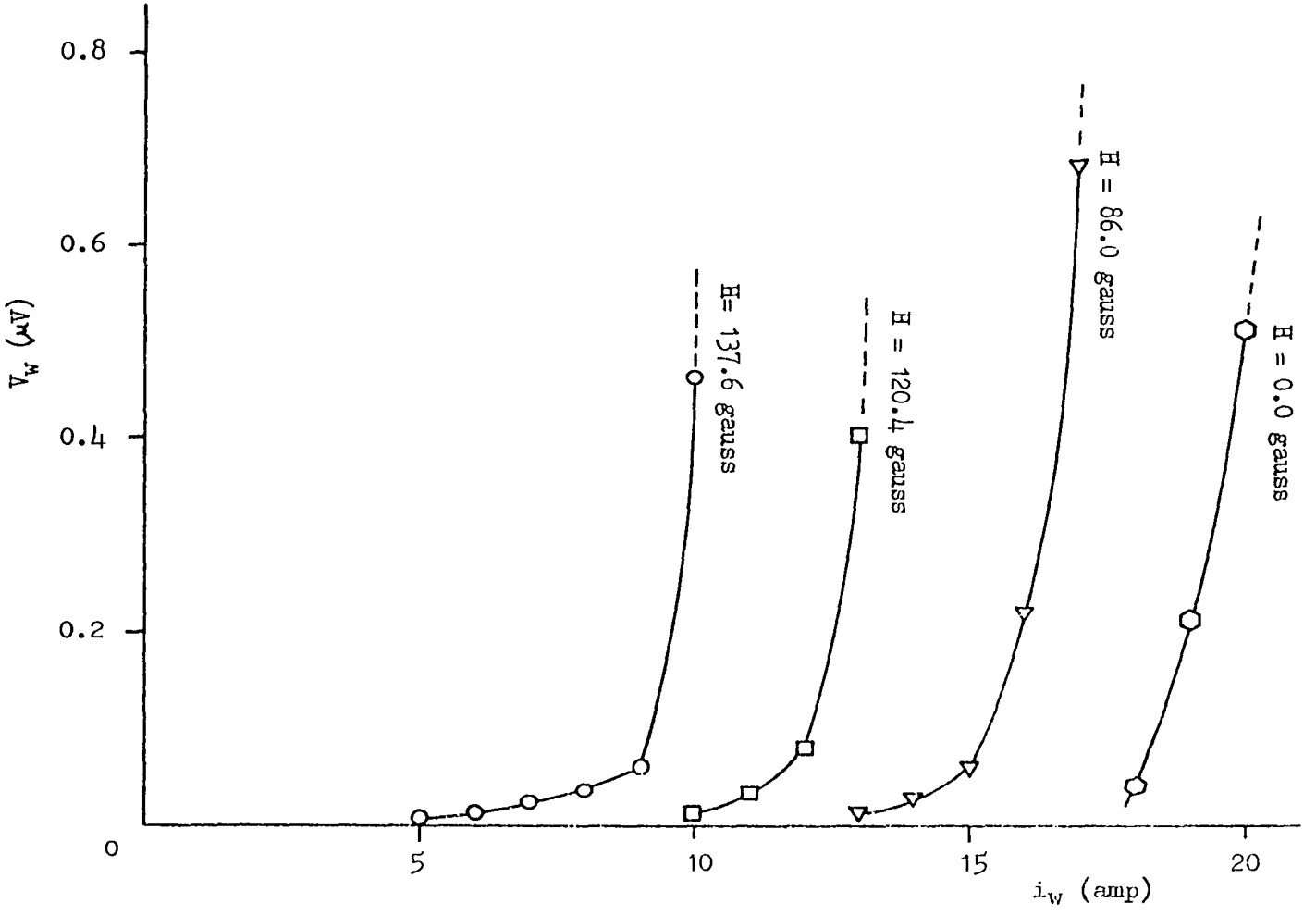


Fig. 14.---Voltage-current characteristics obtained with four-probe technique showing the superconducting-intermediate transitions.

curves are shown, each at a different magnetic field. It is seen that for each magnetic field there is a critical value of current that causes the voltage to rise suddenly above the 0.1 $\mu$V line. (Recall that the critical current is defined here as that current which causes the voltage to rise above 0.1 $\mu$V.) However, note that this is not the current at which a voltage (or resistance) first occurs.

The fact that a voltage appears at currents less than critical has been observed before. For example, see Scott[17] (1948) and Meissner and Zdanis[18] (1958). This is usually attributed to imperfections in the specimen[17]. According to London, a superconducting wire carrying a transport current will enter into the intermediate state <u>at</u> the critical current $i_c$. This superconducting-intermediate (S-I) transition is ideally very sharp and occurs at a unique value of transport current $i_c$. The existence of the voltages before the critical current is reached, indicates that the S-I transition is not something that occurs instantaneously at $i_c$ but takes place over a range of current (refer to Fig. 3).

It is interesting to note that the width of the S-I transition increases with magnetic field. At this point not much significance is attached to the vanishing of the transition width as the field is reduced to zero. It may be possible that the wide transition exists at the low fields but cannot be detected by using the four-probe technique.

The voltages recorded were very sensitive to temperature changes. This indicates that the transition width may also be temperature dependent when measured with the four-probe technique. The results of Meissner and Zdanis[18] suggest a temperature dependence but the variation is too random to make any definite statements.

For the very small voltage readings (on the order of 0.01$\mu$V) it is difficult to distinguish the data points from the noise. The problem of noise must always be dealt with in this type of measurement[34].

## Characteristic Threshold Current

It is proposed that the coupled persistatron may be more sensitive than the four-probe technique for measuring the critical current, when the critical current is defined as the current at which dissipation first occurs in the superconducting wire. The critical current defined in this fashion will be referred to as the "threshold current" $i_{wc}$. In the coupled persistatron, this threshold current $i_{wc}$ first manifests itself as the point at which flux conservation in the superconducting loop breaks down and current is diverted from the wire into the coil (the first critical point). This situation is observed experimentally as an increase in the magnetic field of the solenoid at constant external control current I. The value obtained for $i_{wc}$ is compared to previously published values of the critical magnetic field by means of Silsbee's rule. The published values for the critical field of indium as a function of temperature used here are interpolated from data due to Shaw, et al.[35] and are arranged in Table I.

Preliminary measurements with the coupled persistatron agreed with the four-probe measurements in that the threshold current $i_{wc}$ is found to be less than the critical current $i_c$ (from Eq. (2) using 180 gauss for $H_c$). However, $i_{wc}$ obtained using the coupled persistatron is much lower than that obtained using the four-probe method. The temperature dependence is measured to determine whether the effect of $i_{wc} < i_c$ is a systematic effect (true natural phenomenon) or simply a result caused by the

TABLE I

THE CRITICAL MAGNETIC FIELD
OF INDIUM AS A FUNCTION
OF TEMPERATURE

| T ($^{o}$K) | $H_c$ (gauss) |
|---|---|
| 3.31 | 14.79 |
| 2.99 | 60.98 |
| 2.81 | 85.64 |
| 2.52 | 122.69 |
| 2.20 | 158.94 |
| 2.00 | 180.02 |
| 1.79 | 200.32 |
| 1.46 | 228.07 |

experimental arrangement. In other words, the reproducibility of the threshold current $i_{wc}$ is measured as a function of temperature.

The results for the threshold current $i_{wc}$ as a function of temperature for constant diameter wire are shown in Fig. 15. The "smooth" temperature dependence seen in Fig. 15 and the lack of scatter are taken to be indications that $i_{wc}$ is, in fact, a natural phenomenon. The temperature is measured using a mercury manometer to monitor the vapor pressure of the helium bath. Reference points are chosen on the manometer to give a range of temperatures. The probable error in the pressure is on the order of 3 per cent (valid for all temperatures equal to or greater than 1.8°K), which corresponds to $\pm$ 0.01°K in the neighborhood of 2°K.

The diameter of the indium wire used for this test is 0.546 mm. The current leads and the solenoid are made with HMP Ersin Multicore solder consisting of 93.5 per cent lead (Pb). Its diameter is 1.22 mm. There are tin and silver in this solder making it rigid and easy to work with. Its superconducting properties are well suited for the purposes of the solenoid and current leads.

The procedure for finding the threshold current $i_{wc}$ is to increase manually the external control current I from zero in intervals, allowing the system to remain undisturbed and in equilibrium at each setting of I for a short time (1 or 2 minutes). When the current in the wire reaches $i_{wc}$, the system will not remain in equilibrium. Instead, a current reapportionment will take place within the circuit at constant I (that is, without any external change being made). After this point is reached, I is reduced to zero by turning off the power supply. If $i_{wc}$ has been reached and dissipation has taken place, then there will be a current

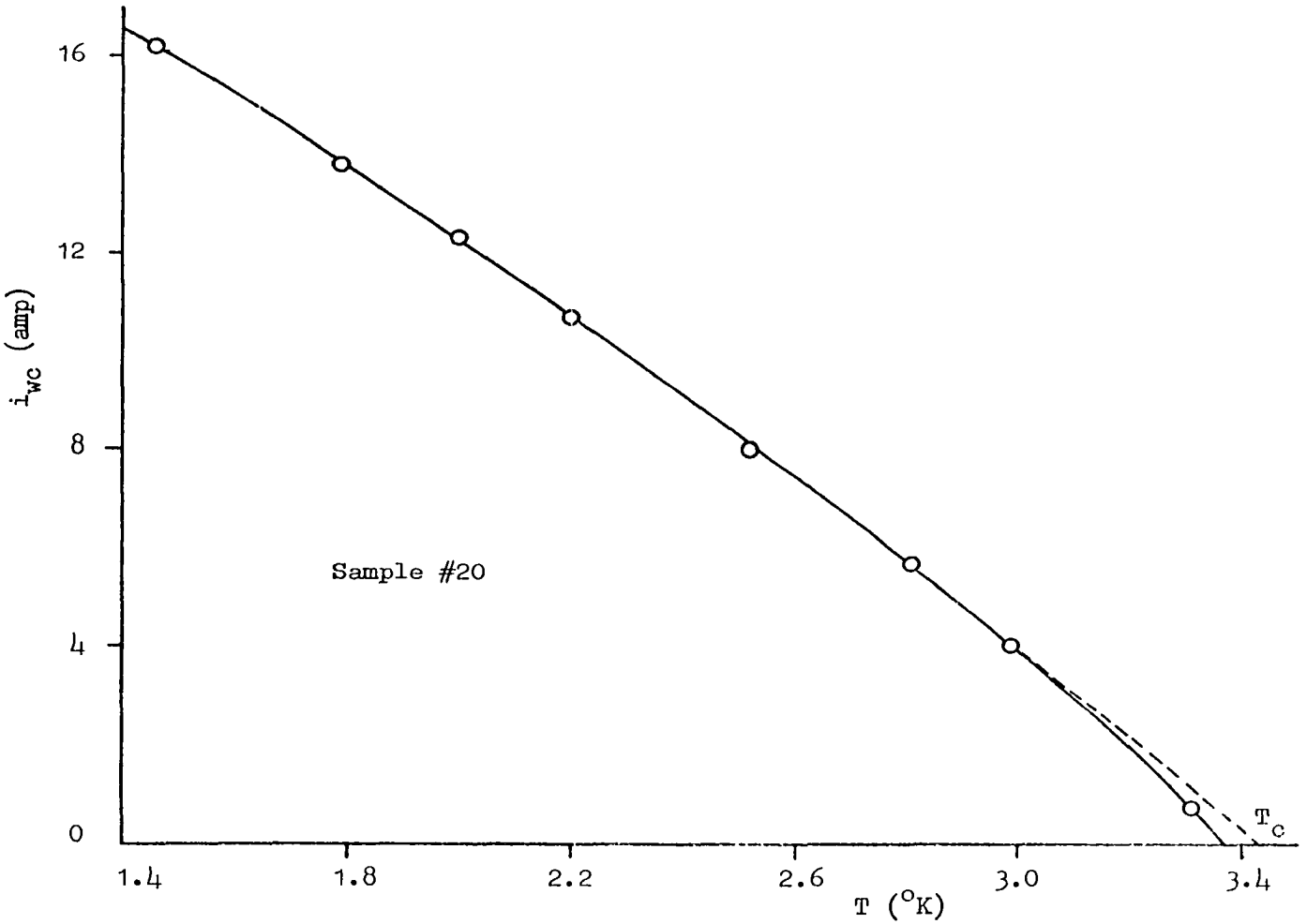


Fig. 15.--The threshold current $i_{wc}$ as a function of temperature.

trapped in the superconducting loop. Before the critical point $I_{1c}$ is reached, the increase in I and the apportionment of this current within the circuit is reversible, and a reduction of I to zero leaves no trapped field or current. The trapped current is cancelled by applying an external current of opposite polarity until the magnetic field of the solenoid is zero, that is, the coupled persistatron is left in the virgin state. The above procedure is repeated until two identical values of the first critical point $I_{1c}$ are obtained consecutively. This usually requires no more than three attempts. The first try might be off by 5 per cent, but gives a good indication of $I_{1c}$ so that the next attempt will yield a reproducible value. The reason for the error in the first effort is that the exact value for $I_{1c}$ might be exceeded due to a choice of the incremental changes of I that is too large.

Note that there is considerable error in the threshold current $i_{wc}$ obtained at $3.31^{\circ}K$, due to the difficulty in maintaining a constant pressure at this temperature with the present experimental arrangement. If the T-I curve, Fig. 15, were extended to pass through $T_c = 3.41^{\circ}K$, then the "correction" that would be made in the reading at $3.31^{\circ}K$ would make $i_{wc}$ about 50 per cent larger. This is not to assume that the linear extrapolation given by the dotted line is the actual behavior. While it is certainly plausible, it cannot be accepted as definitive. Other approaches are possible.

The threshold currents for the different temperatures are correlated by forming the threshold current ratio

$$S_i = i_{wc}/i_c \ ,$$

where $i_{wc}$ is the threshold current of the specimen obtained by using the

coupled persistatron at a given temperature, and $i_c$ is the critical current obtained from the critical magnetic field $H_c$ in Table I. The results are tabulated in Table II.

Another informative way of expressing this threshold ratio is

$$S = H_c'/H_c \ ,$$

referred to as the threshold field ratio where $H_c'$ is the total magnetic field at the surface of the wire when dissipation begins (or ceases depending on whether $i_w$ is increasing or decreasing), that is, the threshold field. For this experimental arrangement, in which the inductance of the coil is much greater than that of the central wire, the field of the solenoid is small compared to the field due to the current in the wire at the first critical point $I_{1c}$ (a factor of about 100 smaller); therefore, to a good approximation

$$S_i = S$$

at the first critical point. (The earth's field is ignored.) The difference between $S_i$ and S is important and will be discussed when more information is available, later in this work.

Notice from Table II that for the wire diameter on the order of 0.5 mm

$$i_{wc} = S_i \, i_c \approx 0.5 \, i_c \ .$$

This effect appears to be independent of temperature and says that the onset of dissipation in this sample occurs at approximately one-half of the conventional bulk critical current. This does not say that the critical current of indium is one-half of what it is predicted to be or measured to be by other techniques. Its interpretation will be treated when more information is available, later in this work.

TABLE II

THE THRESHOLD CURRENT AS A FUNCTION OF TEMPERATURE

| T (°K) | $i_{wc}$ (amp) | $i_c$ (amp) | $S_i$ |
|---|---|---|---|
| 3.31 ± 0.04 | 0.69 | 2.02 | 0.34 |
| 2.99 ± 0.01 | 4.00 | 8.32 | 0.48 |
| 2.81 ± 0.01 | 5.67 | 11.69 | 0.48 |
| 2.52 ± 0.01 | 8.02<br>8.00 | 16.75 | 0.48 |
| 2.20 ± 0.01 | 10.72 | 21.70 | 0.49 |
| 2.00 ± 0.01 | 12.31<br>12.32 | 24.57 | 0.50 |
| 1.79 ± 0.02 | 13.78 | 27.34 | 0.50 |
| 1.46 ± 0.04 | 16.22 | 31.13 | 0.52 |

The previous results indicate that the threshold current $i_{wc}$ is not necessarily equal to the critical current $i_c$. This is a striking result and must be checked thoroughly. A first check can be made on the circuit construction. This is done by using the same sample in several different coils to determine whether or not the solenoid has any systematic effect on the results.

The results of such a measurement are presented in Table III. The Pb-alloy coil is made from the HMP Ersin solder described before. Pure lead (6-9's), which was extruded, is the wire in the Pb coil. Its diameter is about 1.0 mm. The Pb-alloy b coil is the same as coil #1 except that the current leads to the sample (Pb-alloy in each case) are cut and soldered back together with Pb-Sn solder. Coil #4 (Pb-alloy c) is identical to coil #3, but is cycled between room temperature and $2^{o}K$ to see if thermal shock has any effect. Ersin Multicore solder (60 per cent Sn), diameter 1.2 mm, is used for the Pb-Sn coil. Its junction are soldered with pure In solder.

No systematic effect on the threshold current by the particular coil used in the circuit is indicated by the preceding measurements. However, a certain amount of randomness in $S_i$ is introduced when the circuit is mechanically disturbed. The thermal shock does not change the first critical point. It can be assumed that the physical characteristics of the coupled persistatron, at least from the above checks, do not determine the value for the threshold current ratio. It is only necessary for the solenoid to remain completely within the superfluid state at all times during the course of a measurement. There is a similar randomness in the threshold ratio $S_i$ (same order of magitude as that caused by a coil change) over long periods of annealing.

TABLE III

THE THRESHOLD CURRENT AS A FUNCTION
OF THE PICK-UP COIL USED IN CIRCUIT

| Coil # | Type of Coil | $i_{wc}$ (amp) | $S_i$ |
|---|---|---|---|
| 1 | Pb-alloy | 12.32 | 0.50 |
| 2 | Lead (Pb) | 12.92 | 0.52 |
| 3 | Pb-alloy b | 12.62 | 0.51 |
| 4 | Pb-alloy c | 12.61 | 0.51 |
| 5 | Pb-Sn | 13.08 | 0.53 |

The preliminary test have confirmed the existence of dissipation in a current-carrying superconducting wire at a point less than critical. The four-probe measurements indicated that dissipation begins at a current $i_{wc}$ less than the value $i_c$ predicted using Silsbee's hypothesis and that the transition from the superconducting state to the intermediate state ($i_w > i_c$) occurs over a range of current. The coupled persistatron measurements, thus far, have indicated that the threshold current $i_{wc}$ is considerably less (approximately 50 per cent) than the critical current $i_c$. The coupled persistatron results have also shown that $i_{wc}$ relative to $i_c$ is independent of temperature and is not determined by the experimental arrangement or physical characteristics of the circuit.

## Specimen Radius of Curvature

An effort is now made to find a variable on which $i_{wc}$ does depend. Meissner and Zdanis' [18] observations of the resistance transition for indium wires indicate that the onset of dissipation, as evidenced by the toe on the resistance transition curves, seems to be dependent on the radius of curvature or the diameter of the wire. Their data suggest that the smaller the wire the wider the transition. (Here the "transition" is taken to mean the range of currents beginning at the value for which resistance is first observed and extending to the Silsbee's critical current.) In other words, for small wires the onset of resistance occurs at a smaller percentage of the critical current than it does for larger wires. The effect virtually disappears, according to the data of Meissner and Zdanis[18], as the wire diameter exceeds 2 mm.

In order to pursue the possibility of the onset of dissipation being dependent on the radius of curvature of the wire, several specimens

are extruded varying in diameter by a factor of approximately five. The wires are all made from the same batch of indium shot and care is taken to use the same procedure for each wire. The slugs are etched before extrusion. A microscope is used to examine the wires after extrusion to see if there is any visible differences in their structure. They are chosen to be as nearly alike as possible, including length.

The procedure for measuring the threshold current $i_{wc}$ as a function of wire diameter is similar to that used in the temperature measurements. For each wire, the same solenoid constructed of 1.22 mm diameter Pb-alloy wire solder is used. After $i_{wc}$ is measured for one wire, the circuit is removed from the dewar; the sample is replaced by another wire. Without disturbing the solenoid or the wire itself, the specimen holder is put in place and the current leads soldered to the binding post. The results are tabulated in Table IV and presented graphically in Fig. 16.

The threshold ratio $S_i$ for the wires is measured at $2^{o}K$, except for sample #80. The critical current for this wire was too large at $2^{o}K$ for this experimental arrangement. Consequently, $i_{wc}$ for this sample is measured at $2.8^{o}K$ and $3^{o}K$. Two temperatures are used to make sure the values are temperature independent. Ratios at different temperatures differed by less than one per cent.

The large currents associated with samples #60 and #80 call for an additional check on the temperature dependence because of the possibility of heating. This is done using the 1.5 mm (sample #60). Points are checked above and below the lambda point and found to be constant within one per cent. If heating were a factor, its effect would have been detected when the liquid helium surrounding the circuit became superfluid.

TABLE IV

DIAMETER DEPENDENCE OF THE
THRESHOLD CURRENT

| Sample | Diameter in mm | $S_i$ |
|---|---|---|
| 15 | 0.368 ± 2.7% | 0.52 |
| 20e | 0.464 ± 1.5% | 0.51 |
| 20 | 0.546 ± 0.5% | 0.50 |
| 25 | 0.646 ± 0.3% | 0.51 |
| 30 | 0.785 ± 0.9% | 0.49 |
| 35 | 0.776 ± 1.4% | 0.51 |
| 40 | 1.012 ± 2.7% | 0.54 |
| 60 | 1.538 ± 0.3% | 0.63 |
| 80 | 1.951 ± 0.5% | 0.75 |

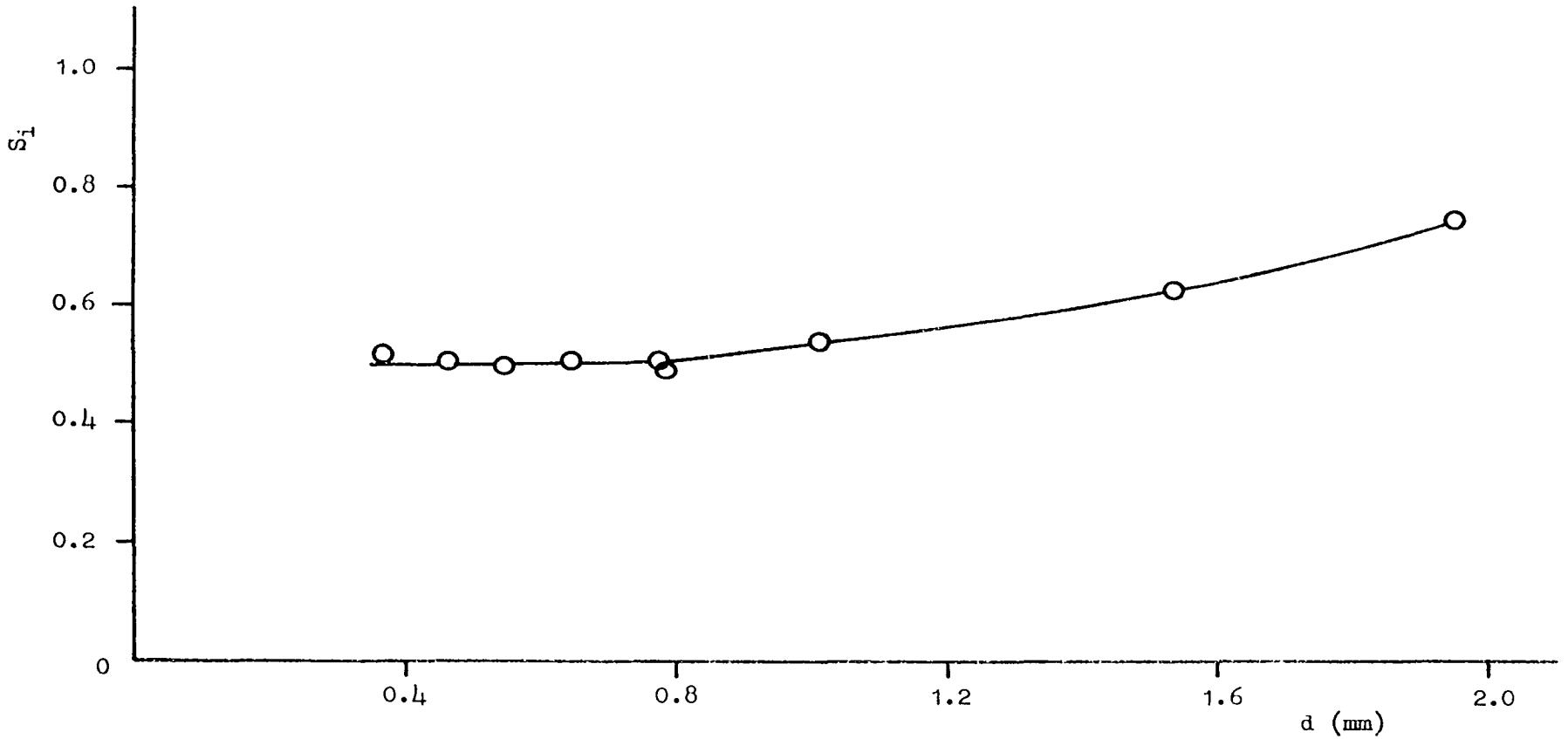


Fig. 16.--Diameter dependence of the threshold current ratio.

Therefore, although an attempt is made to measure the points in Table IV at the same temperature, it is not necessary in determining $S_i$.

Sample #80 (2 mm wire) is the largest one measured because of the inability of this experimental arrangement to maintain constant temperature near $T_c$ and to produce currents above 50 amperes. (The power supply available, item #8 in the equipment list of Appendix B, was capable of producing 50 amp at maximum.) The 0.4 mm wire is the smallest wire which could be easily extruded. Smaller dies would have to be produced by a special process not immediately available to this laboratory. The ones used are made by drilling the holes and the walls of these small holes sometimes break off. When this happens the scratches on the wires are large and the samples are not exactly round. Without the small dies, the making of smaller wires would involve a different technique. It was decided that all the wires for this experiment should be constructed in the same manner and no new technique would be used. Small wires can be made be drawing down glass capillaries filled with indium[18]; they can be made even smaller by etching.

None of the wires which are used in the diameter dependence test are treated in any way after extrusion except sample #20e. The surface of this sample was etched using a 70 per cent solution of nitric acid. This sample was extruded using the 0.5 mm steel die and was etched down to 0.464 mm. After etching the surface was very smooth and shiny in general; however, there was some evidence of pitting. There were "cracks" on the surface which were taken to be grain boundaries. Notice that this process did not affect the threshold current ratio $S_i$.

It can be seen from Fig. 16 that for a range of diameters below 0.8 mm the threshold ratio is a constant. Because of this plateau, the

ratio appeared, at first, to be independent of diameter since the initial wires were all less than 1 mm diameter. Nothing can be said from these results about how far the plateau may extend toward smaller diameters. The results presented in Fig. 16 are very incomplete, but they do indicate that the threshold ratio $S_i$ is a function of diameter.

A result or observation which cannot be represented in the table or on the graph is the response of the wires as $i_{wc}$ is approached. For the small wires, the critical point, $I_{1c}$, is easy to detect since there is a sudden change in the current apportionment of the circuit. However, for the larger wires, $I_{1c}$ is not so well defined because current reapportionment is less abrupt. For these wires, many attempts have to be made since it is easy to overshoot the threshold current. Nonetheless, the critical point can be located to within one per cent when sufficient care is exercised in the recording of the data.

This section has verified that the ratio $S_i$ postulated in Eq. (16) does indeed exist and is a function of the radius of curvature of the specimen. The situation studied in this section is for a negligible applied magnetic field $H_s$; thus, it has not been determined whether or not $S_i$ is a constant for a particular wire.

## Behavior in Critical Region

Dissipation of energy in a current-carrying superconducting wire has been established as beginning at a point less than critical. It remains to be seen how the wire will behave when its transport current $i_w$ is increased above the threshold value $i_{wc}$. The nature of the equilibrium state reached when dissipation ceases must also be investigated.

## Analysis of Observables

Once the threshold current $i_{wc}$ has been reached the circuit passes into the critical region, in which the behavior of the circuit is time dependent. Careful measurements are made of these time dependent characteristics. The actual observables are the chart readings CR, the total external control current I, and the time increments at which the readings are taken. A computer program (see Appendix C) is used to analyze these observables and make a plot of the time curves.

The first step is to convert the chart readings into Hall voltages. This is done by adding each chart reading to the reference Hall voltage, which is the Hall voltage at which the preceding curve came to equilibrium,

$$V_H(t) = V_{Ho} + CR(t) \ .$$

Once the Hall voltage for a particular time is known, the longitudinal magnetic field produced by the solenoid can be found by using the relation

$$H_s(t) = k_H \, V_H(t) \ , \tag{44}$$

where $k_H$ is the calibration constant of the Hall probe. A typical value for the Hall calibration constant is

$$k_H = 28.444 \text{ gauss/mv} \ .$$

The magnetic field of the solenoid yields the current in the solenoid as

$$i_s(t) = H_s(t)/k_s \ ,$$

where $k_s$ is the coil constant for the particular solenoid used, typically

$$k_s = 6.226 \text{ gauss/amp.}$$

In terms of the original observable, the current of the solenoid is given by

$$i_s(t) = k_H \, V_H(t)/k_s \ . \tag{45}$$

The current in the wire at a given time is

$$i_w(t) = I - i_s(t).$$

Again, writing this in terms of the original variables yields

$$i_w(t) = I - k_H V_H(t)/k_s . \qquad (46)$$

This wire current is normalized making it a unitless quantity. The result is

$$i_{wn}(t) = \frac{i_w(t) - i_{wf}}{i_{wo} - i_{wf}} ,$$

where the symbols have been defined in Eq. (27), or

$$i_{wn}(t) = C_1 i_w(t) - C_2 , \qquad (47)$$

where

$$C_1 = 1/(i_{wo} - i_{wf}) ;$$

$$C_2 = i_{wf}/(i_{wo} - i_{wf}) .$$

The wire current is normalized so that it may be easily analyzed graphically and its behavior compared to a pure exponential behavior. The change in wire current itself is not large enough to justify the use of a logarithm scale. A typical range would only involve one or two per cent of one decade. However, the range of $i_{wn}(t)$ spans at least two full decades. Over two decades on a logarithm scale, a reasonable idea of the exponential behavior of the curves may be obtained. As seen in Chapter II, this normalization is equivalent to defining the reapportionment current in terms of the wire current.

Normalizing the wire current in this fashion has several advantages. First of all, it forces the values of $i_{wn}(t)$ for any curve to lie between unity and zero, that is, all of the curves have two points in common:

$$i_{wn}(0) = 1,$$

$$i_{wn}(\infty) = 0.$$

A second advantage of this procedure is that $i_{wn}(t)$ is independent of the constants used in the calculations, and it is independent of variations in the set value of the external current. Variations of the constants ($k_H$, $k_s$, $k_w$) and the external current I do not affect the values obtained for $i_{wn}(t)$. Obviously, the other variables of interest do depend on these constants; so care must be taken in determining the constants and reading the external current.

On the other hand, there is a distinct disadvantage of this method of normalizing. The values of $i_{wn}(t)$ are sensitive to the value chosen for $i_{wf}$ (that is, the final chart reading used). For curves with a very large time constant or rise time, the true final value of the wire current may never be reached. This then requires a decision to be made about how much time must pass before a decent estimate of the final value can be made.

Adjustment of the final chart reading upwards (since the actual curve recorded on the chart is approximately a rising exponential) has a tendency to straighten out the semi-logarithm plot, making it a better exponential fit, as in Fig. 17. If there are only a few points (such as the solid circles of curve a in Fig. 17) which deviate from the exponential line by no more than approximately 80 per cent of the slope of the straight line portion, then the curve can be straightened out by raising the final chart reading by 0.02 mv (which corresponds to lowering $i_{wf}$ by about 0.1 amp), as in curve b of Fig. 17. This increase will cause a decrease in the absolute value of the slope by as much as 15 per cent. A

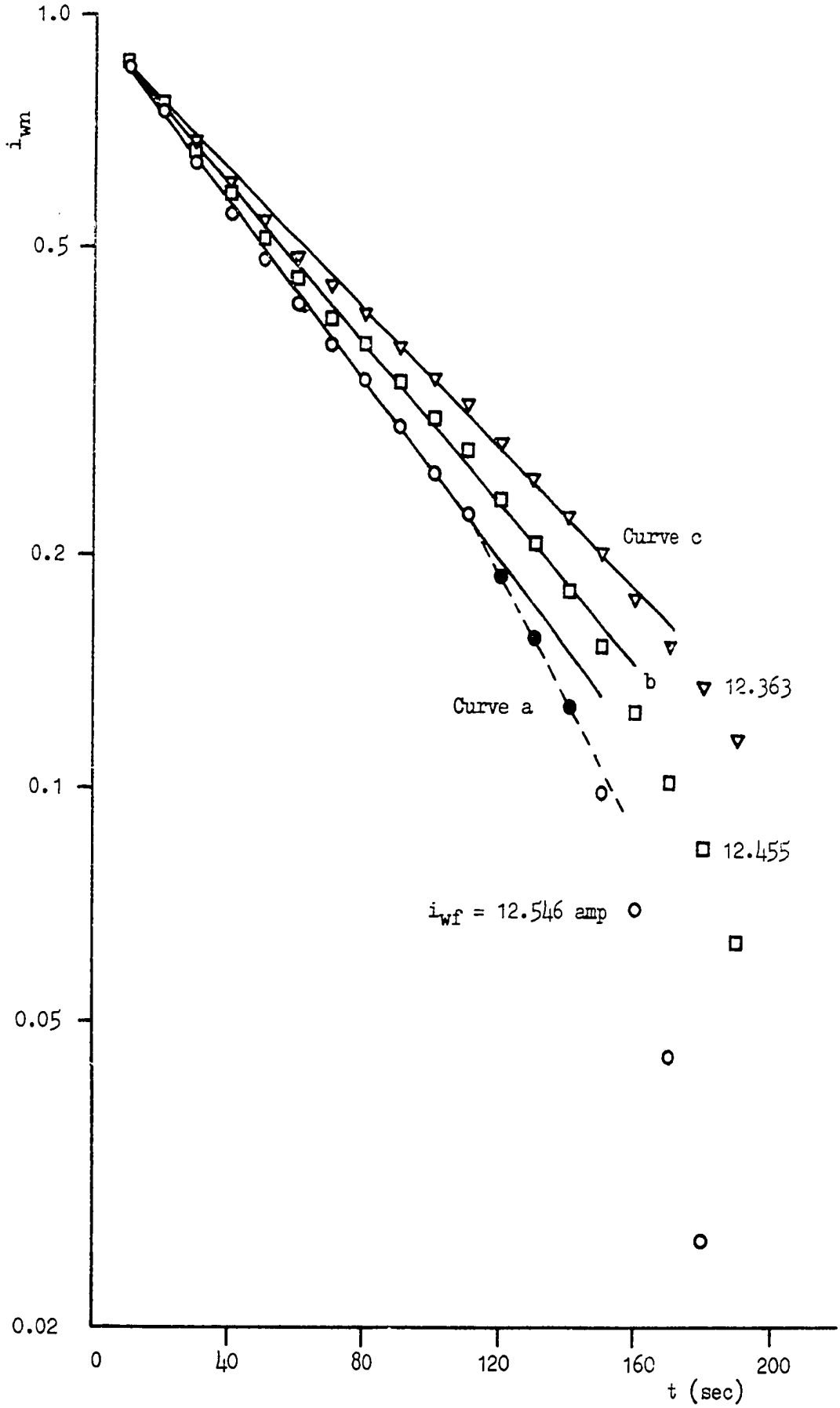


Fig. 17.--The influence of $i_{wf}$ on the time curves.

greater increase in the final reading is not justified experimentally and would cause the straight line portion of the curve to lose its linearity without completely straightening out the curve, as in curve c of Fig. 17.

Therefore, a variation in $i_{wf}$ over a reasonable range of values affects only the slope of the semi-logarithm plot and cannot be said to affect the general behavior of the curve. This problem is not serious whenever a curve with a short rise time is involved. In this case, a much larger percentage of the full exponential curve is observed and the final value or asymptotic value can be estimated very well.

Of course, $i_{wn}(t)$ also depends on $i_{wo}$, but this initial value of the wire current is equal to the final value for the preceding curve (which need not be an equilibrium point as far as $i_{wo}$ is concerned). The value of $i_w(t)$ at which an increase in the external control current is made is known. In other words, $i_w(t)$ need not be constant for a particular value, say

$$i_w(t') = i_w(0),$$

to be known. Consequently, the error in determining $i_{wo}$ may be ignored; it does not affect the behavior of the time curves.

## Relaxation Time Constants

As stated, the time curves are obtained by plotting the natural logarithm of the normalized current as a function of time for a constant external control current I. The rise time of such a curve gives an indication of the time required for the system to "relax" after a change is made in I. This semi-logarithm plot is chosen in order for the experimental curves to be compared with the theoretical exponential relation between $i_{wn}$ and time. Whenever the semi-logarithm plot yields a straight

line the data fits the relation that is exponential in time; a curved line indicates a non-exponential relation and will not be dealt with to any great extent in this work.

The slope of the straight line portion of the curve is calculated by finding the slope of the segment between consecutive points,

$$m = \frac{\ln i_{wn}(t_2) - \ln i_{wn}(t_1)}{t_2 - t_1} \quad ,$$

and averaging over the segments. A cut-off point is chosen, beyond which points deviating from the exponential line are not considered. The standard deviation from such an averaging process merely gives an indication of the scatter of the points from the exponential line, but not necessarily a standard error in the slope, as may be determined from a mathematical fit.

A time curve is plotted for each value of the external control current I at a given annealing time $A_t$. After the same circuit is annealed for several additional days at 100°C, another set of time curves is obtained using the wire. This procedure is continued for a total annealing time of 30 days. Once the relaxation time of the curves has decreased enough, a second set of curves is obtained at a given annealing time, for the same run. When this is done, the value of the external control current I at which the second critical point $I_{2c}$ occurs usually decreases by one ampere. For the circuit ($k_w$ = 7.505 gauss/amp; $k_s$ = 6.226 gauss/amp) used in this investigation of the time curves, the first set of measurements yields

$$I_{2c} = 30.0 \text{ amp}$$

for the second critical point; however, for the second set of measurements this value changes to

$$I_{2c} = 29.0 \text{ amp.}$$

These two sets of measurements are made without changing the temperature of the circuit. The magnetic field trapped in the circuit between runs is cancelled by reversing the external current.

The occurrence of the second critical point at two different values for external current is possibly due to the wire losing slightly more current for each increment of I on the second run. In other words, the longitudinal field $H_s$ could be slightly larger for each I than for the first run. Consequently, the singularity value of $H_s$ is reached for $I = 29.0$ amp rather than for $I = 30.0$ amp. For the first test, when current is passed through the wire, a type of thermally induced pinning center may be relaxed. The absence of these pinning centers for the second test might mean that more current is removed from the wire and added to the solenoid (the shifting of field in the wire can occur for a slightly longer time). It should be emphasized that this possible explanation is a surmise on the part of the author.

Whenever two sets of curves are obtained, a check can be made on the reproducibility of the curves by comparing the data at a given external control current. These curves will not always be identical at the same value of $i_w/I$, but the difference usually does not have any real affect on the shape of the curves. Usually the curves are nearly the same (within experimental error). At times, they are practically identical, even reproducing the same type of scatter from the straight line; on the other hand, there are times when they are completely different. For a given annealing time, the measurements show that curves at some values of I reproduce while curves at other values of I do not. For another annealing time, the same thing will happen but for different values of I. This

tends to indicate that there is a certain amount of fluctuation involved in these results which (it is strongly felt) cannot be attributed to the experimental arrangement. The fact that curves at the same external control current may not have the same range of values for $i_w/I$ may be due to the inability of the reverse current process to completely cancel the magnetic field trapped during a preceding run.

It is found from the time curves that the relaxation time constant,

$$R/L = |\bar{m}| \text{ sec}^{-1},$$

is a function of the duration of annealing $A_t$ and the external control current I. The dependence on I is, more accurately, a dependence on the transport current $i_w$ in the superconducting wire. The wire current $i_w$ decreases as I increases, as seen in Fig. 2. However, during the relaxation time, the variable I is an observable constant and makes a convenient parameter for analyzing the data.

It should be pointed out that the time constant does not depend experimentally on the particular change $\Delta I$ made in the total external control current as long as the final value of I is the same. Neither is the relaxation time affected by the choice of $\Delta I$. However, the linearity of the initial portion of the time curve will be destroyed if the change in the external control current is too large. For example, if $\Delta I \geq 3.0$, the initial slope well be very large; however, it will decrease rapidly to the same value of R/L as for $\Delta I < 3.0$. As I is increased, the initial slope increases, but the curve always levels off to the same value of R/L, as long as the circuit is sitting at the same value of I. The choice of $\Delta I = 1.0$ for these experiments was made after some trial and error. It is a convenient value but is somewhat arbitrary. A change of one ampere

in I gives fairly straight lines and gives a reasonable number of time curves. A smaller value would produce a greater number of time curves which is not necessary. A larger value might not produce enough such curves.

Fig. 18 (data in Table 3 of Appendix B) shows how the time constant varies with I at a given annealing time. This curve summarizes the circuit behavior after 20 days of annealing. It does not necessarily represent any particular functional relationship. Note that the rise time varies as the reciprocal of the time constant, R/L, as plotted in this figure.

Several representative curves are shown in Fig. 19 (data in Table 4 of Appendix B) This along with Fig. 18 demonstrates that the rise time of the curves (or the time required for the circuit to come to equilibrium once a change has been made in I and reapportionment begins) increases rapidly toward the latter part of the critical region. This relaxation time is not chosen as a variable to plot because it has too much scatter, due to the rather arbitrary method used to determine the cut-off time (that is, the choice of $i_{wf}$).

The variation of the time constant due to annealing is shown in Fig. 20 (data in Table 5 of Appendix B). A plot of R/L vs. $A_t$ for one particular value of I may show no general trend. In order to see a general trend, the values for I in the plateau part of the critical region are averaged. (The plateau part of the critical region is characterized by small changes in the equilibrium wire current for different I.) It is the average of the values of R/L for I in the plateau that is represented by the circles in Fig. 20. These circles show that the rise time

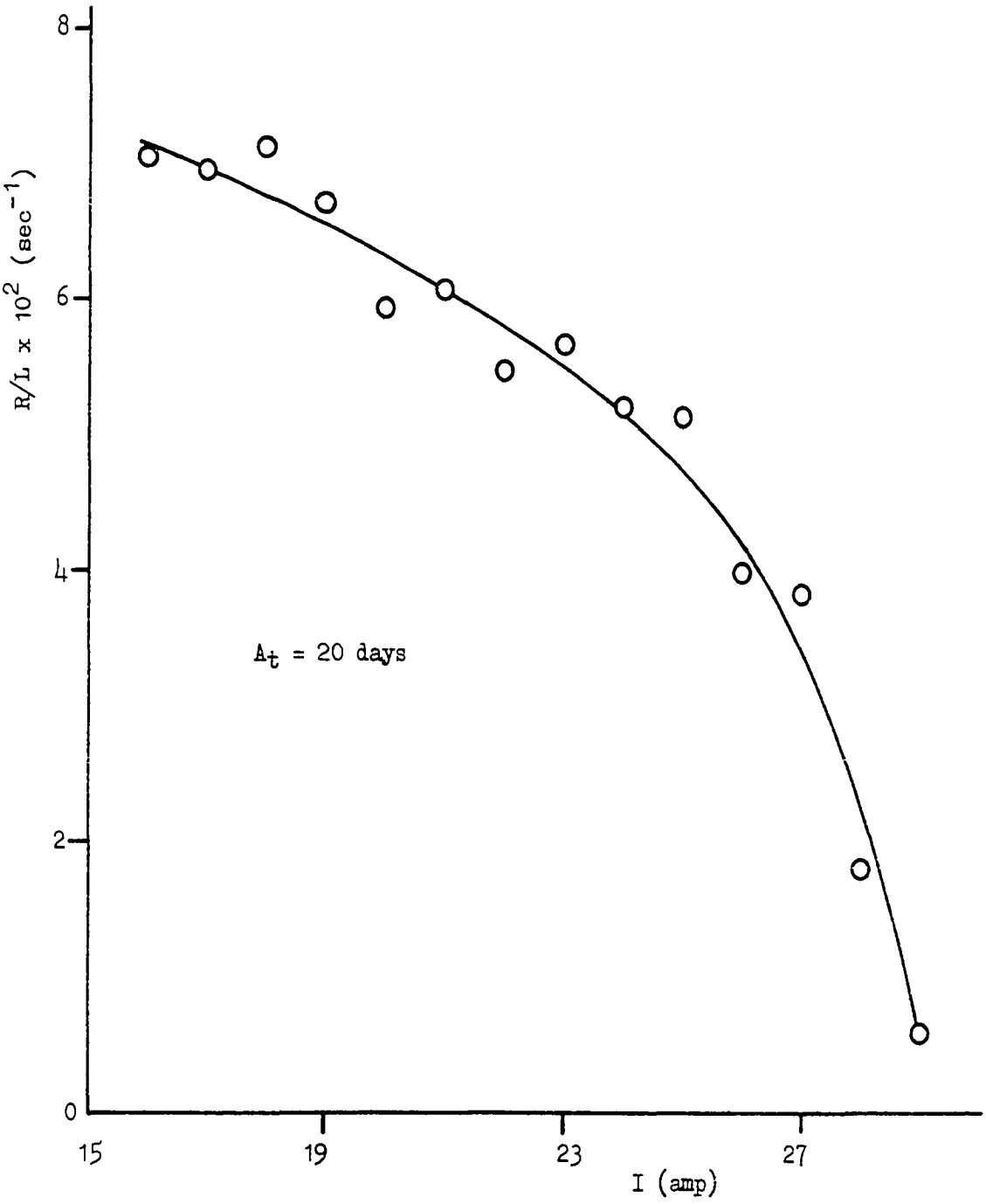


Fig. 18.--The time constant as a function of external control current.

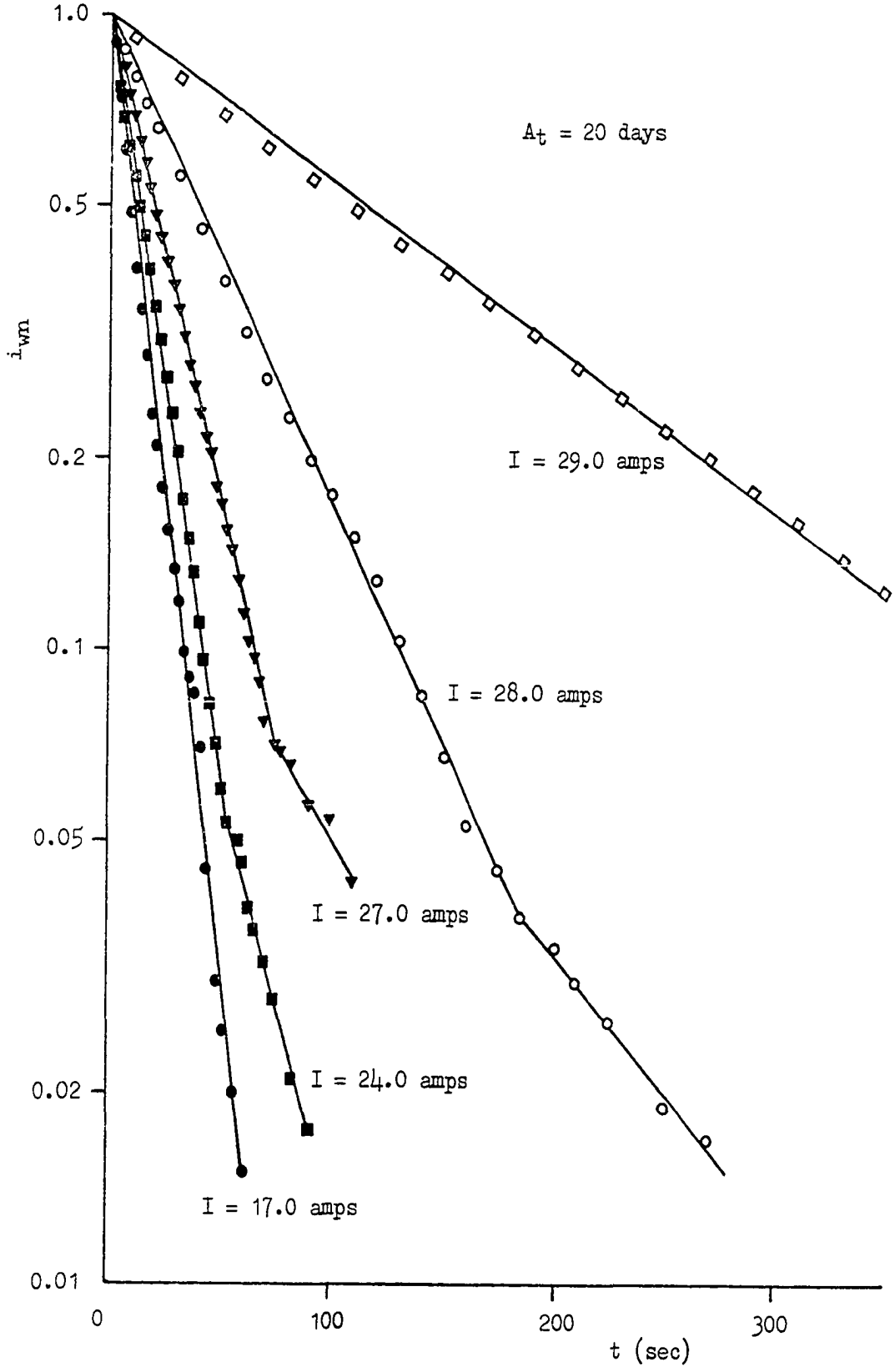


Fig. 19.--The time curves as functions of external control current

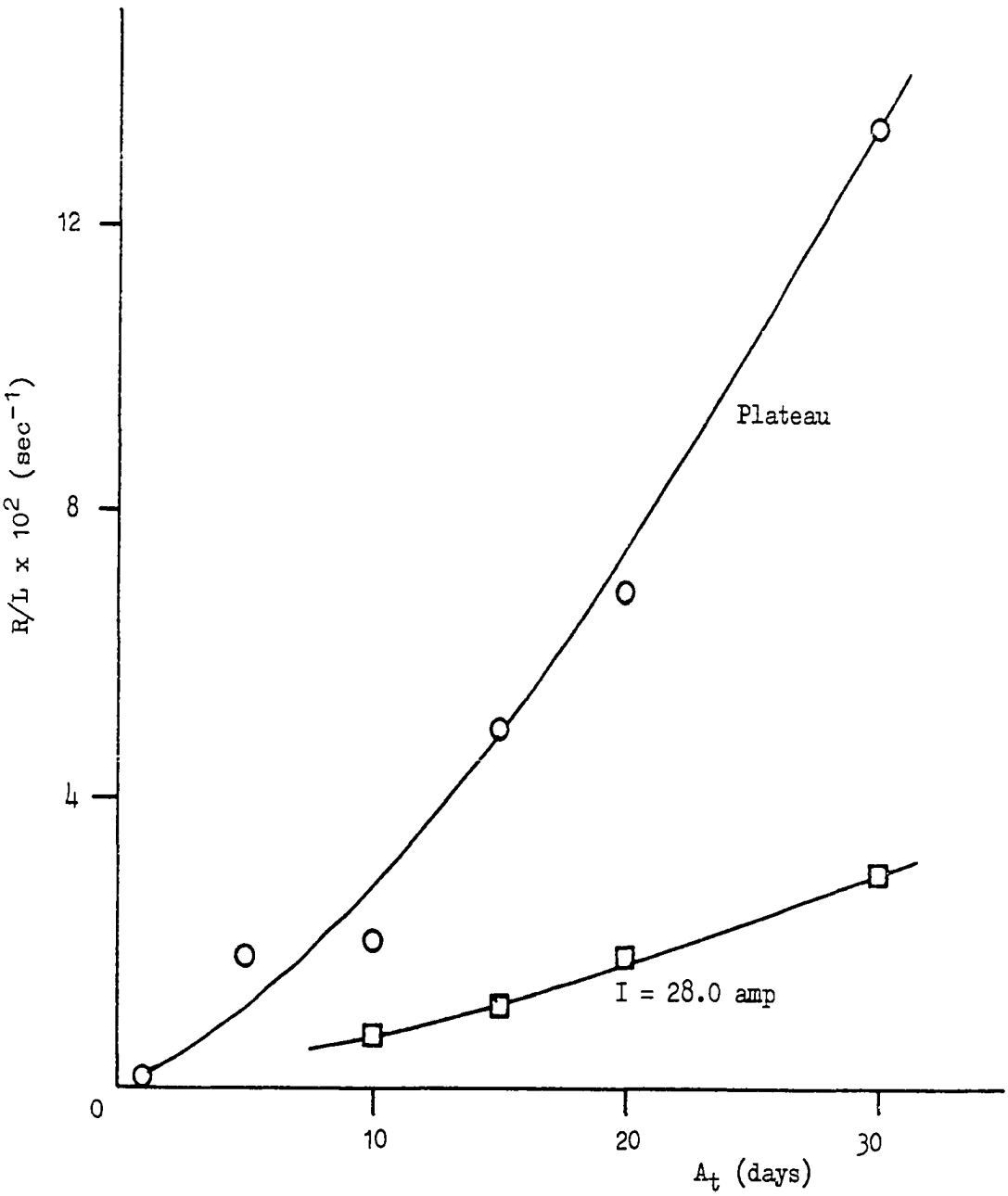


Fig. 20.--The time constant as a function of annealing.

time for the time curves decreases rapidly as the sample is annealed. The squares are values for I = 28.0 amp which is near the end of the critical region. This curve again shows the low values of the time constants associated with large values of external control current.

A few representative curves are presented in Fig. 21 (data in Table 6 of Appendix B), to show the variation of the curve shapes with annealing. Because of the large differences in the relaxation times, the time axis has an "adjusted" scale. One point on each curve is labeled in time. Since each point is taken at equal intervals in time, the actual time scale can be deduced. Notice the increase in R/L and the change in the shape of the curves as the circuit is annealed. The time curve for a sample that has no annealing is not shown. It has a rise time greater than three hours, and a complete set of data cannot be obtained for it with the experimental arrangement used in this investigation. The fact that an unannealed sample could not be completed was learned from some preliminary tests, and consequently such a curve was not attempted for the sample under consideration. The preliminary test indicated that R/L would have been less than 0.001 $sec^{-1}$.

A fact that is not represented in Fig. 19 and Fig. 21 is that there seem to be generally three basic types of curves. These three types are represented in Fig. 22. (The curves shown in Fig. 22 are chosen so as to represent the three classes or types of curves. They are not related in any special sense. The values of I and $A_t$ are given to show that these are actual data curves and not just sketches.)

Type a consists of a long straight line portion followed by a gentle bending of the curve. The bending represents a rapid increase in R/L.

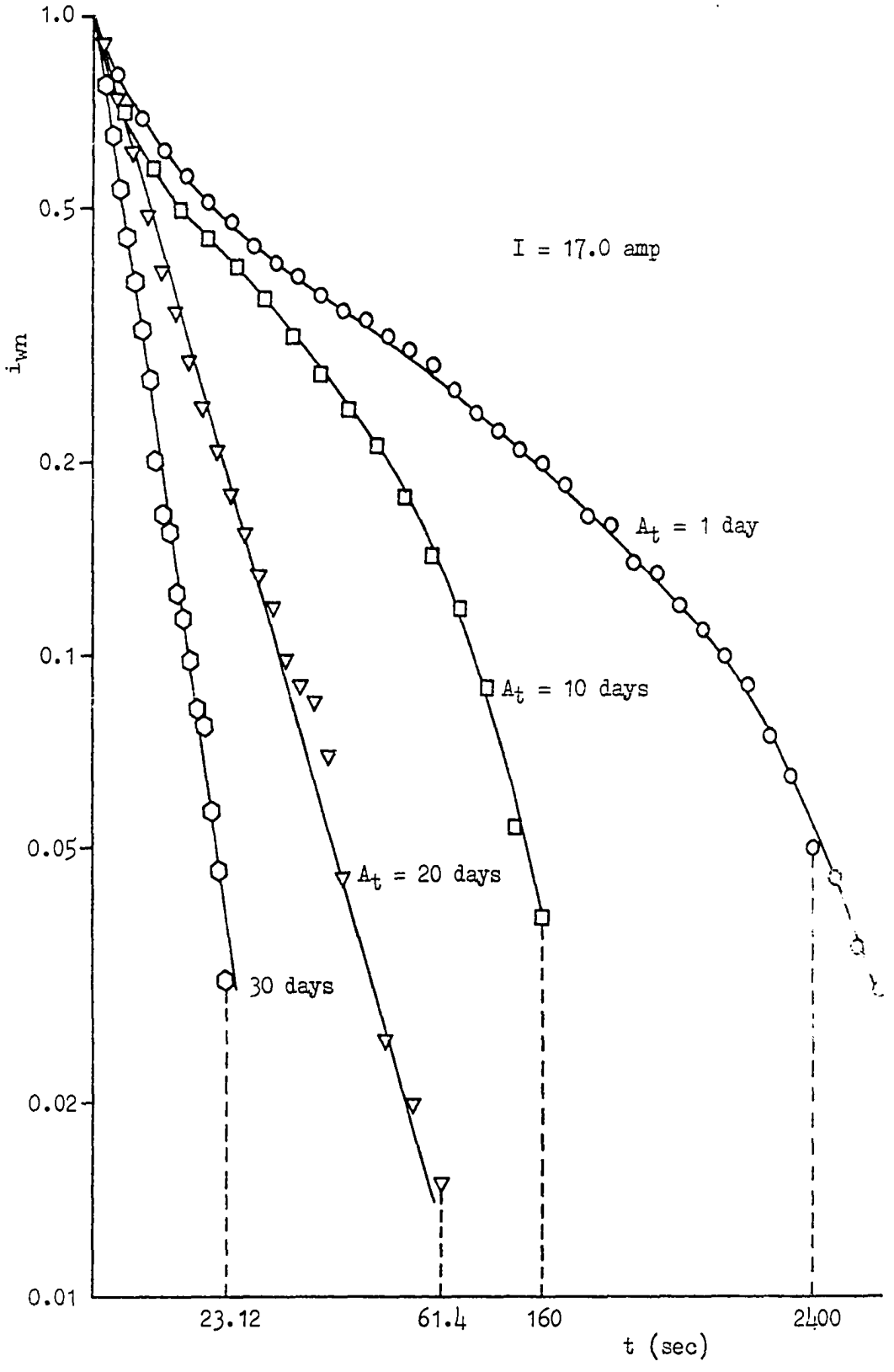


Fig. 21.--The time curves as functions of annealing.

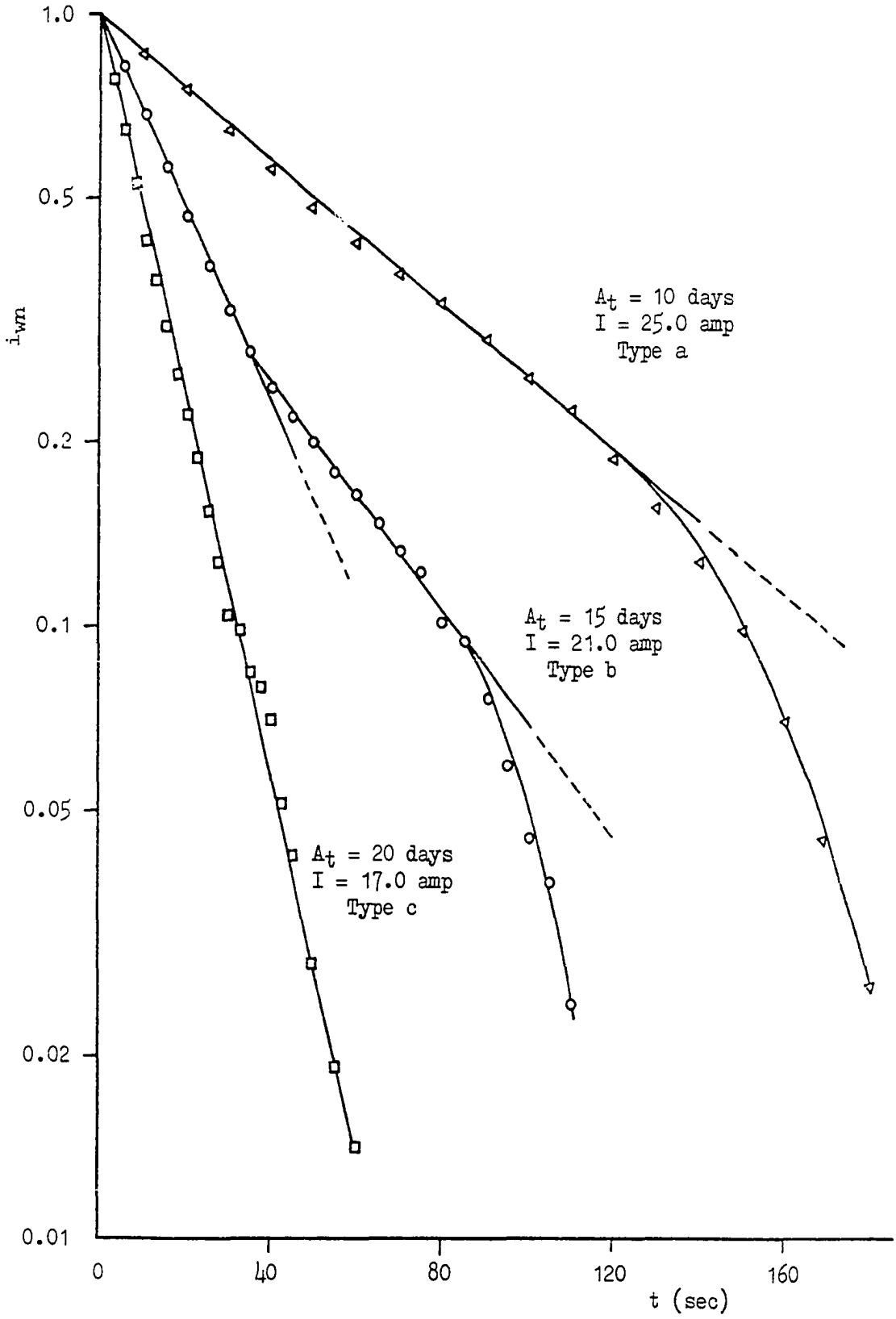


Fig. 22.--Typical behavior of the time curves.

The bending seen in this type of curve cannot be eliminated by a small adjustment in the final value of $i_{wf}$. This is the most predominant type. Type b consists of two straight line portions and a gentle bending away from exponential behavior at the end. This type of curve appears to be prevalent toward the end of the critical region, that is, beyond the plateau; but this is not without exception. Type c is a straight line (constant R/L) over two cycles of the semi-logarithm plot. This type of curve appears often but with little regularity. It is believed to be a special case of the type a curve, where the bending occurs rather suddenly below the two cycles represented. This type of curve is not as common as the other curves.

Whenever the magnetic pressure drops below a certain value, dissipation ceases. As the system approaches this situation, it is assumed that pinning takes place. It is conjectured that whenever pinning begins, the curves lose their exponential behavior and the bending occurs. If there were absolutely no pinning centers, then all of the curves would presumably be type c; that is, they would be pure exponentials. The fact that a few type c curves exist indicates that pinning is statistically a random phenomenon, and its degree of occurrence may be unpredictable.

The general observations that can be made from the entire set of curves are summarized in the following: After one day of annealing, only the plateau part of the critical region can be observed, due to the large relaxation times. The curves are of type a. Five days of annealing produces a greater number of curves of type b, that is, over one-half of the curves have breaks. For the plateau curves, the breaks begin to disappear after ten days of annealing and are gone after fifteen days except for the

end of the plateau (around I = 18.0 amp). Even after twenty days, the 18.0 amp curve still has a break. At this stage, several curves in the upper part of the critical region are found to have breaks. Once the circuit has been annealed thirty days, no breaks occur in the plateau. Most of the curves are type a, but a few breaks still occur in the upper part of the critical region. It is also observed that annealing tends to cause the curves to coalesce (that is, they all look alike and, if plotted on the same graph, cannot be distinguished), and that the curves in the upper part are less reproducible than those in the plateau.

The work presented in this section represents, by far, most of the experimental "labor" of this investigation. Many time curves were measured for several different samples. Much effort was made (cf. Chapter III) to make these curves reproducible. This was accomplished to some extent, and the results (experimental observations) have been discussed here. However, the explicit behavior of the exponential curves (that is, the functional behavior of R/L for a given curve) is a problem of considerable magnitude which has not been dealt with in this investigation.

As far as this investigation is concerned, the most important result from this section is that the wire reduces its current load (if given the opportunity as in a coupled persistatron) when $i_w$ is increased above $i_{wc}$. This current decay is exponential in time and is influenced by the average magnitude of the transport current and the state of annealing of the wire. The existence of this exponential current decay is a good indication that the coupled persistatron is detecting dissipation of energy in a current-carrying superconducting wire.

State of Equilibrium

As the time curves approach their asymptotic values, the system approaches an equilibrium state. This state is different for each value of external control current I or each apportionment of current within the circuit. Some insight into the behavior of the coupled persistatron and the manner in which superconductivity is destroyed in such a circuit can be obtained by studying the equilibrium state of the system as a function of external control current I. The data obtained from the circuit (characterized by $k_w$ and $k_s$) after it had annealed for 10 days was chosen for this purpose. This particular set was chosen because it was the first set which contained the entire critical region.

As the system approaches equilibrium, it follows the hyperbolic curve defined (Eq. (21) and Fig. 6) by the total field at the surface of the straight wire. The portion of the $H_{tot}$ curve which actually corresponds to the path followed by the system for a given I (solid portions shown in Fig. 23) is relatively small compared to the allowed values. The length of the actual path is dictated by the choice of the change in the external control current. The larger the increase in I, then the longer the total field path. Note that here the "lengths" referred to are not in time but ranges of $i_w/I$. Three such portions are shown in Fig. 23. The circles represent points between which data is actually recorded. The curves in Fig. 23 show that the total magnetic field $H_{tot}$ at the surface of the wire decreases during the current reapportionment for values of $i_w/I$ greater than 0.408. It turns out that this is the case for all values of external control current I below 28.0 amperes for this particular experimental arrangement. At I = 28.0 amp, the magnetic field

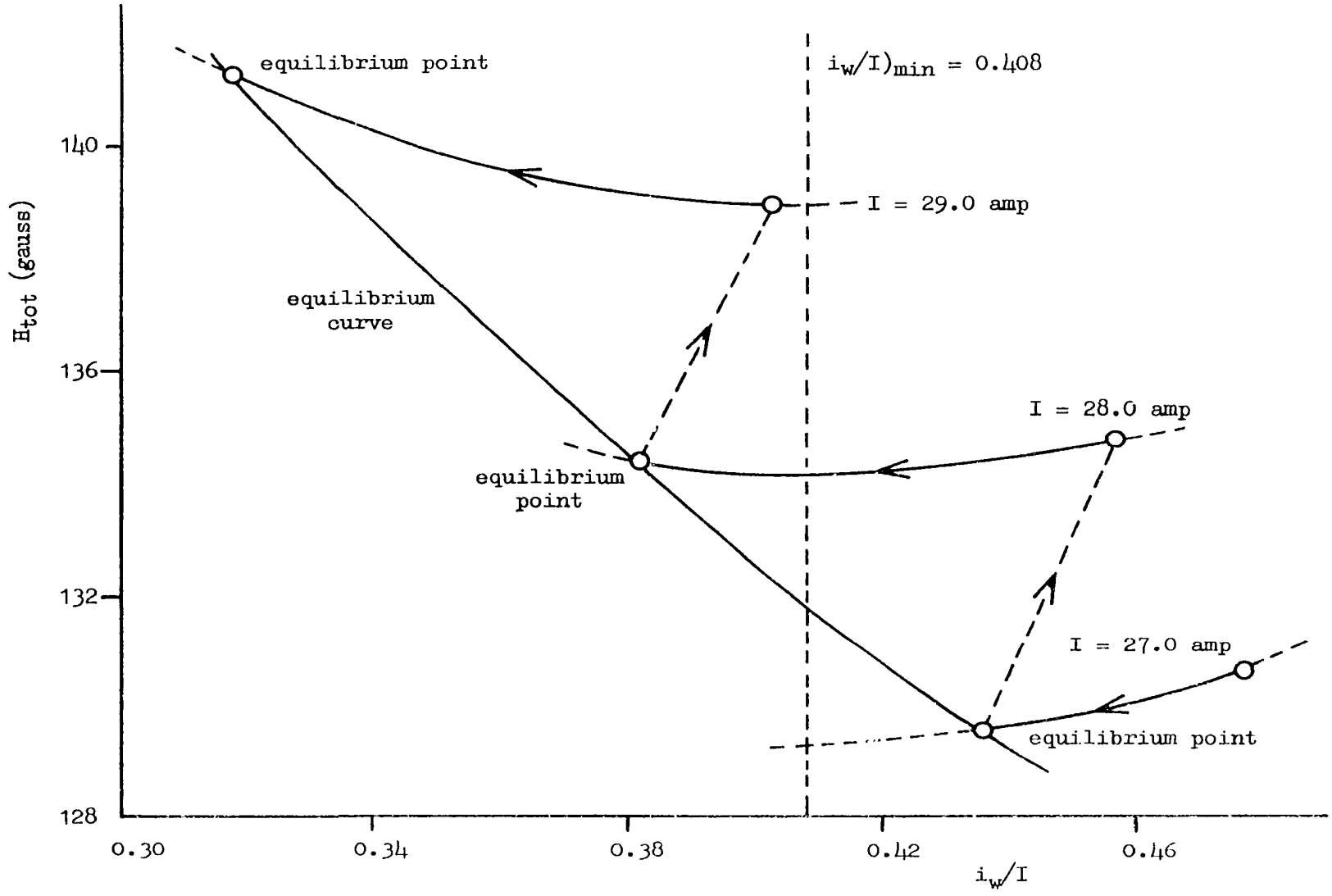


Fig. 23.--Behavior of $H_{tot}$ near $i_w/I)_{min}$.

passes through the minimum, defined by Eq. (22), and begins to increase during the reapportionment. For values of $i_w/I$ less than 0.408, the magnetic field begins an increase as current reapportionment takes place and the wire loses current. Notice that the changes of the total magnetic field involved are less than 5 per cent for the particular value of I used in this investigation. When I is increased, the system moves up to the corresponding $H_{tot}$ curve along the dotted lines shown in Fig. 23. The arrows represent the "path" followed by the circuit during the course of an experiment. The solid lines are for constant I, and the dotted are merely schematic representations of the result of current increases of $\Delta I = 1$ amp.

Dissipation of energy ceases as the wire reduces its current and a steady state is reached. This equilibrium state is defined by Eq. (19). The equilibrium state of the system is characterized by a constant threshold current ratio $S_i$, as may be seen from Table V. In this table, $i_{wc}$ is the steady-state value of $i_w$, $H_s$ is the longitudinal field corresponding to the steady-state value of $i_s$, $i_c$ is the Silsbee critical current as obtained using $H_c = 180$ gauss in Eq. (15), and $S_i$ is the ratio of $i_{wc}$ to $i_c$. Not all of the values for $i_w/I$ are used. For values near the second critical point, $S_i$ does not appear to be a constant. Notice that the functional relation between $i_{wc}$ and $H_s$ is such that the change in $i_{wc}$ is small for a given change in $H_s$ for the range of $H_s$ used here.

The characteristic equilibrium curve is shown in Fig. 24. The solid line in Fig. 24 is the theoretical curve predicted by Eq. (19) and the circles are experimental points (given in Table 8 of Appendix B). The calculated curve is obtained by using the steady-state values of $i_w/I$

TABLE V

THE THRESHOLD CURRENT RATIO FOR VARIOUS VALUES OF APPLIED LONGITUDINAL FIELDS

| $i_{wc}$ | $i_c$ | $S_i$ | $H_s$ |
|---|---|---|---|
| 13.970 | 23.984 | 0.582 | 3.300 |
| 13.762 | 23.966 | 0.574 | 7.708 |
| 13.643 | 23.908 | 0.571 | 14.677 |
| 13.715 | 23.833 | 0.575 | 20.451 |
| 13.718 | 23.718 | 0.577 | 26.908 |
| 13.764 | 23.592 | 0.583 | 32.597 |
| 13.864 | 23.442 | 0.591 | 38.200 |
| 13.677 | 23.206 | 0.589 | 45.596 |
| 13.402 | 22.903 | 0.585 | 53.532 |
| 13.242 | 22.581 | 0.586 | 60.756 |
| 12.976 | 22.176 | 0.585 | 68.635 |
| 12.546 | 21.649 | 0.580 | 77.538 |
| 12.048 | 21.011 | 0.573 | 86.868 |
| 11.787 | 20.400 | 0.578 | 94.718 |

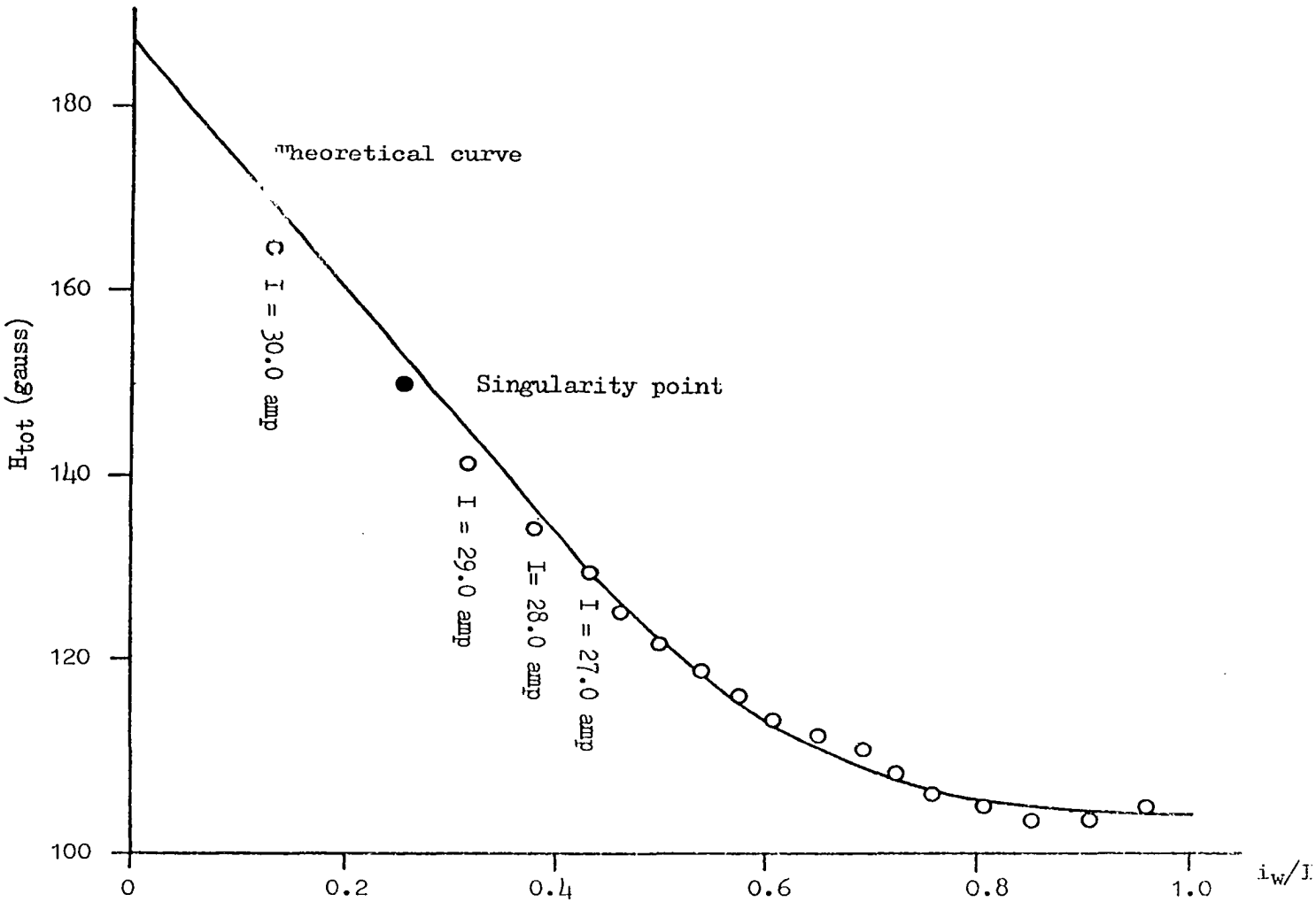


Fig. 24.--The equilibrium curve for the coupled persistatron.

for several I of the experiment in Eq. (19). The point for $i_w/I = 0$ is found by assuming that $S_i = 0$ if there is no current in the wire. The critical field used is $H_c = 180$ gauss. It should be emphasized that the solid line is a curve of constant $S_i$. The close experimental fit in Fig. 24, which verifies the postulated Eq. (16), is one of the most significant accomplishments of this investigation.

When I is increased, the system is moved up to a new $H_{tot}$ curve, off the equilibrium curve, and into a region of instability (as in Fig. 23). The system can reduce the magnetic pressure on the straight wire by reducing the amount of the current carried by the wire. That is, the total magnetic field is reduced until the system returns to the equilibrium curve. (The three equilibrium points of Fig. 23 have been noted on Fig. 24 for comparison.)

If the $H_{tot}$ curve that the system is on has passed through its minimum before reaching the equilibrium curve, the magnetic field must be increased in order for the system to return to this curve. In other words, the system cannot reduce the magnetic pressure on the wire by reducing the wire current, for example the 29.0 amp curve.

The singularity point represented on Fig. 24 is the point beyond which the system cannot come to equilibrium; that is, it is the second critical point of the circuit $I_{2c}$ (refer to Eq. (35) ). For the set of data under consideration, this singularity point occurs for I = 30.0 amp when

$$i_w/I = 0.258,$$

$$H_{tot} = 150.3 \text{ gauss};$$

$$S = 0.835.$$

When the circuit is recycled, that is, returned to the virgin state and

run again, this point where $H_s = 138.6$ gauss occurs for the I = 29.0 amp curve. Notice that the singularity point does not represent the place at which the total magnetic field at the surface of the straight wire becomes critical, that is, $H_{tot} \neq H_c$ at the singularity point. However, the fact that $S = H_{tot}/H_c = 0.835$ indicates that the assumption $H_{tot} = H_c$ at the singularity point is a reasonable one.

In Fig. 24 the point labeled as I = 30.0 amp does not represent an equilibrium point since it is beyond the singularity point. It represents a point recorded during the transition of the wire into the normal state and is rather arbitrary. This transition at the second critical point is very rapid for a well annealed sample. However, for a sample with many pinning centers, this transition may require as long as one hour to complete. This enables the sample to remain in the superconducting state for fields higher than that dictated by the singularity point for a given time. Nonetheless, the system cannot reach a stable equilibrium regardless of the amount of pinning. If the pinning is great enough, it may approach a metastable equilibrium. For example, for an unannealed sample the system will not come to equilibrium in the time observed here (say four to six hours) but neither will it reach the second critical point.

While the system is approaching the equilibrium curve (solid lines of Fig. 23), the Lorentz force on the flux lines is changing. Using the Lorentz force calculated from the perfect diamagnetism model, Eq. (34), a plot of the behavior is shown in Fig. 25 (data may be found in Tables 7 and 8 of Appendix B). As the current reapportionment takes place, and the wire loses current, this Lorentz force decreases. However, it does not decrease to the same value each time, as I is moved upward in steps

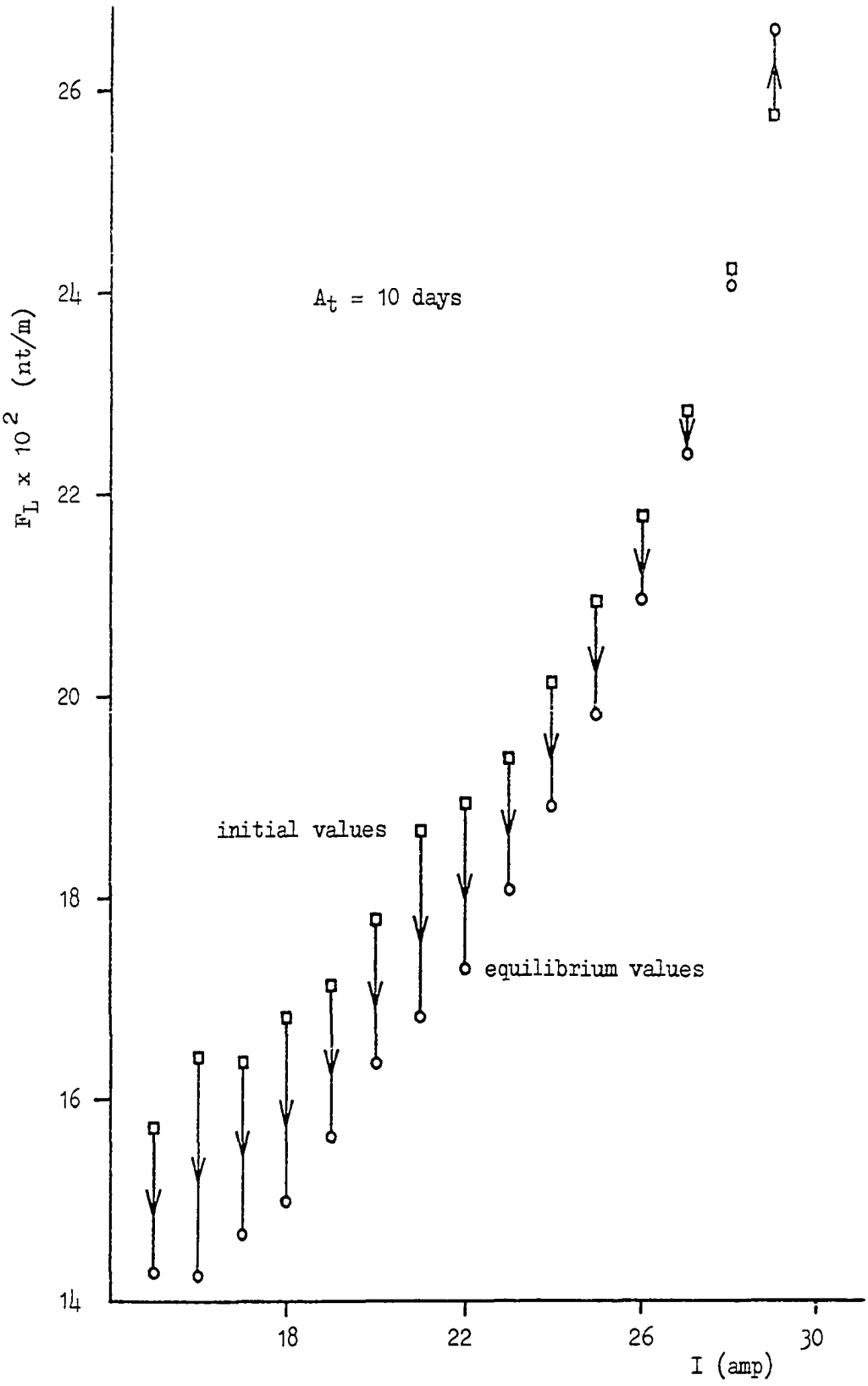


Fig. 25.--Behavior of Lorentz force for each reapportionment.

toward $I_{2c}$. Notice that the final or equilibrium value of the force is larger after every increase in the external control current.

This process of decreasing force with each $\Delta I$ continues until the system reaches a $H_{tot}$ curve for which the equilibrium state is beyond the minimum of the $H_{tot}$ curve. After this occurs, the force begins to increase as the reapportionment takes place. One interesting result from this graph is that the system can come to equilibrium at I = 29.0 amp even though the force is increasing. This can continue to happen until the singularity point is reached. For I = 28.0 amp, the force actually decreases for a while then increases once the minimum is passed; however, the net change results in a decrease.

It is informative to consider the threshold field ratio,

$$S = H_{tot}/H_c',$$

at the equilibrium states. This ratio is plotted as a function of the longitudinal magnetic field $H_s$ at each equilibrium site in Fig. 26 (data in Table 8 of Appendix B). This plot suggests that the threshold field $H_c'$ approaches the critical field as the longitudinal field is increased. In other words, the threshold field ratio S is a function of applied longitudinal field. This plot implies that the threshold ratio increases as the current contribution to the total magnetic field decreases. The value of S for very low fields is not recorded in Fig. 26. When the data on the time curves were recorded, the object was to get the circuit into the critical region and little care was taken in approaching the first critical point.

In this last section, the characteristics of the equilibrium state, to which the system tends, after an increase in $i_w$ have been found. This

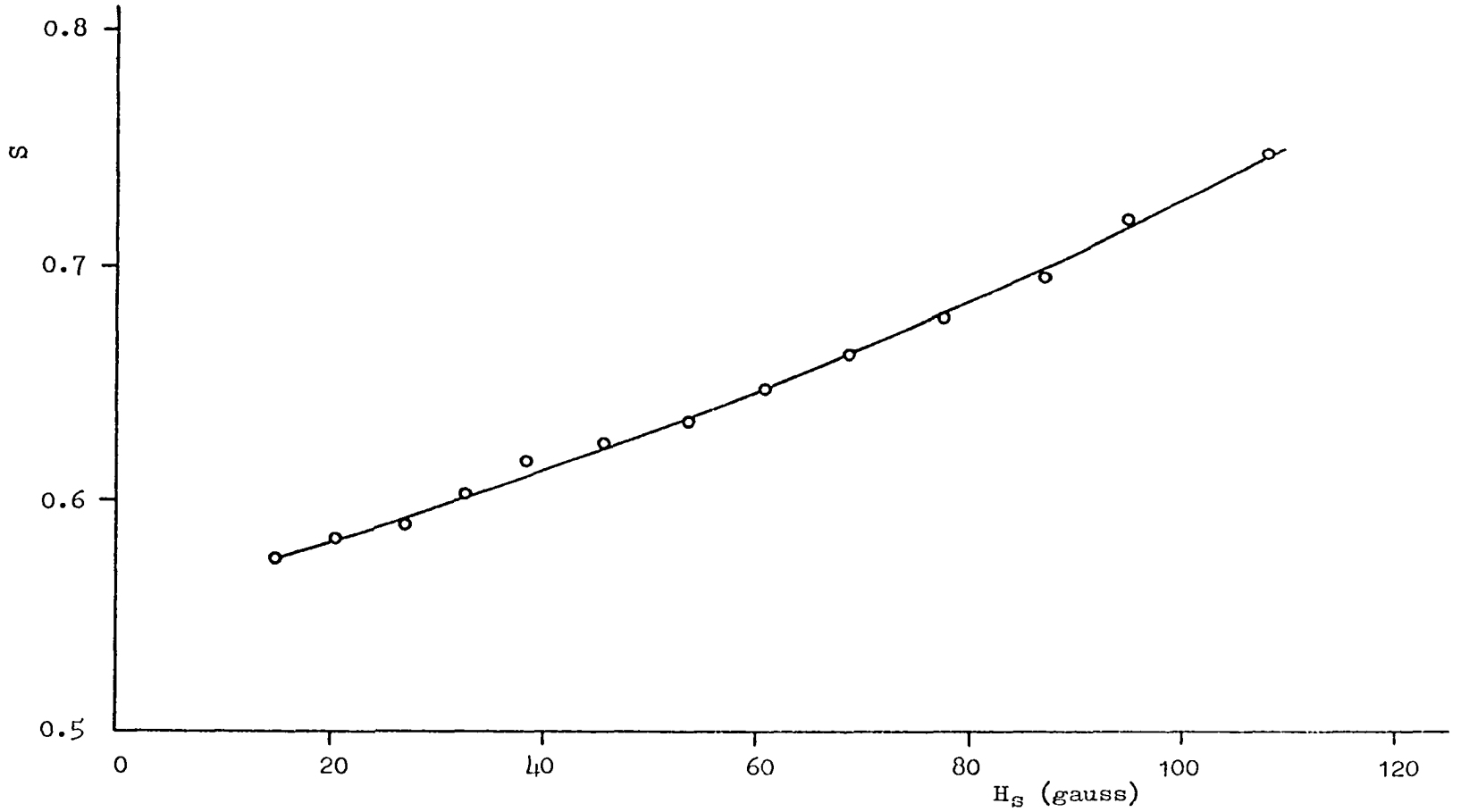


Fig. 26.--Dependence of the threshold ratio on the externally applied longitudinal magnetic field.

steady state is characterized by a constant threshold current ratio $S_i$; that is, the threshold current is a given fraction of the critical current regardless of the applied longitudinal field. This steady state is also characterized by an increasing total equilibrium field; that is, the ratio of the total threshold field to the total critical field increases as the transport current decreases.

# CHAPTER V

## CONCLUSION

The coupled persistatron has been used to study the dissipation of energy in a current-carrying superconducting wire. In other words, the stability of the superconducting state in the presence of a transport current has been investigated for a cylindrical type-I superconductor with its length much greater (by a factor of about 50) than its diameter.

As indicated by four-probe measurements, the earliest dissipation in a wire may occur below the critical current. The point at which dissipation is first observed to occur has been referred to as the threshold point. In the case of decaying current in the wire, this is also the point at which dissipation ceases. In other words, the threshold point is the point at which dissipation begins or ceases depending on the "region" from which the point is approached.

The threshold point is discussed in terms of the threshold field $H_c'$ and the threshold current $i_{wc}$ by forming ratios. The threshold field ratio is given by

$$S = H_c'/H_c,$$

and the threshold current ratio by

$$S_i = i_{wc}/i_c,$$

where $H_c$ is the bulk critical field and $i_c$ is the critical current obtained by applying Silsbee's rule. According to Silsbee's hypothesis,

$$S_i = S = 1.$$

The coupled persistatron in this investigation indicated that these ratios can be as small as 0.5. Rather than contradict Silsbee's hypothesis, the critical current should be redefined as the current for which at least 50 per cent of the normal state resistance is restored to the wire, not the current (since $S < 1$) at which dissipation first begins.

This threshold phenomenon was found to be independent of temperature and the annealing state of the wire. However, it was found to be a function of the diameter of the wire. Since an uncoupled circuit (simple persistatron) yielded much the same results, it is not believed to be a paramagnetic effect[37] for which superconducting regions are aligned with the spiraling magnetic field produced by an azimuthal field and a longitudinal field causing the current to spiral in the same direction giving rise to an internal magnetic field larger than the applied field.

As shown in Fig. 26, the threshold field ratio is a function of applied longitudinal field $H_s$. This ratio increases as the longitudinal field is increased. Since the current-carrying capacity of the wire decreases with increasing applied field, the increase in S with $H_s$ may possibly indicate that S would be unity in the absence of a transport current. In the event of no applied field, $S = S_i$. For a wire of diameter approximately 0.5 mm, this means that

$$H_c' = 0.5\, H_c.$$

Note that this condition when dissipation begins should not be confused with the condition that $H = 0.5\, H_c$ when the intermediate state of a cylinder in a transverse magnetic field first forms. For the latter case, H is the value of the applied transverse field when the superfluid

state of the cylinder breaks down. However, the field strength at the surface of the cylinder or wire is critical. In the former case, which is investigated here, the field $H_c'$ is the field at the surface of the wire when the superfluid state becomes unstable.

The threshold current ratio has been found to be independent of the applied longitudinal field. It is a constant for a particular wire, depending only (as far as the results here indicate) on the diameter of the wire. It is this ratio that is taken to be the fundamental quantity in describing the onset of dissipation. In other words, Silsbee violations are believed to occur only when the total magnetic field is composed in part of an azimuthal field produced by a transport current.

The physical reason for the difference in behavior of a wire when carrying a transport current and when subjected to a longitudinal magnetic field may be seen by considering the stability of the superfluid state. In the case of the longitudinal field, any diameter of superconducting material is stable. This field is not "self-increasing" in the sense that small fluctuations in the superfluid state will not allow a field less than $H_c$ to penetrate the wire. In other words, though fluctuations may occur due to the longitudinal field, there is no tendency for a fluctuation to grow because of the field penetration. However, in the presence of an azimuthal field produced by a transport current, the superfluid state is probably not so stable. A decrease in the effective radius of the superconducting material due, for example, to small fluctuations at the surface would result in an increase in this field strength because of its $1/r$ dependence. Therefore, a wire carrying a current that is near critical is in a far less stable equilibrium than one simply located in a longitudinal field. As soon as any portion of the surface sheath becomes normal,

there is a tendency for the surface current density in that region to increase (due to the admitting of flux at that spot) and precipitate the transition into the normal state[38].

This investigation suggests that the superfluid state becomes unstable in the presence of a transport current considerably below the superconducting-normal transition, and the superconductor passes into a superconducting-intermediate transition state. It should be emphasized that the S-I transition state,

$$S_i \; i_c \leq i \leq i_c,$$

is not an intermediate state. The intermediate state is taken to be that state for which macroscopic normal domains exist in the superconductor; for a current-induced intermediate state, the transport current is greater than $i_c$. This means that the voltages which may be observed in the intermediate state are due to the transport current flowing through normal regions which span the whole specimen.

The dissipation observed in this investigation is not believed to be due to this mechanism, but is assumed to be due to fluctuations. Consider the surface sheath of the superconducting wire in which the current flows to be divided into many small segments. The probability that a segment or spot will suffer a fluctuation to the normal state is nonzero. As the transport current is increased more segments will undergo, simultaneously, a fluctuation between the superconducting and normal states (s-n fluctuation). At some point the number of such events will be sufficient to produce observable dissipation in the wire. It is suggested that this point is the threshold point. Microscopically this threshold point is not a sharply-defined point at which dissipation begins, if it

is to be attributed to fluctuations. As sensitivity is increased, probably smaller dissipation yet could be seen.

Consider now the radius dependence of the threshold current ratio $S_i$ as observed in this work. The basic reason to expect this is that in a smaller wire a smaller s-n fluctuation can be effective in producing dissipation. In the longitudinal field configuration, there is no "regenerative" process which causes fluctuations to grow. In the current-produced case, a fluctuation reduces the effective radius of the superconducting material at a spot, that is, increases the effective current density, and thereby increases the azimuthal field produced by the current in the wire. This in turn causes the growth of this small normal volume until some flux is admitted. This all is assumed to occur on a microscopic scale and the normal spots formed are not "strong" enough to cause a cascading effect which precipitates the normal state. Instead, these spots probably tend to "drift" away and the current sheath at the place where it is formed "heals" itself after a short time. If the spots are strong enough, they will not drift away, and the spot may increase in size.

The first objective of finding the point at which dissipation begins has been accomplished. Further work is needed beyond this to verify that dissipation of energy is indeed occurring and to verify the conclusion that the threshold current ratio is a constant, characteristic of the particular wire diameter. This work has been done by observing the behavior of the wire when $i_w$ is increased above $i_{wc}$ and by observing the equilibrium state of the system.

Consider now the behavior of the wire when the current is increased above the threshold point. Langer and Amegaokar[39] asserted that "any state

of nonzero supercurrent is metastable in the sense that there is a topologically accessible fluctuation which leads to a state of lower current and, therefore, lower free energy". These fluctuations are dominant near the superconducting-normal transition[40]. Near the transition temperature and close to the critical current, small segments of the superconductor undergo a thermodynamic fluctuation to the normal state. Intrinsic quantum fluctuations have been observed in tin whisker crystals[41].

It is believed that dissipation-producing fluctuations are observed for this work even though the state of the sample is well below the transition temperature. When $i_w$ is increased above $i_{wc}$, a current reapportionment occurs within the coupled persistatron during which the wire loses current to the solenoid. The current decay in the wire is observed to be exponential in time.

The time constant of the exponential was found to be a function of both the annealing and the transport current $i_w$. Fig. 18 shows how the time curves become very long (small time constants) as the wire loses current (for large values of I). As already implied, it is the azimuthal field $H_w$ of the transport current that causes the superfluid state to become unstable below the critical point. Therefore, as $i_w$ decreases, the superconducting state becomes more stable; that is, it is presumably more capable of resisting the magnetic pressure. As a possible consequence, the magnetic field change takes a longer time to complete due to the decrease in regenerative fluctuations.

The time constant is also a function of the duration of annealing. A sample with little annealing has very long rise times (small R/L), as shown in Fig. 20. As the specimen is annealed, the time required for the

reapportionment to take place decreases. The time constant increases by a factor of more than 100 over a period of 30 days at 100°C. It is believed that the long relaxation time for the imperfect indium crystalline samples is due to flux trapping by grain boundaries[42]. While reapportionment is taking place in the circuit, the magnitude and direction of the magnetic field inside a surface layer, on the order of the penetration depth, is changing. The grain boundaries, consisting of atoms with high free energy, offer impedance to this motion. As the grains grow and the boundaries disappear, this impedance to flux changes is reduced.

As the wire loses current to the solenoid during current reapportionment, the system approaches the state of equilibrium shown in Fig. 24. This equilibrium curve was predicted by assuming that the threshold current $i_{wc}$ is a constant fraction of the critical current $i_c$, Eq. (16). The procedure is to modify the Silsbee hypothesis, as done in Eq. (17). The resulting equilibrium curve, Eq. (19), is shown in Fig. 24 as a solid line. It should be emphasized that the solid line in this figure is an actual theoretical curve drawn through calculated points not shown on the graph.

The exponential decay of $i_w > i_{wc}$ is a good indication that the phenomenon investigated here is, in fact, dissipation of energy, and the close experimental fit to Eq. (19) indicates that this dissipation occurs below the critical current. It also supports the assertion that $S_i$ is a constant for a particular wire. (This fit was done using $H_c$ = 180 gauss, which shows that the decision to use this value throughout was a good one.)

The results of this investigation suggest several areas of further study:

(1) A more complete diameter-dependence curve, Fig. 16, should be

obtained. This would involve using wires up to 4 mm in diameter and down to less than 0.1 mm in diameter. The range of the flat portion of the curve should be investigated.

(2) A good check on these results, which would possibly be easier to analyze, would be to use the uncoupled circuit (simple persistatron) to study the dependence of $S_i$ and S on a longitudinal field (applied by a source external to the loop) and a transport current. A heater or field coil could be used to keep the sensing solenoid (high inductance branch of the simple persistatron) normal as a current larger than the threshold current is applied to the wire (low inductance branch of the simple persistatron). The control coil could then be switched off and the time behavior of the resulting apportionment monitored. In this manner the actual critical current (as opposed to the threshold current) of the wire could be reached.

(3) The constants of the circuit could be adjusted so that the critical region would span a wider range of values. In this way, the equilibrium curve, Fig. 24, could be experimentally extended to $i_w/I = 0$.

(4) More extensive work could be done with the four-probe technique for the purpose of comparison.

(5) Superheating in the straight wire of the coupled persistatron was observed several times during the course of this investigation. It did not occur with enough regularity to be studied in detail. The experimental manifestation of this phenomenon was the occasional absence of a time curve once the external control current was increased. In other words, the indium wire would take the full increase in I (sometimes as much as two or three amperes without dissipating energy. The amount of

recrystallization and the rate of annealing (as well as the temperature of annealing) probably determine the amount of superheating observed. Such results did not appear in the data used in this thesis.

(6) The entire investigation should be repeated for other type-I materials, such as tin and lead, and possibly for a type-II material such as In-Tl.

(7) A liquid helium analog could probably be found. The angular momentum of a rotating system could be the analog of the magnetic field. The angular velocity of a channel through which superfluid helium is flowing could possibly affect the rate at which vortices are formed in the channel.

LIST OF REFERENCES


1. M. J. Buckingham, Proc. Vth Int. Conf. on Low Temp. Physics and Chemistry, (edited by J. R. Dillinger), p. 229, University of Wisconsin Press, Madison (1958).

2. K. J. Carroll, H. L. Laquer, E. F. Hammel, Bull. Am. Phys. Soc. 11, 345 (1966).

3. H. L. Laquer, K. J. Carroll, E. F. Hammel, Phys. Lett. 21, 397 (1966).

4. P. T. Sikora, E. F. Hammel, W. E. Keller, Physica 32, 1693 (1966).

5. W. M. Van Alphen, R. DeBruyn Ouboter, K. W. Taconis, Phys. Lett. 24A, 380 (1967).

6. P. T. Sikora, K. J. Carroll, L. K. Sisemore, J. E. Nicholson, Cryogenics 10, 233 (1970).

7. A. C. Rose-Innes, E. H. Rhoderick, Introduction to Superconductivity, Pergamon Press, New York (1969).

8. F. B. Silsbee, Bull. Bur. Stand. 14, 301 (1918).

9. E. A. Lynton, Superconductivity, Barnes & Noble, Inc., New York (1964).

10. A. Meshkovsky, A. Shalnikov, JETP USSR 17, 871 (1947).

11. T. E. Faber, Proc. Roy. Soc. (London) 248A, 460 (1958).

12. D. C. Baird, Canad. J. Phys. 42, 1682 (1964).

13. W. DeSorbo, Phil. Mag. 112, 853 (1965).

14. P. Laeng, F. Haenssler, L. Rinderer, J. Low Temp. Phys. 4, 533 (1971).

15. F. London, Superfluids, vol. 1, Dover Publications Inc., New York (1961).

16. R. Freud, Acta. Phys. Polon. 35, 925 (1969).

17. R. B. Scott, J. Research Natl. Bur. Stand. 41, 581 (1948).

18. H. Meissner, R. Zdanis, Phys. Rev. 109, 681 (1958).

19. D. C. Baird, B. K. Mukherjee, Phys. Rev. B 3, 1043 (1958).

20. N. V. Sarma, A. Wilcockson, Phil. Mag. 20, 539 (1969).

21. P. R. Solomon, Phys. Rev. 179, 475 (1969).

22. A. M. Shrager, Elementary Metallurgy and Metallography, MacMillan Company, New York (1949).

23. A. W. Grosvenor, Basic Metallurgy, vol. 1, American Soc. for Metals, Cleveland (1954).

24. J. Newton, An Introduction to Metallurgy, John Wiley & Sons, Inc., New York (1951).

25. M. C. Smith, Principles of Physical Metallurgy, Harper & Brothers, New York (1956).

26. W. Boas, An Introduction to the Physics of Metals and Alloys, John Wiley & Sons, Inc., New York (1949).

27. C. Dasarthy, Z. Metallkunde 61, 121 (1970).

28. L. K. Sisemore, Behavior of a Self-Interacting, Multiply-Connected Superconducting Circuit, Thesis, University of Oklahoma, Norman (1969).

29. A. C. Rose-Innes, Low Temperature Techniques, The English Universities Press Ltd., Great Britian, p. 48 (1964).

30. A. C. Rose-Innes, Brit. J. Appl. Phys. 10, 452 (1959).

31. H. Levy, P. P. M. Meincke, Appl. Phys. Lett. 14, 387 (1969).

32. J. J. Winter, J. T. Breslin, H. A. Leupold, J. Appl. Phys. 40, 3862 (1969).

33. P. S. Swartz, H. R. Hart, Jr., Phys. Rev. 137, A818 (1965).

34. H. Meissner, Phys. Rev. 109, 668 (1958).

35. R. W. Shaw, D. E. Mapother, D. C. Hopkins, Phys. Rev. 120, 88 (1960).

36. J. E. Nicholson, Flux Motion in Lead-Indium Wires with Longitudinal Magnetic Fields, Dissertation, University of Oklahoma, Norman (1972).

37. H. Meissner, Phys. Rev. 97, 1627 (1955).

38. A. B. Pippard, Phil. Mag. 41, 243 (1950).

39. J. S. Langer, V. Amegaokar, Phys. Rev. 164, 498 (1967).

40. R. D. Parks, R. P. Groff, Phys. Rev. Lett. 18, 342 (1967).

41. W. W. Webb, R. J. Warburton, Phys. Rev. Lett. 20, 461 (1968).

42. J. C. Thompson, Phys. Rev. 102, 1004 (1956).

## APPENDIX A

### EQUIPMENT LIST

1. Ammeter, D. C., Weston Instruments, Inc., Model 931, No. 77636, 0 - 15 amp.

2. Ammeter, D. C., Weston Instruments, Inc., Model 931, No. 73556, 0 - 50 amp.

3. Chart Recorder, Keithley Instruments, Model 370.

4. Dewar System, H. S. Martin & Son, 4-inch inner dewar with matching nitrogen jacket dewar.

5. Furnace, Hevi-Duty Electric Co., Type 051-PT, 0 - 1000°C.

6. Hall Probe, Siemens RHY 18.

7. Milliammeter, D. C., Western Electric, KS-20006 L2, 0 - 50 milliamp.

8. Power Supply, Regulated D. C., Hewlett-Packard, Harrison 6428A, 0 - 20 volt, 0 - 45 amp.

9. Power Supply, Regulated D. C., Hewlett-Packard, Harrison 6268A, 0 - 40 volt, 0 - 30 amp.

10. Power Supply, D. C., Hewlett-Packard, 6217A, 0 - 50 volt.

11. Power Supply, Regulated D. C., Hewlett-Packard, 6214A, 0 - 10 volt, 0 - 1.0 amp.

12. Voltmeter, Digital D. C., Computer Products, 0 - 1.999 volt.

13. Voltmeter, D. C. Microvolt-Ammeter, Keithley Instruments, Model 153.

14. Voltmeter, D. C. Nanovolt Null Detector, Keithley Instruments, Model 147.

15. Vacuum Pump, Kinney Extra-High Volume Mechanical Pump.

16. Vacuum Pump, Welch Duo-Seal, Model 1400.

# APPENDIX B

## MISCELLANEOUS DATA TABLES

### TABLE 1

### DATA FOR THE $i_w(H)$ CURVE IN FIG. 13

| H (gauss) | $i_w$ (amp) | H (gauss) | $i_w$ (amp) |
|---|---|---|---|
| 0.000 | 18.45 | 89.456 | 15.35 |
| 3.441 | 18.45 | 92.896 | 15.00 |
| 6.881 | 18.40 | 96.337 | 14.75 |
| 10.322 | 18.40 | 99.777 | 14.40 |
| 13.762 | 18.35 | 103.218 | 14.20 |
| 17.203 | 18.30 | 106.659 | 13.85 |
| 20.644 | 18.30 | 110.099 | 13.50 |
| 24.084 | 18.25 | 113.540 | 13.00 |
| 27.525 | 18.10 | 116.980 | 12.65 |
| 30.965 | 18.10 | 120.421 | 12.20 |
| 34.406 | 18.05 | 123.862 | 11.85 |
| 37.847 | 17.90 | 127.302 | 11.30 |
| 41.287 | 17.80 | 130.743 | 10.80 |
| 44.728 | 17.65 | 134.183 | 10.30 |
| 48.168 | 17.50 | 137.624 | 9.70 |
| 51.609 | 17.40 | 141.065 | 9.15 |
| 55.050 | 17.30 | 144.505 | 8.45 |
| 58.490 | 17.15 | 147.946 | 7.70 |
| 61.931 | 16.95 | 151.386 | 6.75 |
| 65.371 | 16.80 | 154.827 | 5.70 |
| 68.812 | 16.70 | 158.268 | 3.75 |
| 72.253 | 16.35 | 159.988 | 3.00 |
| 75.693 | 16.20 | 160.848 | 2.60 |
| 79.134 | 16.10 | 161.708 | 2.00 |
| 82.574 | 15.85 | 162.568 | 1.40 |
| 86.015 | 15.60 | 163.428 | 0.20 |

TABLE 2

DATA FOR THE $V_w(i_w)$ CURVES OF FIG. 14

| $i_w$ (amp) | $V_w$ (μvolt) |
|---|---|
| H = 00.0 gauss | |
| 18.0 | 0.040 |
| 19.0 | 0.213 |
| 20.0 | 0.511 |
| 21.0 | 0.982 |
| H = 34.4 gauss | |
| 16.0 | 0.013 |
| 17.0 | 0.026 |
| 18.0 | 0.117 |
| 19.0 | 0.373 |
| 20.0 | 0.780 |
| H = 68.8 gauss | |
| 15.0 | 0.013 |
| 16.0 | 0.046 |
| 17.0 | 0.168 |
| 18.0 | 0.544 |
| 18.5 | 0.775 |
| H = 86.0 gauss | |
| 13.0 | 0.011 |
| 14.0 | 0.026 |
| 15.0 | 0.060 |
| 16.0 | 0.220 |
| 17.0 | 0.680 |

| $i_w$ (amp) | $V_w$ (μvolt) |
|---|---|
| H = 103.2 gauss | |
| 10.0 | 0.008 |
| 11.0 | 0.037 |
| 12.0 | 0.060 |
| 13.0 | 0.080 |
| 14.0 | 0.122 |
| 15.0 | 0.340 |
| 16.0 | 0.935 |
| H = 120.4 gauss | |
| 10.0 | 0.011 |
| 11.0 | 0.031 |
| 12.0 | 0.079 |
| 13.0 | 0.400 |
| 14.0 | 0.955 |
| H = 137.6 gauss | |
| 5.0 | 0.006 |
| 6.0 | 0.012 |
| 7.0 | 0.022 |
| 8.0 | 0.035 |
| 9.0 | 0.060 |
| 10.0 | 0.460 |

TABLE 3

DATA FOR THE R/L(I) CURVE IN FIG. 18
$A_t$ = 20 DAYS

| I (amp) | R/L ($sec^{-1}$) |
|---|---|
| 16.0 | 0.0704 |
| 17.0 | 0.0695 |
| 18.0 | 0.0712 |
| 19.0 | 0.0671 |
| 20.0 | 0.0593 |
| 21.0 | 0.0607 |
| 22.0 | 0.0547 |
| 23.0 | 0.0567 |
| 24.0 | 0.0520 |
| 25.0 | 0.0513 |
| 26.0 | 0.0398 |
| 27.0 | 0.0382 |
| 28.0 | 0.0180 |
| 29.0 | 0.0059 |

TABLE 4

DATA FOR $i_{wn}(t)$ FOR VARIOUS I IN FIG. 19
$A_t$ = 20 DAYS

| I = 24.0 amp | | | I = 27.0 amp | | |
|---|---|---|---|---|---|
| t (sec) | $i_w$ (amp) | $i_{wn}$ | t (sec) | $i_w$ (amp) | $i_{wn}$ |
| 0.00 | 14.360 | 1.000 | 0.00 | 13.408 | 1.000 |
| 0.47 | 14.342 | 0.986 | 0.16 | 13.386 | 0.986 |
| 2.97 | 14.196 | 0.872 | 2.66 | 13.253 | 0.903 |
| 5.47 | 14.059 | 0.765 | 5.16 | 13.143 | 0.834 |
| 7.97 | 13.958 | 0.687 | 7.66 | 13.020 | 0.757 |
| 10.47 | 13.867 | 0.616 | 12.66 | 12.824 | 0.634 |
| 12.97 | 13.789 | 0.555 | 15.16 | 12.746 | 0.586 |
| 15.47 | 13.716 | 0.498 | 17.66 | 12.664 | 0.534 |
| 17.97 | 13.652 | 0.448 | 20.16 | 12.586 | 0.486 |
| 20.47 | 13.584 | 0.395 | 22.66 | 12.522 | 0.446 |
| 22.97 | 13.520 | 0.345 | 25.16 | 12.463 | 0.409 |
| 25.47 | 13.469 | 0.306 | 27.66 | 12.413 | 0.377 |
| 27.97 | 13.419 | 0.267 | 32.66 | 12.307 | 0.311 |
| 30.47 | 13.378 | 0.235 | 35.16 | 12.257 | 0.280 |
| 32.97 | 13.337 | 0.203 | 37.66 | 12.225 | 0.260 |
| 35.47 | 13.296 | 0.171 | 40.16 | 12.189 | 0.237 |
| 37.97 | 13.268 | 0.149 | 42.66 | 12.157 | 0.217 |
| 40.47 | 13.246 | 0.132 | 45.16 | 12.134 | 0.203 |
| 42.97 | 13.218 | 0.110 | 47.66 | 12.097 | 0.180 |
| 45.47 | 13.200 | 0.096 | 52.66 | 12.056 | 0.154 |
| 47.97 | 13.182 | 0.082 | 55.16 | 12.038 | 0.143 |
| 50.47 | 13.168 | 0.071 | 57.66 | 12.015 | 0.129 |
| 52.97 | 13.154 | 0.060 | 60.16 | 11.992 | 0.114 |
| 55.47 | 13.145 | 0.053 | 62.66 | 11.974 | 0.103 |
| 60.47 | 13.140 | 0.050 | 65.16 | 11.965 | 0.097 |
| 62.97 | 13.136 | 0.046 | 67.66 | 11.951 | 0.089 |
| 65.47 | 13.127 | 0.039 | 75.16 | 11.924 | 0.071 |
| 67.97 | 13.122 | 0.036 | 77.66 | 11.919 | 0.069 |
| 72.97 | 13.118 | 0.032 | 82.66 | 11.915 | 0.066 |
| 77.97 | 13.113 | 0.028 | 90.16 | 11.901 | 0.057 |
| 85.47 | 13.104 | 0.021 | 100.16 | 11.896 | 0.054 |
| 92.97 | 13.099 | 0.018 | 110.16 | 11.878 | 0.043 |
| --- | 13.077 | 0.000 | --- | 11.809 | 0.000 |

TABLE 4--Continued

| I = 28.0 amp | | | I = 29.0 amp | | |
|---|---|---|---|---|---|
| t (sec) | $i_w$ (amp) | $i_{wn}$ | t (sec) | $i_w$ (amp)[a] | $i_{wn}$ |
| 0.00 | 12.809 | 1.000 | 0.00 | 12.128 | 1.000 |
| 5.62 | 12.567 | 0.887 | 20.00 | 11.635 | 0.854 |
| 15.62 | 12.225 | 0.726 | 60.00 | 10.968 | 0.656 |
| 25.62 | 11.960 | 0.603 | 80.00 | 10.726 | 0.584 |
| 35.62 | 11.750 | 0.504 | 100.00 | 10.511 | 0.520 |
| 45.62 | 11.567 | 0.419 | 140.00 | 10.164 | 0.417 |
| 55.62 | 11.425 | 0.353 | 160.00 | 10.018 | 0.374 |
| 65.62 | 11.284 | 0.286 | 180.00 | 9.885 | 0.335 |
| 75.62 | 11.201 | 0.248 | 220.00 | 9.657 | 0.267 |
| 85.62 | 11.133 | 0.216 | 240.00 | 9.556 | 0.237 |
| 95.62 | 11.069 | 0.186 | 260.00 | 9.474 | 0.213 |
| 105.62 | 11.009 | 0.158 | 300.00 | 9.328 | 0.169 |
| 115.62 | 10.959 | 0.135 | 320.00 | 9.264 | 0.150 |
| 125.62 | 10.918 | 0.115 | 340.00 | 9.209 | 0.134 |
| 135.62 | 10.877 | 0.096 | 380.00 | 9.099 | 0.102 |
| 145.62 | 10.836 | 0.077 | 400.00 | 9.063 | 0.091 |
| 155.62 | 10.799 | 0.060 | 420.00 | 9.035 | 0.083 |
| 170.62 | 10.781 | 0.051 | 460.00 | 8.958 | 0.060 |
| 180.62 | 10.763 | 0.043 | 480.00 | 8.930 | 0.051 |
| 195.62 | 10.749 | 0.036 | 500.00 | 8.898 | 0.042 |
| 205.62 | 10.740 | 0.032 | 540.00 | 8.834 | 0.023 |
| 215.62 | 10.731 | 0.028 | 570.00 | 8.811 | 0.016 |
| 225.62 | 10.726 | 0.026 | 590.00 | 8.784 | 0.008 |
| 235.62 | 10.722 | 0.024 | 630.00 | 8.770 | 0.004 |
| 250.62 | 10.712 | 0.019 | 650.00 | 8.766 | 0.003 |
| 270.62 | 10.708 | 0.017 | 670.00 | 8.761 | 0.001 |
| ---- | 10.671 | 0.000 | ---- | 8.757 | 0.000 |

[a] There is a systematic error of +0.457 amp in the values of $i_w(t)$ for I = 29.0 amp due to a mistake in nulling the Hall voltage for the I = 28.0 amp curve. However, this does not affect the values of $i_{wn}(t)$.

TABLE 5

DATA FOR THE R/L($A_t$) CURVES IN FIG. 20

| | R/L ($sec^{-1}$) | |
|---|---|---|
| $A_t$ (days) | Plateau[a] | I = 28.0 amp |
| 1 | 0.0011 | ---- |
| 5 | 0.0180 | ---- |
| 10 | 0.0201 | 0.0073 |
| 15 | 0.0497 | 0.0112 |
| 20 | 0.0689 | 0.0180 |
| 30 | 0.1334 | 0.0294 |

[a] The "plateau" refers to the range of external control current given by the following: $15.0 \leq I \leq 18.0$ amp. The R/L value recorded in this column is an average over the plateau region.

TABLE 6

DATA FOR THE $i_{wn}(t)$ CURVES FOR
VARIOUS $A_t$ FOUND IN FIG. 21
I = 17.0 AMP

| $A_t$ = 30 days | | | $A_t$ = 20 days | | |
|---|---|---|---|---|---|
| t (sec) | $i_w$ (amp) | $i_{wn}$ | t (sec) | $i_w$ (amp) | $i_{wn}$ |
| 0.00 | 15.401 | 1.000 | 0.00 | 15.013 | 1.000 |
| 0.94 | 15.305 | 0.906 | 1.40 | 14.926 | 0.905 |
| 2.19 | 15.182 | 0.785 | 3.90 | 14.775 | 0.741 |
| 3.44 | 15.040 | 0.646 | 6.40 | 14.656 | 0.612 |
| 4.69 | 14.912 | 0.520 | 8.90 | 14.542 | 0.488 |
| 5.94 | 14.830 | 0.439 | 11.40 | 14.460 | 0.398 |
| 7.19 | 14.771 | 0.381 | 13.90 | 14.410 | 0.343 |
| 8.44 | 14.729 | 0.341 | 16.40 | 14.359 | 0.289 |
| 9.69 | 14.675 | 0.287 | 18.90 | 14.309 | 0.234 |
| 10.94 | 14.633 | 0.247 | 23.90 | 14.259 | 0.179 |
| 12.19 | 14.583 | 0.197 | 26.40 | 14.236 | 0.154 |
| 13.44 | 14.556 | 0.170 | 28.90 | 14.218 | 0.134 |
| 14.69 | 14.519 | 0.135 | 31.40 | 14.204 | 0.119 |
| 15.94 | 14.496 | 0.112 | 33.90 | 14.186 | 0.099 |
| 17.19 | 14.474 | 0.090 | 36.40 | 14.177 | 0.090 |
| 18.44 | 14.455 | 0.072 | 38.90 | 14.172 | 0.085 |
| 19.69 | 14.432 | 0.049 | 43.90 | 14.135 | 0.045 |
| 20.94 | 14.423 | 0.040 | 48.90 | 14.122 | 0.030 |
| 22.19 | 14.410 | 0.027 | 51.40 | 14.117 | 0.025 |
| 23.44 | 14.400 | 0.018 | 56.40 | 14.113 | 0.020 |
| 25.94 | 14.391 | 0.009 | 61.40 | 14.108 | 0.015 |
| 28.44 | 14.387 | 0.004 | 68.90 | 14.099 | 0.005 |
| --- | 14.382 | 0.000 | --- | 14.094 | 0.000 |

TABLE 6--Continued

| $A_t$ = 10 days | | | $A_t$ = 1 day | | |
|---|---|---|---|---|---|
| t (sec) | $i_w$ (amp) | $i_{wn}$ | t (min) | $i_w$ (amp) | $i_{wn}$ |
| 0.00 | 14.643 | 1.000 | 0.00 | 14.062 | 1.000 |
| 10.00 | 14.373 | 0.709 | 1.25 | 13.889 | 0.810 |
| 20.00 | 14.250 | 0.576 | 2.50 | 13.779 | 0.690 |
| 30.00 | 14.177 | 0.498 | 5.00 | 13.660 | 0.560 |
| 40.00 | 14.131 | 0.448 | 7.50 | 13.583 | 0.475 |
| 50.00 | 14.090 | 0.404 | 10.00 | 13.523 | 0.410 |
| 60.00 | 14.049 | 0.360 | 12.50 | 13.482 | 0.365 |
| 70.00 | 14.008 | 0.315 | 17.50 | 13.423 | 0.300 |
| 80.00 | 13.971 | 0.276 | 20.00 | 13.386 | 0.260 |
| 90.00 | 13.939 | 0.241 | 22.50 | 13.354 | 0.225 |
| 100.00 | 13.912 | 0.212 | 25.00 | 13.331 | 0.200 |
| 110.00 | 13.880 | 0.177 | 28.75 | 13.295 | 0.160 |
| 120.00 | 13.848 | 0.143 | 32.50 | 13.258 | 0.120 |
| 130.00 | 13.825 | 0.118 | 37.50 | 13.217 | 0.075 |
| 140.00 | 13.797 | 0.089 | 40.00 | 13.194 | 0.050 |
| 150.00 | 13.765 | 0.054 | 42.50 | 13.181 | 0.035 |
| 160.00 | 13.752 | 0.039 | 46.25 | 13.167 | 0.020 |
| 170.00 | 13.720 | 0.005 | 48.75 | 13.153 | 0.005 |
| ---- | 13.715 | 0.000 | --- | 13.149 | 0.000 |

TABLE 7

INITIAL VALUES OF USEFUL QUANTITIES

| I (amp) | $i_w$ (amp) | $i_w/I$ | $H_w$ (gauss) | $H_s$ (gauss) |
|---|---|---|---|---|
| 14.5 | 14.148 | 0.976 | 106.181 | 2.190 |
| 15.0 | 14.470 | 0.965 | 108.597 | 3.300 |
| 16.0 | 14.762 | 0.923 | 110.789 | 7.708 |
| 17.0 | 14.643 | 0.861 | 109.896 | 14.677 |
| 18.0 | 14.715 | 0.818 | 110.436 | 20.451 |
| 19.0 | 14.678 | 0.772 | 110.158 | 26.908 |
| 20.0 | 14.764 | 0.738 | 110.804 | 32.597 |
| 21.0 | 14.864 | 0.708 | 111.554 | 38.200 |
| 22.0 | 14.677 | 0.667 | 110.151 | 45.596 |
| 23.0 | 14.402 | 0.626 | 108.087 | 53.532 |
| 24.0 | 14.242 | 0.593 | 106.886 | 60.756 |
| 25.0 | 13.976 | 0.559 | 104.890 | 68.635 |
| 26.0 | 13.546 | 0.521 | 101.663 | 77.538 |
| 27.0 | 13.048 | 0.483 | 97.925 | 86.868 |
| 28.0 | 12.787 | 0.457 | 95.966 | 94.719 |
| 29.0 | 11.685 | 0.403 | 87.696 | 107.803 |
| 30.0 | 10.223 | 0.341 | 76.724 | 123.134 |

TABLE 7--Continued

| $H_w/H_s$ | $H_{tot}$ (gauss) | sin θ | $F_L$ ($10^4$nt/m) |
|---|---|---|---|
| 48.484 | 106.204 | 0.9998 | 1503 |
| 32.908 | 108.647 | 0.9995 | 1573 |
| 14.373 | 111.057 | 0.9976 | 1643 |
| 7.488 | 110.872 | 0.9912 | 1638 |
| 5.400 | 112.314 | 0.9833 | 1681 |
| 4.094 | 113.397 | 0.9714 | 1713 |
| 3.399 | 115.499 | 0.9593 | 1778 |
| 2.920 | 117.913 | 0.9461 | 1865 |
| 2.416 | 119.215 | 0.9240 | 1894 |
| 2.019 | 120.617 | 0.8961 | 1938 |
| 1.759 | 122.947 | 0.8694 | 2014 |
| 1.528 | 125.350 | 0.8368 | 2094 |
| 1.311 | 127.857 | 0.7951 | 2178 |
| 1.127 | 130.902 | 0.7480 | 2283 |
| 1.013 | 134.838 | 0.7116 | 2423 |
| 0.813 | 138.968 | 0.6309 | 2574 |
| 0.623 | 145.081 | 0.5289 | 2804 |

TABLE 8

EQUILIBRIUM VALUES OF USEFUL QUANTITIES

| I (amp) | $i_w$ (amp) | $i_w/I$ | $H_w$ (gauss) | $H_s$ (gauss) |
|---|---|---|---|---|
| 14.5 | 13.970 | 0.963 | 104.845 | 3.300 |
| 15.0 | 13.762 | 0.917 | 103.284 | 7.708 |
| 16.0 | 13.643 | 0.853 | 102.391 | 14.677 |
| 17.0 | 13.715 | 0.807 | 102.931 | 20.451 |
| 18.0 | 13.678 | 0.760 | 102.653 | 26.908 |
| 19.0 | 13.764 | 0.724 | 103.299 | 32.597 |
| 20.0 | 13.864 | 0.693 | 104.049 | 38.200 |
| 21.0 | 13.677 | 0.651 | 102.646 | 45.596 |
| 22.0 | 13.402 | 0.609 | 100.582 | 53.532 |
| 23.0 | 13.242 | 0.576 | 99.381 | 60.756 |
| 24.0 | 12.976 | 0.541 | 97.385 | 68.635 |
| 25.0 | 12.546 | 0.502 | 94.158 | 77.538 |
| 26.0 | 12.048 | 0.463 | 90.420 | 86.868 |
| 27.0 | 11.787 | 0.436 | 88.461 | 94.718 |
| 28.0 | 10.685 | 0.382 | 80.191 | 107.803 |
| 29.0 | 9.223 | 0.318 | 69.219 | 123.134 |
| 30.0 | 4.023 | 0.134 | 30.193 | 161.733 |

TABLE 8--Continued

| $H_w/H_s$ | $H_{tot}$ (gauss) | S | sin θ | $F_L$ ($10^4$nt/m) |
|---|---|---|---|---|
| 31.771 | 104.897 | 0.583 | 0.9995 | 1466 |
| 13.400 | 103.571 | 0.575 | 0.9972 | 1429 |
| 6.976 | 103.438 | 0.574 | 0.9899 | 1426 |
| 5.033 | 104.943 | 0.583 | 0.9808 | 1467 |
| 3.815 | 106.121 | 0.589 | 0.9673 | 1500 |
| 3.169 | 108.320 | 0.602 | 0.9536 | 1563 |
| 2.724 | 110.840 | 0.616 | 0.9388 | 1637 |
| 2.251 | 112.317 | 0.624 | 0.9139 | 1681 |
| 1.879 | 113.940 | 0.633 | 0.8828 | 1730 |
| 16.36 | 116.481 | 0.647 | 0.8532 | 1808 |
| 1.419 | 119.141 | 0.662 | 0.8175 | 1891 |
| 1.214 | 121.975 | 0.678 | 0.7720 | 1982 |
| 1.041 | 125.387 | 0.696 | 0.7212 | 2095 |
| 0.934 | 129.603 | 0.720 | 0.6826 | 2238 |
| 0.744 | 134.358 | 0.749 | 0.5969 | 2405 |
| 0.562 | 141.256 | 0.785 | 0.4899 | 2659 |
| 0.187 | 164.527 | 0.914 | 0.1840 | 3597 |

## APPENDIX C

### COMPUTER PROGRAM

```
C     TIME CONSTANT CURVE
C     HC .. HALL CONSTANT
C     CK .. COIL CONSTANT
C     XI .. EXTERNAL CURRENT
C     N ... NUMBER OF POINTS
C     VH .. INITIAL HALL VOLTAGE
C     TI .. FIRST NON-ZERO VALUE OF TIME
C     XT .. INCREMENT OF TIME
C     MM .. SPACES BETWEEN POINTS ON PLOT
      DIMENSIONYY(101),A(2),T(100),VH(100),CR(100),XI1(100),XI2(
     +100),R(100),F(100)
C     THESE ARE SET FOR 360 OR 1130
      NW=5
      NR=2
C     INPUT PLOTTING FACTORS
      READ(NR,5)A(1),A(2)
    5 FORMAT(2A1)
C     HEADER CARDS
   82 READ(NR,501)
  501 FORMAT(80H
     +                                   )
      READ(NR,503)
  503 FORMAT(80H
     +                                   )
      READ(NR,505)
  505 FORMAT(80H
     +                                   )
C     INPUT HC,CK,XI
      READ(NR,1)HC,CK,XI
    1 FORMAT(3F10.2)
C     A CARD WITH HC=0 ENDS PROGRAM
      IF(HC)80,80,81
C     ENTER 1 FOR GRAPH OR 2 FOR TABLE AND GRAPH
C     ENTER 1 FOR RESISTANCE OR 0 FOR NONE
C     ENTER 1 FOR GIVEN END POINTS OR 2 FOR CALCULATED POINTS
   81 READ(NR,2)NN,MN,NPC
    2 FORMAT(I1,9X,I1,9X,I1)
C     INPUT N,VH,TI,XT,MM
      READ(NR,3)N,VH(1),TI,XT,MM
    3 FORMAT(I2,8X,3F10.2,I2)
```

```
      C=HC/CK
      T(1)=0.0
      TT=-XT
      DO 22 I=1,N
   22 CR(I)=0.0
C     ENTER CHART READINGS
      READ(NR,4)(CR(I),I=1,N)
    4 FORMAT(8F10.2)
      DO 10 I=1,N
      IF(CR(I))61,60,61
   60 IF(I-1)61,61,63
   61 VH(I)=VH(1)+CR(I)
      F(I)=HC*VH(I)
      XI2(I)=C*VH(I)
      XI1(I)=XI-XI2(I)
      GO TO 65
   63 XI1(I)=0.0
   65 TT=TT+XT
      TX=TI+TT
      II=I+1
   10 T(II)=TX
      C1=1.0/XI1(1)-XI1(N))
      C2=XI1(N)/(XI1(1)-XI1(N))
      IF(NN-1)90,90,91
   91 WRITE(NW,500)
  500 FORMAT(1H1)
      WRITE(NW,501)
      WRITE(NW,300)
  300 FORMAT(1H ,/)
      WRITE(NW,102)
  102 FORMAT(1H ,8X,'T',8X,'CR',8X,'H',8X,'I2',7X,'I1',8X,'R')
   90 DO 12 I=1,N
C     THIS STATEMENT CHECKS FOR A BLANK READING
      IF(XI1(I))71,70,71
   71 R(I)=C1*XI1(I)-C2
      T(I)=T(I)+0.005
      F(I)=F(I)+0.0005
      XI2(I)=XI2(I)+0.0005
      IF(XI1(I))99,96,96
   96 XI1(I)=XI1(I)+0.0005
   99 R(I)=R(I)+0.0005
C     THIS FORCES R(1)=1 AND R(N)=0
      R(1)=1.0
      R(N)=0.0
      IF(NN-1)12,12,92
   92 IF(N-1)7,7,6
    6 WRITE(NW,104)T(I),CR(I),F(I),XI2(I),XI1(I),R(I)
  104 FORMAT(1H ,5X,F7.2,3X,F6.3,3X,F7.3,3X,F7.3,3X,F7.3,3X,F6.3)
      GO TO 12
    7 WRITE(NW,106)CR(I),F(I),XI2(I),XI1(I),R(I)
  106 FORMAT(1H ,15X,F6.3,3X,F7.3,3X,F7.3,3X,F7.3,3X,F6.3)
      GO TO 12
```

```
   70 R(I)=0.0
      IF(NN-1)12,12,93
   93 WRITE(NW,105)T(I)
  105 FORMAT(1H ,5X,F7.2)
   12 CONTINUE
C     THIS BEGINS THE PLOTTING ROUTINE
      WRITE(NW,500)
      WRITE(NW,503)
      DO 42 I=1,N
      IF(R(I))44,44,43
   43 R(I)=ALOG(R(I))
      GO TO 42
   44 R(I)=0.0
   42 CONTINUE
C     THIS DECIDES WHETHER OR NOT TO CALCULATE THE END POINTS
      GO TO(72,73),NPO
   72 B=0.0
C     THIS DETERMINES NUMBER OF LOG CYCLES TO BE USED IN PLOT
      S=ALOG(0.01)
      IF(XT-TI)75,76,75
   75 II1=2
      GO TO 74
   76 II1=1
      GO TO 74
C     SEARCH FOR MAX AND MIN R
   73 IF(XT-TI)94,95,94
   94 B=R(2)
      S=R(2)
      I1=3
      II1=2
      GO TO 40
   95 B=R(1)
      S=R(1)
      I1=2
      II1=1
   40 DO 20 I=I1,N
      IF(R(I)21,20,21
   21 IF(R(I)-B)15,15,11
   11 B=R(I)
      GO TO 20
   15 IF(R(I)-S)16,20,20
   16 S=R(I)
   20 CONTINUE
   74 WRITE(NW,200)S,B
  200 FORMAT(1H ,F9.3,92X,F9.3)
C     CALCULATION OF SCALING FACTOR
      SC=(B-S)100.0
      WRITE(NW,202)
  202 FORMAT(1H ,8X,'*',99X,'*')
      WRITE(NW,201)
  201 FORMAT(1H ,7X,'-....+....+....+....+....+....+....+....+
     +....+....+....+....+....+....+....+....+....+....+....+
     +....+.')
```

```
C     PLOTTING OF DATA
      DO 30 I=II1,N
      DO 32 JJ=1,101
   32 YY(JJ)=A(2)
      IF(R(I))34,33,34
   34 NY=(R(I)-S)/SC+1
      IF(S-R(I))36,36,37
   37 I=N+1
      GO TO 30
   36 YY(NY)=A(1)
      GO TO 35
   33 NY=1
   35 WRITE(NW,204)T(I),(YY(KJ),KJ=1,NY)
  204 FORMAT(1H ,F7.2,'-',101A1)
C     THIS CHOOSES SCALE ALONG X-AXIS
      IF(N-I)53,30,53
   53 M=MM
   52 IF(M)30,30,51
   51 WRITE(NW,205)
  205 FORMAT(1H ,7X,'-')
      M=M-1
      GO TO 52
   30 CONTINUE
      WRITE(NW,201)
      WRITE(NW,203)SC
  203 FORMAT(1H ,'THE SCALING FACTOR IS...',F8.5)
C     THIS CALCULATES SLOPE R/L=RESISTANCE/INDUCTANCE
C     IF MORE THAN ONE ZERO BETWEEN NONZERO POINTS DON'T USE
      IF(MN-1)82,83,83
   83 WRITE(NW,500)
      WRITE(NW,505)
      WRITE(NW,300)
      WRITE(NW,502)
  502 FORMAT(1H ,20X,'T',15X,'R/L')
      TR=((T(2)/2.0)+0.005)-XT
      M=N-2
      DO 86 I=1,M
      IF(XI1(I))89,86,89
   89 IF(XI1(I+1))84,85,84
   84 D=SI1(I)-XI1(N)
      E=XI1(I+1)-XI1(N)
      IF(I-1)97,98,97
   97 TR=T(I)+XT/2.0
      Q=XT
      GO TO 88
   98 TR=(TI/2)+0.005
      Q=TI
      GO TO 88
   85 D=XI1(I)-XI1(N)
      E=XI1(I+2)-XI1(N)
      TR=T(I)+XT
      Q=2.0*XT
```

```
88 G=D/E
   P=ALOG(G)
   RL=P/Q
   WRITE(NW,87)TR,RL
87 FORMAT( 1H ,17X,F7.2,9X,F8.4)
86 CONTINUE
   GO TO 82
80 WRITE(NW,500)
   CALL EXIT
   END
```

## APPENDIX D

## SYMBOLS

$i_s$ current in the solenoid of the coupled persistatron

L referred to as the self-inductance of the solenoid, may include mutual-inductance term

$H_s$ magnetic field produced by the solenoid, longitudinal to the central wire

$i_w$ the transport current in the wire sample

I $i_s + i_w = I$, the external control current supplied to the coupled persistatron from an external source

$H_w$ azimuthal magnetic field produced by the current in the central wire $i_w$

$H_c$ bulk critical magnetic field for indium based on values published by Shaw, et al.

d diameter of central measured in cm

$I_{1c}$ first critical point of circuit, the value of I for which dissipation begins

$k_s$ coil constant, one of the constants describing the circuit, relates $H_s$ to $i_s$

$k_w$ wire constant, other constant of circuit relating $H_w$ to $i_w$, $k_w = 2/5d$

$i_{wc}$ threshold current, the current in the wire for which dissipation is first observed

$I_{2c}$ second critical point, value of I at singularity

$H_{tot}$ total magnetic field at surface of the wire at all times

$S_i$ threshold current ratio, ratio of the threshold current to the critical current

$i_c$ critical current as obtained from $H_c$ using Silsbee's rule

$H_c'$ threshold field, total field at the surface of the wire when dissipation begins or ceases, equilibrium value of $H_{tot}$

$\phi$ pitch angle of magnetic field

$\theta$ pitch angle of total current

R effective resistance of central wire

R/L time constant of time curves

i reapportionment current

$i_{wo}$ initial value of $i_w$ for a given change in I

$i_{wf}$ final value of $i_w$ recorded for a given change in I

$i_{wT}$ total current in wire, including shielding current

$F_L$ Lorentz force in units of $10^4$nt/m

CR chart reading

$V_H$ Hall voltage used to obtain $H_s$

S threshold field ratio, $H_c'/H_c$

$i_{wn}$ normalized wire current

$k_H$ Hall probe calibration constant

$A_t$ annealing time of the wire sample